Life in a moving world

Scaling movement ecology from species traits to communities

Dissertation
to fulfill the requirements for the degree of
„doctor rerum naturalium“ (Dr. rer. nat.)

submitted to the Council of the Faculty of Biological Sciences
of the Friedrich Schiller University Jena

by M.Sc.
Myriam Brose-Hirt

born on 16.03.1988 in Ebersberg

Leipzig, 2018

Reviewers
Prof. Dr. Nico Eisenhauer, University of Leipzig
Prof. Dr. Kirsten Küsel, University of Jena
Prof. Dr. Florian Jeltsch, University of Potsdam

Date of defense: 16.11.2018

Table of Contents

General Discussion

Appendix

Summary

Movement is the core process driving interactions between species and their environment, and is therefore vital to all animals. Only by moving, animals find food, shelter, mating partners or new territories. Only by moving, they can directly react to changed environmental conditions if they are unable to adapt. Only by moving, they can attack others or escape predation in the absence of defense mechanisms. Thus, movement is a central determinant of species interactions and consequently shapes communities. Moreover, by inducing exchange between habitat patches, it creates spatial networks and couples subpopulations.

The increasing general and scientific interest in animal movement has led to a massive amount of data gathered over the last years. Advances in tracking technologies helped generate high-resolution movement paths and more and more measureable movement parameters, including body posture or behavioral changes. While this enables analyses of individual tracks in unprecedented detail, new challenges in data management and general analyses emerge. This requires a detailed understanding of the general processes underlying these movement patterns as well as of the main parameters driving them. The physiological and morphological capacity of an animal determines how it moves and thereby affects many important movement parameters such as speed. Speed is the most fundamental constraint on movement, as it has subsequent effects on other movement parameters (e.g. maneuverability or dispersal distances) as well as on species interactions and animal space use. For example, speed affects encounter rates between predator and prey and determines who can catch whom in a one-to-one chase. Moreover, it defines the distances an animal can travel and, consequently, which patches in a landscape it can connect. As it is impossible to measure movement parameters for all species separately, it is useful to apply trait-based

scaling relationships of these parameters (e.g. body-mass dependent (allometric) scaling relationships). This enables generalized predictions of their effects on movement patterns and their consequences for species interactions and communities.

In this thesis, I analyze the general determinants of individual movement, their consequences for species interactions and, thereby, finally scale movement ecology from species traits to communities. In **Chapter 1** and **2**, I provide new insight into how movement speed scales with the body mass of animals. In **Chapter 1**, I develop a general mechanistic model showing that the maximum speed of animals follows a hump-shaped relationship with body mass, finally explaining why the largest animals are not the fastest. This finding is based on the assumption that larger animals could theoretically reach higher speeds, as they have more muscle tissue and therefore more energy available for acceleration. However, due to mass-dependent inertia, they need more time to accelerate to the same speed than smaller animals, causing that their energy reserves run out before actually reaching their top speed. I test this model by a new extensive empirical database and interestingly, it does not only predict the maximum speed of animals highly accurately but also holds across ecosystems, taxonomic groups, and movement modes. However, there is a clear data bias towards vertebrate species caused by difficulties in tracking small-bodied organisms.

In **Chapter 2**, I contribute to filling this gap by measuring the exploratory (voluntary) speed of invertebrates in the laboratory using automated image-based tracking. Thereby, I provide a first general empirically-derived allometric scaling relationship of exploratory speed across broad taxonomic groups of invertebrates. Moreover, I show that there is substantial variation in this scaling relationship between taxonomic groups and feeding types, which probably arises from differences in body shape and other functional traits. Exploratory speed is a key component of species interactions, for example by driving encounter and attack rates between predator and prey. Therefore, it is essential to integrate species traits such as speed in all movement ecology fields, including movement modelling. Current state-of-the-art movement models are either random, ignoring differences in animal movement capacities, or highly specific, thereby rendering generalizations for modelling communities impossible.

In **Chapter 3**, I present a framework how to integrate the allometric scaling of movement speed (**Chapter 1** and **2**) in random walk models, generating movement trajectories within a realistic and species-specific spatial scale. I demonstrate in two worked examples how this framework can be used to (1) correctly predict predator-prey attack rates as an example for species interactions and (2) generate species-specific connectivities of spatial networks and thereby predict large-scale biodiversity patterns in fragmented landscapes. This clearly demonstrates that allometric random walks represent the movement of real species better than random walks with stochastic parameters and that they can be generalized more easily across species and communities. Moreover, this framework emphasizes the importance of movement speed for predator-prey interactions. While exploratory speed affects encounter and attack rates between predator and prey, the maximum speed has strong implications for the outcome of this encounter.

In **Chapter 4**, I explore the role of maximum speed as a general determinant of predator-prey interactions and show that trophic niches need to be extended from a simple prey range to a two-dimensional prey space including body mass as well as maximum speed as key drivers. This prey space is constrained by three limits. The "energetic limit" and the "subdue limit" are only body-mass dependent and reveal that the prey needs to be large enough to meet the energetic demand of the predator but small enough to be successfully subdued. The newly established "speed limit" implies that the predator should be faster than its prey to be able to catch it in a chase. I test this concept of a two-dimensional prey space using a new database combining body mass and maximum speed of various mammalian predators and their prey. Thereby, I show that (1) the prey space is significantly affected by the hunting strategy of the predator (pursuit predator, group hunter, ambusher) and (2) that these different prey spaces and therefore hunting strategies have a specific energetic optimum along the body-mass axis. Therefore, this novel concept also provides a mechanistic understanding how energy and speed limits prevent the existence of small-bodied group hunters and large pursuit predators.

Overall, in this thesis, I demonstrate the importance of applying generalized allometric scaling relationships of movement parameters to understand the drivers of natural movement patterns and illustrate how they can be scaled up to making predictions on species interactions, communities, and animal space use.

Zusammenfassung

Bewegung ist der Kernprozess, der Interaktionen zwischen Arten sowie mit ihrer Umwelt antreibt und ist deshalb essentiell wichtig für alle Tierarten. Nur durch Bewegung können Tiere Nahrung finden genauso wie Unterschlupf, Partner oder neue Reviere. Nur durch Bewegung können sie direkt auf sich verändernde Umweltbedingungen reagieren, wenn es ihnen nicht möglich ist, sich daran anzupassen. Nur durch Bewegung können sie Beute erlegen oder Prädation entkommen, wenn es keine Verteidigungsmechanismen gibt. Folglich spielt Bewegung eine zentrale Rolle in zwischen- und innerartlichen Interaktionen und verändert dadurch auch die Zusammensetzung von Artgemeinschaften. Desweitern wird durch Bewegung Austausch zwischen verschieden Lebensräumen ermöglicht, wodurch räumliche Netzwerke entstehen können.

Das wachsende wissenschaftliche wie auch allgemeine Interesse an der Bewegung von Tieren hat dazu geführt, dass über die letzten Jahre enorme Datenmengen gesammelt wurden. Dazu trugen unter anderem auch die technischen Fortschritte bei, durch die extrem hochauflösende Trajektorien generiert und immer mehr Parameter gemessen werden konnten, darunter zum Beispiel die Körperhaltung des Tieres oder Verhaltensänderungen. Dies ermöglicht es zwar, individuelle Bewegungsmuster in nie da gewesener Genauigkeit zu analysieren, stellt uns aber vor neue Herausforderungen, diese Daten zu verwalten sowie generelle Analysen durchzuführen. Dafür benötigen wir ein gutes Verständnis davon, welche generellen Prozesse diesen Mustern zugrunde liegen und welche Parameter dafür hauptsächlich verantwortlich sind. Die physiologische und morphologische Kapazität eines Tieres ist dabei von zentraler Bedeutung und bedingt viele wichtige Bewegungsparameter wie zum Beispiel die Geschwindigkeit, mit der Tiere sich fortbewegen. Geschwindigkeit ist die grundlegendste Eigenschaft von Bewegung und hat

weiterführende Auswirkungen sowohl auf andere Bewegungsparameter (z.B. Manövrierfähigkeit oder Ausbreitungsdistanz) als auch auf Artinteraktionen und Raumnutzung. So bedingt sie zum Beispiel, wie häufig Räuber und Beute einander begegnen (Begegnungsrate) und wer als Gewinner aus diesem Zusammentreffen hervorgeht. Darüber hinaus sagt Geschwindigkeit auch etwas über die Strecke aus, die ein Tier zurücklegen kann und somit auch welche Teilhabitate es in einer Landschaft vernetzen kann. Bewegungsparameter wie Geschwindigkeit für alle Tiere einzeln zu messen ist allerdings unmöglich. Daher ist es sinnvoll, allometrische (körpermassenabhängige) Skalierungsverhältnisse dieser Parameter zu identifizieren. Dadurch lassen sich generelle Vorhersagen machen, wie sie sich auf Bewegungsmuster auswirken und welche Konsequenzen dies für Artinteraktionen und Artgemeinschaften hat.

In dieser Arbeit möchte ich die generellen Determinanten von Bewegung analysieren und ihre Konsequenzen für Artinteraktionen erfassen, um darüber letztendlich Bewegungsökologie von Arteigenschaften bis zu Artgemeinschaften zu skalieren. In den **Kapiteln 1** und **2** beschäftige ich mich damit, wie Bewegungsgeschwindigkeit mit der Körpermasse von Tieren skaliert. In **Kapitel 1** entwickle ich ein generelles, mechanistisches Modell, das einen parabelartigen Zusammenhang zwischen Maximalgeschwindigkeit und Körpermasse von Tieren beschreibt und letztendlich erklärt, warum die größten Tiere nicht die schnellsten sind. Dieses Modell beruht auf der Annahme, dass große Tiere zwar theoretisch höhere Geschwindigkeiten erreichen könnten, da sie mehr Muskelgewebe und dadurch mehr Energie für die Beschleunigung zur Verfügung haben; durch Massenträgheit jedoch brauchen sie mehr Zeit als kleinere Tiere, um auf die gleiche Geschwindigkeit zu beschleunigen, so dass ihre Energiereserven verbraucht sind, bevor sie ihre Maximalgeschwindigkeit erreichen können. Ich teste diese Theorie anhand einer neuen umfangreichen Datenbank und interessanterweise sagt das Modell nicht nur die Maximalgeschwindigkeit von Tieren mit sehr hoher Genauigkeit vorher, es hat auch über Ökosysteme, taxonomische Gruppen und Bewegungstypen hinweg Gültigkeit. Diese Datenbank beinhaltet allerdings deutliche mehr Vertebraten als Invertebraten, was vor allem an der Schwierigkeit liegt, kleine Organsimen zu „tracken".

In **Kapitel 2** möchte ich diese Lücke teilweise schließen, indem ich die Normalgeschwindigkeit von Invertebraten im Labor mithilfe von automatisierten,

bildbasierten Trackingmethoden messe. Dadurch entwickle ich das erste generelle, empirisch-hergeleitete allometrische Modell von Normalgeschwindigkeit über eine große Zahl taxonomischer Gruppen von Invertebraten hinweg. Desweitern zeige ich, dass es in diesem Skalierungsverhältnis substantielle Variation zwischen taxonomischen Gruppen und Ernährungstypen gibt, welche vermutlich von Unterschieden in Körperbau und funktionellen Merkmalen bedingt wird. Die Normalgeschwindigkeit von Tieren ist ein wichtiges Element von Artinteraktionen und bestimmt zum Beispiel Begegnungs- und Angriffsraten zwischen Räuber und Beute. Daher ist es essentiell, Arteigenschaften wie Geschwindigkeit in alle bewegungsökologische Wissenschaftsbereiche zu integrieren, unter anderem auch in die Modellierung tierischer Bewegung. Derzeitige Bewegungsmodelle sind entweder zufällig, das heißt sie ignorieren Unterschiede in den Bewegungskapazitäten von Tieren, oder sie sind sehr spezifisch für einzelne Arten, wodurch die generelle Modellierung größerer Artgemeinschaften unmöglich wird.

In **Kapitel 3** stelle ich ein Konzept vor, wie man die allometrische Skalierung von Bewegungsgeschwindigkeit (**Kapitel 1** und **2**) in sogenannte „random walk"-Modelle integrieren kann, um dadurch Trajektorien auf einer realistischen und artspezifischen räumlichen Skala zu generieren. In zwei ausgearbeiteten Beispielen lege ich dar, wie man dieses Konzept nutzen kann, um (1) Angriffsraten zwischen Räuber und Beute korrekt vorherzusagen und (2) artspezifische Konnektivitäten räumlicher Netzwerke generieren kann, um darüber Biodiversitätsmuster in fragmentierten Lebensräumen auf großen Skalenebenen vorherzusagen. Diese Anwendungsmöglichkeiten zeigen, dass „allometrische random walks" die Bewegung von echten Tieren deutlich besser widerspiegeln als „random walks" mit stochastischen Parametern und dass sie wesentlich einfacher für andere Arten und Gemeinschaften generalisiert werden können. Überdies verdeutlicht dieses Kapitel noch einmal die Bedeutung von Bewegungsgeschwindigkeit für Räuber-Beute Interaktionen. Während Normalgeschwindigkeit die Begegnungs- und Angriffsraten zwischen Räuber und Beute bestimmt, hat die Maximalgeschwindigkeit starke Auswirkungen darauf, wie diese Begegnungen ausgehen.

In **Kapitel 4** analysiere ich, welche Rolle Maximalgeschwindigkeit als eine generelle Determinante in Räuber-Beute Interaktionen spielt und entwickle das Konzept trophischer Nischen von einem einfachen Beutebereich zu einem zweidimensionalen Beuteraum

weiter, indem ich sowohl Körpermasse als auch Maximalgeschwindigkeit als Nischendimensionen miteinbeziehe. Dieser Beuteraum ist durch drei Grenzen eingefasst. Die „Energiegrenze“ und die „Überwältigungsgrenze“ sind körpermassenabhängig und sagen aus, dass die Beute groß genug sein muss, um den energetischen Bedürfnissen des Räubers zu entsprechen, aber klein genug, um überwältigt werden zu können. Die neu eingeführte „Geschwindigkeitsgrenze“ sagt aus, dass der Räuber schneller als seine Beute sein muss, um sie in einer Verfolgungsjagd fangen zu können. Dieses Konzept eines zweidimensionalen Beuteraums teste ich anhand einer neuen Datenbank, die Körpermassen und Maximalgeschwindigkeiten von verschieden Säugetier-Räubern und ihrer Beute beinhaltet. Dadurch zeige ich, dass (1) der Beuteraum signifikant von der Jagdstrategie des Räubers (Verfolgungsjäger, Gruppenjäger, Lauerjäger) abhängt und (2) diese verschiedenen Beuteräume und damit auch Jagdstrategien spezifische energetische Optima entlang der Körpermassenachse haben. Daher eröffnet dieses neue Konzept auch ein mechanistisches Verständnis, wie Energie- und Geschwindigkeitsgrenzen die Existenz von kleinen Gruppenjägern und großen Verfolgungsjägern verhindern.

Im Großen und Ganzen lege ich in dieser Arbeit die hohe Bedeutung generalisierter Skalierungsmodelle von Bewegungsparametern für ein umfassendes Verständnis der Bewegungsökologie von Tieren dar. Darüber hinaus zeige ich, wie mithilfe dieser Skalierungsmodelle natürliche Bewegungsmuster von Tieren besser verstanden und Vorhersagen für Artinteraktionen, Artgemeinschaften und Raumnutzung getroffen werden können.

List of Figures

List of Tables

Author Contributions

Chapter 1 | A general scaling law reveals why the largest animals are not the fastest

Myriam R. Hirt, Walter Jetz, Björn C. Rall & Ulrich Brose

M.R.H. and U.B. developed the model. M.R.H. gathered the data. M.R.H. and B.C.R. carried out statistical analyses. W.J. was involved in study concept and data analyses. M.R.H. and U.B. wrote the paper. All authors discussed the results and commented on the manuscript.

Published in *Nature Ecology and Evolution*, 2017, 1:1116 –1122, doi:10.1038/s41559-017-0241-4

Chapter 2 | The little things that run: a general scaling of invertebrate exploratory speed with body mass

Myriam R. Hirt*, Tobias Lauermann*, Ulrich Brose, Lucas P.J.J. Noldus & Anthony I. Dell

A.I.D. designed the study. T.L. gathered the data. M.R.H. analyzed the data and wrote the manuscript. M.R.H. and U.B. carried out statistical analyses. All authors discussed the results and commented on the manuscript. * These authors contributed equally.

Published in *Ecology*, 2017, 98: 2751–2757. doi:10.1002/ecy.2006

Chapter 3 | Bridging scales - allometric random walks link movement and biodiversity research

Myriam R. Hirt, Volker Grimm, Yuanheng Li, Björn C. Rall, Benjamin Rosenbaum, & Ulrich Brose

M.R.H and U.B. developed the overall concept. M.R.H. and B.R. implemented beta distributions in the concept. M.R.H. and V.G. merged the concept with individual-based modelling. Y.L and B.C.R. conducted simulations of worked example I. M.R.H. wrote the manuscript and all authors discussed the results and commented on the manuscript.

Published in *Trends in Ecology and Evolution*

Chapter 4 | Rethinking trophic niches: speed and body mass co-limit prey space of mammalian predators

Myriam R. Hirt, Thomas Müller, Benjamin Rosenbaum, Marlee Tucker & Ulrich Brose

M.R.H, T.M., M.T. and U.B. developed the concept. M.R.H. and M.T. established the database. M.R.H. and B.R. carried out statistics. M.R.H. wrote the manuscript and all authors discussed the results and commented on the manuscript.

General Introduction

Movement research

What we see, what is behind it, and what it tells us

Movement is one of the most fundamental processes of live. It has a determining influence on where species live and how they interact with their environment as well as on how they coexist and interact with other species (Nathan et al. 2008, Jeltsch et al. 2013). A holistic picture of movement research includes *causes*, *mechanisms*, *patterns*, and *implications* of movement (Figure I.1). Movement patterns are **what we see** in nature. As an example, there is extensive data on the movement pattern of elk (*Cervus elaphus*) in the Yellowstone National Park (USA) gathered by tracking them in the field. We can analyze these movement patterns to understand what caused them (**what is behind it**) and which implications they have for other species and the environment (**what it tells us**). The causes ("why move") and mechanisms ("how to move") of movement are what shapes these movement patterns (Nathan et al. 2008). For example, the elk move in search of food as well as in response to predation risk (Ripple et al. 2001, Ripple and Beschta 2004). Their physical and morphological capacity determines how fast and far they can move. Their movement has, of course, also direct implications for their environment (e.g. by browsing tree bark or sprouts) and other species (e.g. for predators or for species that compete for the same resources) (Ripple and Beschta 2004). Thus, animal movement is complex and needs to be addressed on all these levels – separately as well as interactively.

Data on animal movement patterns are currently available in large amounts due to tremendous advances in animal tracking technologies (Kays et al. 2015). The problem is that analyzing all these movement patterns individually is impossible and the benefit of this high data availability therefore remains limited. A general understanding of the underlying processes and mechanism is necessary to be able to make generalized predictions of the implications of movement patterns. This includes, for example, figuring out how different

traits such as body mass (how big you are) or movement mode (if you run, swim, or fly) affect important movement parameters such as movement speed [→ **Chapter 1 & 2**]. By identifying these general relationships between traits, we can more easily assess the movement patterns we observe and better understand their implications for species interactions [→ **Chapter 3 & 4**], communities, and biodiversity [→ **Chapter 3**].

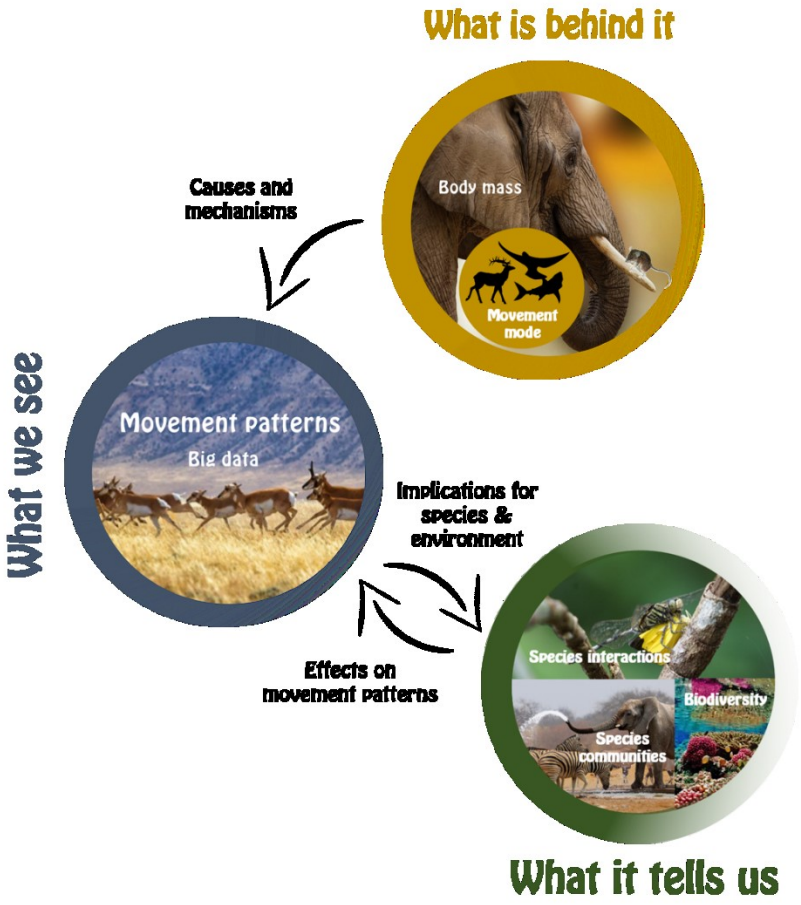

Figure I.1 | Movement research compartments: movement patterns, causes and mechanisms of movement, implications for species and environment. Movement patterns are **what we see** in nature and currently have enormous amounts of data on. To understand these movement patterns, we need to identify the general underlying mechanisms of movement processes, e.g. how body size and movement mode (if animals run, swim or fly) affect important movement parameters such as movement speed (**what is behind it**). By gaining insight in these processes, we strongly facilitate the evaluation of the available data concerning animal movement patterns in terms of their implications for species interactions, communities, and biodiversity, as well as their feedback effects (**what it tells us**).

What we see

Gathering movement data by animal tracking in the field

Despite the major scientific interest in animal movement, the limited possibilities for gathering data in the wild led to only sparse information on movement patterns and processes until recently. Since the 1960s, scientists have been using radio telemetry to gather animal movement data (Ropert-Coudert and Wilson 2005, Urbano et al. 2010, Kays et al. 2015). Telemetry comes from the Greek words *tele*, far, and *metros*, measurement, and aims at tracking animals from the distance. Thereby, a transmitting device (tag) is affixed to the animal and signals emitted by this tag are recorded by a radio receiver and an antenna system (Ropert-Coudert and Wilson 2005). Gathering as well as evaluation of these data was tough, as scientists had to repeatedly localize their tagged animals in the field and track them manually by using antennas. From own experience, I can approve that this is a time-consuming process with limited information gained. When I tracked partridges during my master thesis, a whole day of work yielded tracking data on 10 individuals – but only one data point each. Substantial advances in tracking technologies have now facilitated the study of animal movement and helped generate enormous amounts of movement data from all over the globe (Urbano et al. 2010, Kays et al. 2015). The major step here was that both – the sensory and the recording system – were now attached to the animal. This precluded the need for manually obtaining locations, as the accurate position of the animal could be directly transmitted and downloaded to the computer. Modern tracking methods use Global Positioning System (GPS) devices that are able to record animal movement nearly continuously and in high spatial and temporal resolution. The addition of secondary sensors to the tracking tags offered new insights into the animal's behavior, physiology, and environment. So-called accelerometers, for example, provide information on behavior-specific body posture and body movements (e.g. distinguishing between resting and moving

periods, and information about energy use, Brown et al. 2013). Moreover, physiological parameters such as heart rate or internal temperature can be recorded via implanted electronics (Rattenborg et al. 2008, Signer et al. 2010).

Figure I.2 | Tagged animals of decreasing body mass from a-f*. (**a**) plains zebra (*Equus quagga*), (**b**) three-toed sloth (*Bradypus variegatus*), (**c**) fisher (*Pekania pennant*), (**d**) Lyle's flying fox (*Pteropus lylei*), (**e**) ground beetle (*Carabus ullrichii*), (**f**) bumblebee (*Bombus terrestris*); **a-d* from Kays et al. 2015, *e* from Růžičková & Veselý 2016, and *f* from Kissling et al. 2015.

The majority of animals currently tracked with GPS accuracy are medium- or large-sized vertebrates (Figure I.2 a-d) leaving a distinct threshold below which animals cannot be accurately tracked (Figure I.3). Minimum tag size is highly restricted (currently limited to ~5 g) due to a trade-off between transmitter weight vs. power (i.e. range) and battery life (Wikelski et al. 2007, Kissling et al. 2014). Thus, small vertebrates are not able to carry current tags, as they should be less than 5% of the body weight of the animal to minimize negative effects on behavior and survival (Kays et al. 2015). However, rapid technological development lead to continuously shrinking tag sizes over the last 40 years (Figure I.3a), which is likely to continue in the future and facilitate the tagging of small vertebrates.

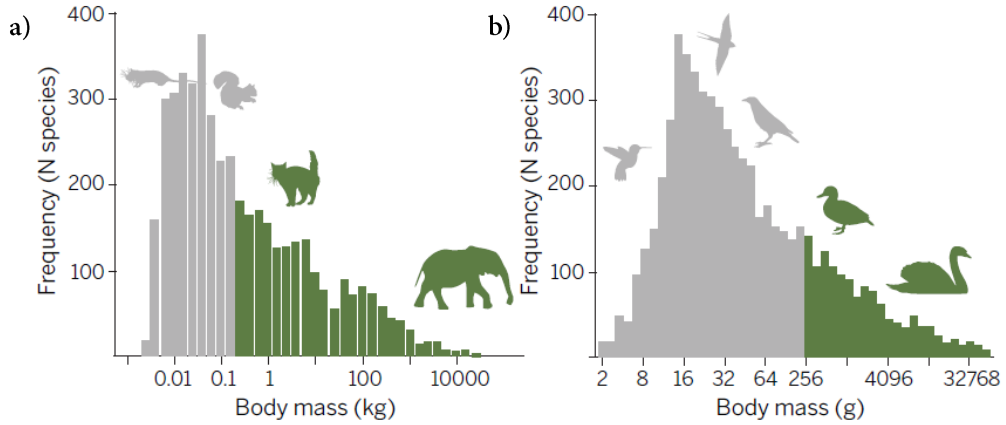

Figure I.3 | Overview of the body masses of currently tracked vertebrates. Body-mass distributions for all known mammals (**a**) and birds (**b**), illustrating the proportion of species that can be tracked with GPS accuracy with today's technology (green bars). Figure from Kays et al. 2015.

However, Figure I.3 only shows the proportion of *vertebrate* species that can be tracked. Another challenge is the tracking of smaller organisms such as invertebrates. Information on invertebrate ecology is crucial as they are "the little things that run the world" (Wilson 1987) not only by sheer abundance and diversity but also by contributing to key ecosystem structure, functions, and services (Wilson 1987, Hochkirch 2016). This is even more true for microbes and unicells. Microbial communities are ideal model systems for addressing ecological key questions and for testing concepts of evolution (Jessup et al. 2004, Altermatt et al. 2015). Thus, tracking both invertebrates and microbes is essential for understanding the ecological and evolutionary consequences of current and altered movement behavior. Due to their small size, invertebrates cannot be tracked by GPS technology, as the weight of

these transmitters is too heavy. The small (non-GPS) tags that are currently used in insect telemetry (Figure I.2 e-f) have a much shorter life span and a limited tracking range. These technical difficulties complicate movement parameter measurements, but new methods of invertebrate movement tracking evolve. First, so-called automated image-based tracking enables tracking of invertebrates in the laboratory (Dell et al. 2014a) (**→ Chapter 2**). This method is based on filming by cameras and does not require tagging of the animals. The advantage of this approach is the continuous recording of individuals under controlled conditions. Therefore, this method is also suitable for tracking microbes or unicells (Pennekamp and Schtickzelle 2013, Pennekamp et al. 2017). The disadvantage is that it requires high-contrast images so that organisms can be discerned from their surrounding background and, thus, a simple environmental landscape is inevitable. Hence, implementing more complex environments with physical structure, such as plant cover or soil, is difficult. A possibility to track animals in complex environments lies in passive transmitting systems like radio-frequency identification (RFID) (Aguzzi et al. 2011). This method requires tagging of the animals. The passive tag, however, does not need a battery and is therefore much lighter than a GPS tag. The smallest tags only weigh around 0.9 mg. However, there is a trade-off between tag size and distance to the reader, which records the animal: the smaller the tag, the lower the minimum distance required. In a current project, we effectively attach 30 mg tags to Carabid beetles of at least 500 mg and aim to track them in experimental meta-communities (**→ Outlook**).

In summary, the tremendous advances in tracking technologies opened up unprecedented insights into the movement behavior of animals. The easy and continuous data generation produced a vast amount of movement patterns mainly from medium- to large-sized vertebrates. However, advances in the field of invertebrate and microbial movement tracking are clearly necessary. Moreover, there is an evident need for a general data analysis to handle the mass of data, which requires good knowledge of the underlying causes and mechanisms of movement.

What is behind it

Causes and mechanisms of movement

An animal's physiological and morphological capacity ("how to move") paired with its internal motivation ("why move") is what eventually generates the movement patterns we see in nature (Nathan et al. 2008). Thus, knowledge on these aspects is crucial to analyze the numerous animal movement patterns we currently have data on. The internal motivation of an animal addresses the question "why move?" and can include one or more of the following proximate intentions: searching for food, escaping from predators, following adults, or searching for mating partners, which translate into the general goals of gaining energy, seeking safety, learning, and reproducing (Nathan et al. 2008). The physiological and morphological capacity determines how an animal moves and defines many important movement parameters such as speed or maneuverability (Wilson et al. 2018). Speed is the fundamental constraint on movement. It determines, for example, the distances an animal can travel and, thereby, which patches in a landscape it can connect. Moreover, it has important implications for predator-prey interactions by setting the basic rules of who can catch whom in a one-to-one chase. Therefore, I would call movement speed the "primary movement parameter", which has subsequent effects on other movement parameters (e.g. maneuverability or dispersal distances) as well as on their consequent patterns such as space use capacities (e.g. home range sizes) and connectivity potential (e.g. patch integration in fragmented landscapes). Particularly important is the maximum speed an animal can reach. While the realized movement of animals might be largely driven by ecological factors such as landscape structure, habitat quality, or sociality, the range within which this realized movement occurs, meets its upper limit at the maximum movement speed.

As it is impossible to measure movement parameters for all species separately, it is useful to identify traits that characterize a species and its other relevant features. A so-called "super-trait" in ecology is the *body mass* of an animal (Peters 1986, West et al. 1997) as it determines many other species traits. For example, the metabolic rate increases with body mass while mortality and reproduction rates decrease (Brown et al. 2004, Savage et al. 2004). Most of these scaling relationships follow a power law, indicating that an animal's feature (Y) changes as some power (b) of its body mass (M):

$$Y = a\, M^b$$

The scaling exponent b has several implications for this scaling relationship. Positive values indicate an increase and negative values a decrease with body mass. An exponent of one would indicate that an animal's feature and body mass change at the same rate (*isometric scaling relationship*). In biological systems, however, they usually change at different rates with an animal's feature increasing at a higher ($b > 1$) or lower rate ($b < 1$) than the body mass. Therefore, these scaling relationships are often referred to as *allometric relationships.* The most basic physiological process is the metabolism of an animal. According to the Metabolic Theory of Ecology, the metabolic rate of an animal increases with body mass to an exponent of approximately ¾ (Peters 1986, West et al. 1997). Therefore, it is assumed that other physiological rates should scale as multiples of 0.25. However, the universality of the ¾ exponent as well as the applicability of a simple power law is strongly debated (Kolokotrones et al. 2010, White 2010, Capellini et al. 2010).

Besides physiological rates, body mass also determines interaction strengths with co-existing species (Petchey et al. 2008, Rall et al. 2012), behavioral characteristics (Dial et al. 2008), and movement parameters and patterns. For instance, movement speed has been shown to increase with body mass (Peters 1986, Van Damme and Vanhooydonck 2001, Iriarte-Díaz 2002, Hedenström 2003, Bejan and Marden 2006). Speed has direct consequences for the space use of animals and the distances that can be covered. Consequently, also home range size (Jetz et al. 2004, Tamburello et al. 2015), and dispersal and migration distances (Sutherland et al. 2000, Hein et al. 2012) increase with body mass. While most of these parameters follow a power-law relationship with body mass, some

research suggests that the maximum movement speed of vertebrates might scale differently. Already in the 1980's, scientists came across the fact that in running animals, the largest are not the fastest (Garland 1983). The fastest animals such as cheetahs or marlins are of intermediate size indicating that a hump-shaped pattern may be more realistic. This phenomenon caught my particular interest because despite numerous attempts to describe it (Garland 1983, Iriarte-Díaz 2002, Clemente and Richards 2013, Fuentes 2016), a general mechanistic model was still lacking. I deal with this issue in **Chapter 1** developing a model that predicts the large-scale pattern of maximum speed across all taxonomic groups, ecosystem types and movement modes. The *movement mode* - telling if an animal runs, swims, or flies - is an important trait, which significantly affects allometric scaling relationships of movement parameters (e.g Bejan and Marden 2006b, Hein et al. 2012a). For instance, flying animals cover longer distances during migration than running or swimming animals (Hein et al. 2012). Therefore, I also consider this trait when analyzing the allometric scaling of maximum speed.

Most research in this field is conducted on vertebrates due to the earlier mentioned limitations of invertebrate movement tracking (Kissling et al. 2014). Therefore, data on the allometric scaling of movement parameters for invertebrates are sparse. For instance, few empirical studies present allometric scaling relationships of invertebrate movement speed and at the same time only focus on a single taxonomic group (e.g. ants (Hurlbert et al. 2008) or beetles (Forsythe 1983)). In **Chapter 2**, I present a first general empirical analysis of the allometry of invertebrate speed across broad taxonomic and functional groups.

But how can knowledge on these allometric scaling relationships specifically facilitate movement research? First, developing *mechanistic models* to describe allometric patterns of movement parameters helps gaining a better general understanding of the mechanisms of movement. For example, developing a model to predict the scaling of speed with body mass requires a good knowledge on the physiology and morphology of animals and an understanding of how these aspects translate into movement. Second, allometric scaling relationships enable *predictions* of movement parameters for species, on which data is not available. A systematic measurement of movement parameters for the several million species on this planet is impossible and thus the potential to predict these parameters is of immense importance. For example, if we need information on the home range size of an

animal, we do not need to measure it but can predict it simply by using its body mass and the allometric scaling relationship of home-range size (Tamburello et al. 2015). Third, allometric scaling relationships can be used to construct trait-based *movement models*. State-of-the-art movement models are either random or highly specific, so that they cannot be generalized for modeling communities that consist of species with considerable variation in traits and thus movement patterns. By using species traits such as body mass, we can develop trait-based movement models that generate trait-specific and therefore more realistic movement paths (trajectories). In **Chapter 3**, I develop a concept how to achieve this by integrating the allometric scaling of movement speed in current movement models.

Thus, allometric scaling relationships of movement parameters are an important tool to understand the mechanisms of movement and make generalized predictions on movement patterns such as space use or movement trajectories. However, they also facilitate predictions on the implications of movement patterns for other species and the environment.

What it tells us

Implications for species and environment

So far, we have seen how movement data are effectively gathered by using high-tech tracking devices. Moreover, we have understood the importance of identifying general allometric scaling relationships of movement parameters to analyze these data. Now, we want to understand how we can use this information on natural movement patterns to deduce how species react to and interact with other species and their environment. As mentioned earlier, speed is the fundamental constraint on movement as it affects other movement parameters and patterns. Therefore, it has also cascading effects on species interactions and communities, and consequently biodiversity patterns.

For example, a predator-prey interaction is usually based on the encounter between two mobile organisms or a mobile and an immobile organism. The encounter of two mobile animals typically leads to an attack by the predator and defense or flight behavior by the prey. How often predator and prey encounter each other strongly depends on the perception range of the predator and the movement speed of both while exploring the habitat: the higher their movement speed, the higher the encounter rate. This, in turn, leads to higher attack rates by the predator (Mittelbach 1981, Pawar et al. 2012, Polidori et al. 2013), which affect interaction strengths and ultimately community attributes such as persistence and stability (May 1972, McCann et al. 1998, Gross et al. 2009). For instance, links with weak interaction strengths dampen oscillations between consumers and resources and therefore stabilize food web dynamics by decreasing the statistical chance that a population will go extinct (McCann et al. 1998). Just as movement speed, attack rates and therefore interaction strengths strongly depend on body mass (Rall et al. 2012). Thus, to be able to make adequate predictions of these parameters, it is critical to apply allometric scaling relationships of movement speed. This can be done, for example, in movement

modelling. As I have outlined earlier, state-of-the-art movement models are conceptually simple and do not include allometric scaling relationships of species traits. However, this is critically important not only to generate more realistic movement trajectories but also to make realistic predictions on species-interaction parameters such as predator-prey attack rates and consequently community attributes and biodiversity patterns. In **Chapter 3**, I show how the allometric scaling of empirical attack rates can be correctly predicted by using trait-based movement models. Certainly, movement speed also plays a critical role in non-trophic interactions and networks, which will not be further addressed in this thesis. This includes for example competition, mutualism or pollination networks. Due to its substantial effect on encounter rates, movement is of eminent importance to all types of interactions and therefore also community patterns.

Besides its implications for encounter and attack rates, movement speed plays another important role in predator-prey interactions: the movement speed determines who can catch whom in a one-to-one chase. Capture success can be maximized by a combination of speed and other species attributes such as maneuverability, acceleration and deceleration, as well as behavioral strategies. For example, locomotor characteristics of predator and prey have a strong influence on the outcome of a pursuit hunt. Predators need to be more athletic in terms of muscle power, speed, and acceleration capacity, but the prey can match this through higher maneuvering capacity (Wilson et al. 2013, 2018). Higher maneuverability (i.e. turn capacity), however, is negatively linked to movement speed: the higher the speed, the lower the turn capacity. Thus, invoking multiple rapid turns of the prey might be a good predatory strategy as it inevitably leads to a reduction in the prey's speed (Wilson et al. 2013, 2015). This seems contradictory and shows how closely predator and prey athletic capabilities match up. Probably, timing is a relevant factor deciding on the hunting success. Only when turns by the prey are timed correctly (not too far from or too close to the predator), the faster predator will overshoot (Wilson et al. 2015) and, thus, enabling prey escape. Furthermore, unpredictable escape behavior favors prey survival. This type of antipredator behavior uses unpredictable escape trajectories that are mostly directed away from the threat, but with a high variability (Domenici et al. 2008, 2011). Determinants of cursorial predator-prey pursuits have been intensely studied, but other hunting styles might favor different locomotor abilities and behaviors. For example, self-defense in prey such as

large body mass and weaponry, which are likely to trade-off against speed, is of high importance against ambush predators (Caro 2005, Bro-Jørgensen 2013). When mainly confronted with group hunters, there might also be a high evolutionary pressure on endurance speed of both predator and prey. Moreover, a higher body mass to stand against multiple simultaneous attacks is favorable (Bailey et al. 2013). Thus, hunting strategy as well as movement speed and body mass are critical components in predator-prey chases. But how exactly do these attributes interactively control who feeds on whom? I try to answer this question in **Chapter 4** developing a concept on how the prey space available to predators is bordered by an energetic, subdue, and speed limit, and systematically varies with predatory hunting strategy.

Thus, movement has important implications for species interactions and these interactions have again feedback effects on the movement behavior. For example, animals move in response to predation risk or intraspecific relationships (Hamilton and May 1977, Mitchell and Lima 2002). Besides that, also abiotic environmental conditions are a major driver of movement. This includes most importantly the spatial distribution of suitable habitat, and the availability and quality of resources (Van Moorter et al. 2013). These aspects are strongly affected by ongoing global change. Habitats are thereby altered by increasing temperatures as well as human land-use change (Haddad et al. 2015, Newbold et al. 2015, Huang et al. 2016, Reed and Stringer 2016). With increasing temperatures, animals might be forced to disperse in search of new suitable habitat as can be seen in the northward or elevational range shifts of different species (Parmesan et al. 1999, Colwell et al. 2008). But also locally, animals need to adapt their movement behavior to changing habitat conditions, for example due to habitat fragmentation. Thus, it is critically important to understand how species connect spatial networks depending on their movement capacity. I address this question in **Chapter 3,** demonstrating how body mass and movement speed can drive species-specific network connectivities by affecting the maximum distances that can be covered between habitat patches. Moreover, I illustrate how these models can be used to make predictions at larger spatial scales and how this finally helps predict changes in biodiversity patterns. The importance of movement for biodiversity models has long been acknowledged. For example, in island biogeography (MacArthur and Wilson 1963), meta-community theory (Leibold and Chase 2017), or neutral theory (Hubbell 2001), movement

is the central process that leads to an equilibrium between the global species pool and the local communities. Also, in predictive models that seek to understand biodiversity responses to environmental change (Urban and Keitt 2001, Thuiller et al. 2013), movement is often included in form of dispersal affecting ecological and evolutionary processes (Norberg et al. 2012). However, movement in these models is mostly random and trait-based movement models as presented in **Chapter 3** that include movement speeds would enable more precise predictions on biodiversity changes following environmental alterations (e.g. habitat fragmentation).

Overall, this shows that movement speed has direct effects on movement parameters, patterns, and spatial networks as well as cascading effects on species interactions and communities, and finally biodiversity patterns. This clearly emphasizes the predictive power of movement speed not only for proximate but also for ultimate aspects of movement.

Study outline

While developing ideas for my thesis, I gained a major interest in synthesizing and analyzing the huge amount of available movement data. To be able to identify and extract the relevant information from the millions of movement tracks, knowledge on species-specific movement properties is crucial. Thus, before analyzing data on movement patterns, I needed to understand what drives them and how they differ from species to species. As shown before, speed is the primary movement parameter and, hence, understanding the allometric scaling of movement speed is essential for the analysis of large amounts of movement data. During my research, I came across two major issues: first, there is no good mechanistic model of how maximum speed scales with body mass, and, second, there is only little data available on the speed of invertebrates. Thus, I decided to tackle these issues in the chapters of my thesis. In addition, I address the implications of movement speed for movement modelling, species interactions, and community patterns.

In **Chapter 1**, I develop a mechanistic model showing that maximum speed follows a hump-shaped scaling relationship with body mass, implying that medium-sized animals are the fastest. This finding is based on two simple assumptions. First, animals reach their maximum speeds during comparatively short sprints, for which the body uses energy stored in the muscles and which is exhausted relatively quickly. Larger animals have more muscle tissue and can therefore theoretically reach higher speeds. Second, according to Newton's laws of motion, mass has to overcome inertia, and so larger animals cannot accelerate as quickly as smaller ones. By the time large animals get up to full speed while sprinting, their rapidly available energy reserves also soon run out, reducing their realized maximum speed. Taken together, this leads to the well-known pattern that maximum speed increases from small to medium-sized animals and then decreases to the largest again. I tested this model by an empirical database containing 474 species ranging from 30 mg (a mite) to 100 tons (the blue whale) in body mass and found that it predicts maximum speeds across ecosystems and movement modes with almost 90% accuracy. This database also included maximum

speeds of 53 invertebrate species. In contrast, data on the normal (exploratory) speed of invertebrates are much sparser. Therefore, we tracked the exploratory speed of 62 invertebrate species across different taxonomic groups and feeding types in the laboratory using so-called automated image-based tracking.

In **Chapter 2,** I show that across all individuals, invertebrate exploratory speed scales with body mass following a power-law relationship with a scaling exponent of 0.19. Moreover, there is substantial variation in this scaling relationship between taxonomic groups and feeding types, which probably arises from differences in body shape and other functional traits related to locomotion. Information on exploratory speed is crucial for an overarching movement research as it drives key components of species interactions such as encounter and attack rates. Therefore, I think it is critical to give species traits a higher priority in movement modelling. The ecological applicability of state-of-the-art movement models to natural movement patterns is limited as they usually ignore their difference in movement capacities and space use. So-called individual-based models already include decisions of animals in response to their aims and current situation in the landscape and are therefore more realistic. The problem is that these models are highly specific and cannot be generalized for modelling communities comprising species with substantial variation in traits.

In **Chapter 3,** I conceptualize ways to develop trait-based movement models by integrating allometric scaling relationships of movement speed. This generates movement trajectories within a realistic and species-specific spatial scale. The advantage of this approach is that it enables general predictions of species-interaction traits, meta-community structures, and biodiversity patterns. I show in two worked examples how applying allometric movement models (1) leads to correct predictions of predator-prey attack rates compared to non-allometric models, and (2) enables predictions of large-scale biodiversity patterns in fragmented landscapes. For predicting predator-prey attack rates, we applied a self-designed allometric movement model and a standard non-allometric movement model to simulate predator-prey pairs with body masses ranging from 0.1 - 500 mg, and a predator-prey body-mass ratio of 100 characterizing typical natural invertebrate communities. We then compared our simulated attack rates to published empirical data on attack rates of terrestrial invertebrates. The results confirmed our assumption that only the

allometric movement model generates the realistic pattern of an increase in attack rate with body mass compared to the flat relationship produced by the non-allometric model. In the second example, we apply allometric random walks to predict maximum patch-bridging distances of species of different body masses. This generates species-specific network connectivities of spatial networks and enables predictions of the consequences of ongoing fragmentation. Over a larger body mass scale, the network connectivity increases with body mass following a hump-shaped relationship and with higher fragmentation (i.e. larger distances between patches), the increase of this curve is shifted towards higher body masses, implying that species of the same body mass have a lower connectivity in more fragmented landscapes. By combining this information with ecological network analyses, we can even predict how strongly biodiversity declines in altered landscapes. In a simple scenario, we randomly knock out patches from a fictional landscape matrix and show how to infer trait-based extinction probabilities of species of different body mass depending on the number of habitat patches they still connect in the network as well as their population density. This approach suggests that the largest species may have the highest extinction risk because of their low abundance and the low connectivity of their spatial networks. Hence, I show how allometric movement models can be used to simulate how species connect patch networks depending on their traits and how these networks change with ongoing fragmentation in terms of important biodiversity variables, such as species number and body-mass distribution. In this research project, I was particularly surprised by how well we were able to predict the empirical allometric scaling relationship of predator-prey attack rates by applying an allometric movement model, which includes speed as the most important movement parameter. Even the scaling exponent fits perfectly with 0.29 as a result of our modelling compared to 0.3 of the empirical data. This clearly emphasizes the importance of movement speed for predator-prey interactions and it made me think about the consequences of the hump-shaped scaling of maximum speed with body mass (**Chapter 1**) for these interactions.

Thus, in **Chapter 4,** I explore the role of maximum speed as a general determinant in predator-prey interactions. Traditionally, the prey range that can be exploited by a predator was defined on a single body-mass axis: the prey has to be large enough to meet the energetic demands of the predator ("energetic limit") but small enough to be effectively subjugated

("subdue limit"). I add a second dimension to this *prey range* by incorporating the hump-shaped maximum-speed to body-mass scaling (**Chapter 1**), thereby creating a two-dimensional *prey space*. Moreover, I also take into account the predatory hunting strategy and thus consider effects of pursuit predation, group hunting, and ambushing. Thereby, I develop a concept of how body mass and movement speed should mutually determine the prey space of predators of different hunting strategies and test it by empirical data on predator-prey pairs. I found that the prey space of pursuit predators significantly differs from those of group hunters and ambushers. Pursuit predators only hunt prey that is smaller and slower, whereas group hunters focus on larger but mostly slower prey. Ambushers also focus on larger prey, which can be faster or slower than they are. Therefore, they occupy a similar niche as group hunters but are less restricted by the speed limit at the cost of other constraints such as lower search spaces. This indicates that group hunters and ambushers have evolved different strategies to avoid competition with pursuit predators. Moreover, I show that these different hunting strategies have specific energetic optima along the body-mass axis, which prevents the existence of small-bodied group hunters ("micro-lions") or mega-carnivores ("mega-cheetahs"). This clearly demonstrates the importance of advancing the concept of trophic niches from prey ranges to prey spaces by including maximum speed as a second dimension. Moreover, this novel approach will improve our predictive understanding of predator-prey interactions, food web structure, species extinctions, and ecosystem functions.

Overall, this thesis studies the mechanisms of movement ("what is behind it") and their relevance for natural movement patterns ("what we see"). Moreover, it demonstrates ways how to apply trait-based scaling relationships of movement parameters to make profound predictions on the consequences of movement for species interactions and community patterns ("what it tells us"), and thereby clearly fosters the synthesis and general analysis of big data.

Research Chapters

nature ecology & evolution
ARTICLES
DOI: 10.1038/s41559-017-0241-4

1

A general scaling law reveals why the largest animals are not the fastest

Myriam R. Hirt, Björn C. Rall, Walter Jetz & Ulrich Brose

Abstract

Speed is the fundamental constraint on animal movement, yet there is no general consensus on the determinants of maximum speed itself. Here, we provide a general scaling model of maximum speed with body mass, which holds across locomotion modes, ecosystem types and taxonomic groups. In contrast to traditional power-law scaling, we predict a hump-shaped relationship due to a finite acceleration time for animals, which explains why the largest animals are not the fastest. This model is strongly supported by extensive empirical data (474 species with body masses ranging from 3x10-8 to 108,400 kg) from terrestrial as well as aquatic ecosystems. Our approach unravels a fundamental constraint on the upper limit of animal movement, thus enabling a better understanding of realized movement patterns in nature and their multifold ecological consequences.

Introduction

Movement is one of the most fundamental processes of life. The individual survival of mobile organisms depends on their ability to reach resources and mating partners, escape predators, and switch between habitat patches or breeding and wintering grounds. By creating and sustaining individual home ranges (Jetz et al. 2004) and meta-communities (Bauer and Hoye 2014), movement also profoundly affects the ability of animals to cope with land-use and climate changes (Parmesan and Yohe 2003). Additionally, movement determines encounter rates and thus the strength of species interactions (Pawar et al. 2012), which is an important factor influencing ecosystem stability (Neutel et al. 2007). Accordingly, a generalized and predictive understanding of animal movement is crucial (Hussey et al. 2015, Kays et al. 2015).

A fundamental constraint on movement is maximum speed. The realized movement depends on ecological factors such as landscape structure, habitat quality, or sociality, but the range within which this realized movement occurs meets its upper limit at maximum movement speed. Similar to many physiological and ecological parameters, movement speed of animals is often thought to follow a power-law relationship with body mass (Peters 1986, Hedenström 2003, Bejan and Marden 2006). However, scientists have always struggled with the fact that in running animals the largest are not the fastest (Garland 1983, Iriarte-Díaz 2002, Clemente and Richards 2013, Fuentes 2016). In nature, the fastest animals such as cheetahs or marlins are of intermediate size indicating that a hump-shaped pattern may be more realistic. There have been numerous attempts to describe this phenomenon (Garland 1983, Van Damme and Vanhooydonck 2001, Iriarte-Díaz 2002, Clemente et al. 2009, Fuentes 2016). While biomechanical and morphological models were tailored to explain this within taxonomic groups (Van Damme and Vanhooydonck 2001, Clemente et al. 2012, Clemente and Richards 2013, Dick and Clemente 2017), a general mechanistic model predicting the large-scale pattern (over the full body-mass range) across all taxonomic groups and ecosystem types is still lacking. Here, we fill this void by a novel maximum-speed model based on the concept that animals are limited in their time for maximum acceleration due to restrictions on the quickly available energy. Consequently, acceleration time becomes the critical factor determining the maximum speed of animals.

In the following, we first develop the maximum-speed model (in equations that are illustrated in the conceptual Figure 1.1), test the model predictions employing a global database and eventually illustrate its applications to advance a more general understanding of animal movement.

Results

Model development

Consistent with prior models (Peters 1986, Bejan and Marden 2006), we start with a power-law scaling of theoretical maximum speed $v_{max(theor)}$ of animals with body mass M:

$$v_{\max(theor)} = aM^b \qquad (1)$$

During acceleration, the speed of an animal over time t saturates (Elliott et al. 1977, Huey and Hertz 1984, Alexander 2003) (Figure 1.1a, solid lines) approaching $v_{max(theor)}$ (Figure 1.1a, dotted lines):

$$v(t) = v_{\max(theor)} \, (1 - e^{-kt}) \quad (2)$$

The acceleration constant k describes how fast an animal reaches $v_{max(theor)}$. In analogy to Newton's second law, the acceleration k should scale relative to the ratio between maximum force, F, and body mass, M: $k \sim F/M$. Knowing that maximum muscle force is roughly proportional to body mass as: $F \sim M^d$, this yields a general power law scaling of k with body mass M:

$$k = c \, M^{d-1} \qquad (3)$$

with constants c and d. As the allometric exponent d of the muscle force falls within the range 0.75 to 0.94 (Garcia and da Silva 2004, Biewener 2005, Clemente and Richards 2013) the overall exponent (d-1) should be negative, implying that larger animals need more time to accelerate to the same speed than smaller ones (conceptual Figure 1.1a, color code exemplifies four animals of different size). Note that this general scaling relationship also allows for the special cases of a constant acceleration across species or a linear relationship

with body mass. While prolonged high speeds are related to the maximum aerobic metabolism, maximum burst speeds are linked to anaerobic capacity (Jones and Lindstedt 1993, Weyand and Bundle 2005). For maximum aerobic speed, so-called slow twitch fibers are needed, which are highly efficient at using oxygen for generating adenosine triphosphate (ATP) to fuel muscle contractions.

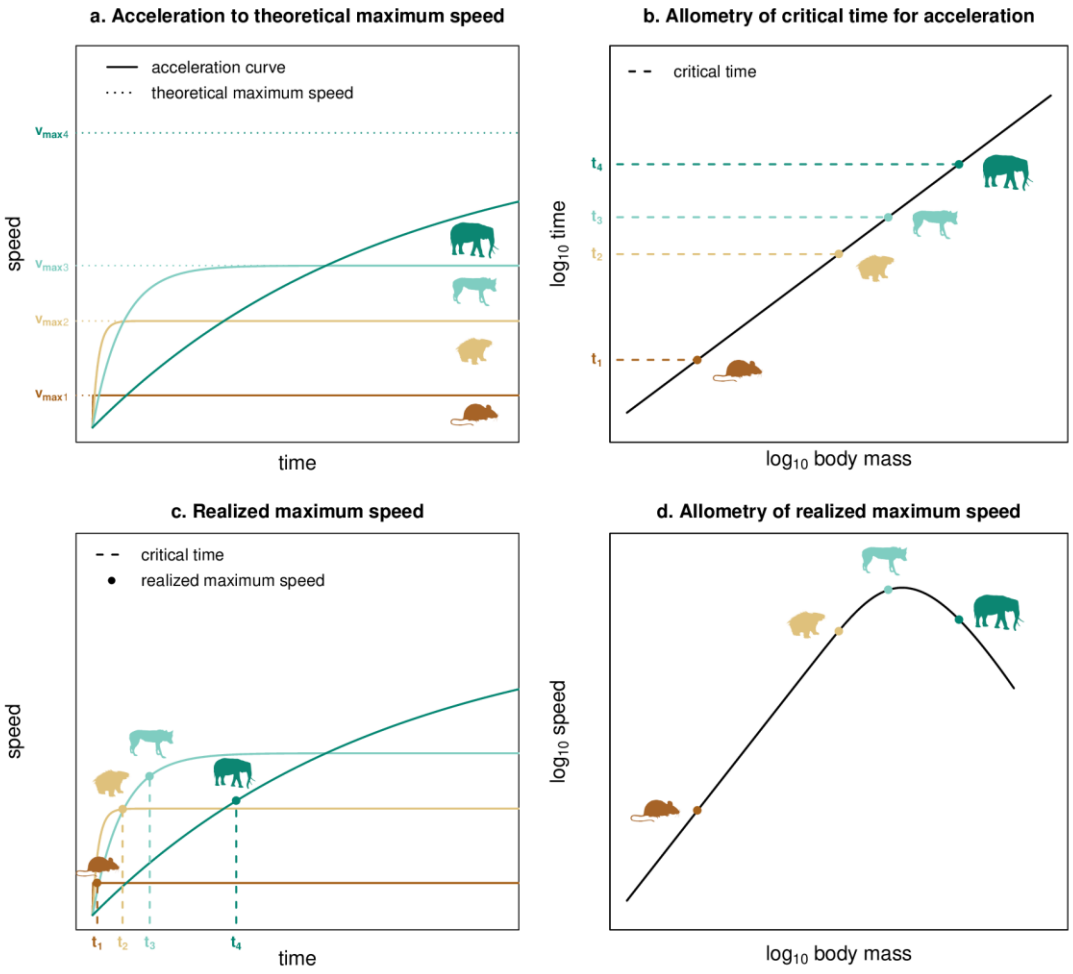

Figure 1.1 | Concept of time- and mass-dependent realized maximum speed of animals. (a) Acceleration of animals follows a saturation curve (solid lines) approaching the theoretical maximum speed (dotted lines) depending on body mass (color code). (b) The time available for acceleration increases with body mass following a power law. This critical time determines the realized maximum speed (c) yielding a hump-shaped increase of maximum speed with body mass (d).

Thus, they produce energy more slowly but for a long period of time before they fatigue and allow for continuous, extended muscle contractions. In contrast, maximum anaerobic speed is fueled by a special type of so-called fast twitch fibers, which use ATP from the ATP storage of the fiber until it is depleted. Thus, they produce energy more quickly but also fatigue very fast and only allow for short bursts of speed. As our maximum speed model is based on this maximum anaerobic capacity, the critical time available for maximum acceleration τ is limited by the amount of fast twitch fibers and their energy storage capacity. This storage capacity is correlated with the amount of muscle tissue mass, which is directly linked to body mass. Thus, similar to the muscle tissue mass, τ should follow a power law:

$$\tau = f\ M^{g} \quad (4),$$

where the allometric exponent g should fall in the range 0.76 to 1.27 documented for the allometric scaling of muscle tissue mass (Maloiy et al. 1979, Alexander et al. 1981, Pollock and Shadwick 1994, Bennett 1996). This power-law implies that larger animals should have more time for acceleration (dashed lines in conceptual Figure 1.1b and c). However, the power-law relationship of the critical time τ in our model allows for a negative or positive scaling of energy availability with body mass as well as the lack of a relationship (constant energy availability across body masses (f = 0)). While we included power-law relationships of k and τ (equations (3) and (4)) in our model, these scaling assumptions are not strictly necessary. Instead, our only critical assumptions are that acceleration over time follows a saturation curve (equation (1)) and that the time available for anaerobic acceleration is limited.

Within the critical time τ, after which the energy available for acceleration is depleted, the animal reaches its realized maximum speed v_{max} (points in Figure 1.1c), which may be lower than the theoretical maximum speed (Figure 1.1a, dotted lines). Combining equations (1) – (4) with $t = \tau$ yields $v_{max} = a\ M^{b}\ \left(1 - e^{-cfM^{d-1+g}}\right)$ which simplifies to

$$v_{max} = a\ M^{b} \quad \left(1 - e^{-\ hM^{i}}\right) \quad (5)$$

where $i = d - 1 + g$ and $h = cf$. This equation predicts a hump-shaped relationship between realized maximum speed and body mass (conceptual Figure 1.1d). The limiting term $1 - e^{-hM^i}$ represents the fraction of the theoretical maximum speed that is realized and is defined on the interval]0;1[. For low body masses, this term is close to 1 and the realized maximum speed approximates the theoretical maximum speed. With increasing body masses, this term decreases and reduces the realized maximum speed. Put simply, small to medium-sized animals accelerate quickly and have enough time to reach their theoretical maximum speed whereas large animals are limited in acceleration time and run out of readily mobilizable energy before being able to reach their theoretically possible maximum speed. Therefore, they have a lower realized maximum speed than predicted by a power-law scaling relationship.

Test of model predictions by empirical database

To test the model predictions (Figure 1.1d), we compiled literature data on maximum speeds of running, flying and swimming animals including not only mammals, fish and bird species but also reptiles, mollusks and arthropods. Body masses of these species range from $3x10^{-8}$ to 108,400 kg. Statistical comparison amongst multiple models (see Methods) shows that the time-dependent maximum speed model is the most adequate (see Supplementary Table 1.3). Our model (Figure 1.2, parameter values in Supplementary Table 1.4) shows that the initial power-law increase of speed with body mass is similar for running and flying animals (b = 0.26 and 0.24, respectively). However, flying animals are nearly six times faster than running ones (a = 143 and 26, respectively). For swimming animals, the power-law increase in speed is steeper (b = 0.36, Figure 1.2a). This is due to the fact that in contrast to air (in which both flying and running animals move), water is 800 times denser and 60 times more viscous (Dejours 1987). Small aquatic animals are slower than running animals of the same body size while larger species approach a similar speed as their running equivalents. This implies that in water, body size brings a greater benefit in gaining speed. The second exponent is lower for flying animals (i = -0.72) than for running (i = -0.6) and swimming ones (i = -0.56). Future research will need to disentangle the relative importance of anaerobic and musculoskeletal constraints on movement speed by measuring muscle force, muscle mass, body mass and maximum acceleration for the same species to narrow down

this large range of possible exponents. Furthermore, this may allow us to address the systematic differences in the exponent *i* between the locomotion modes as well as potential morphological side effects (e.g. quadrupedal vs. bipedal running or soaring vs. flapping flight).

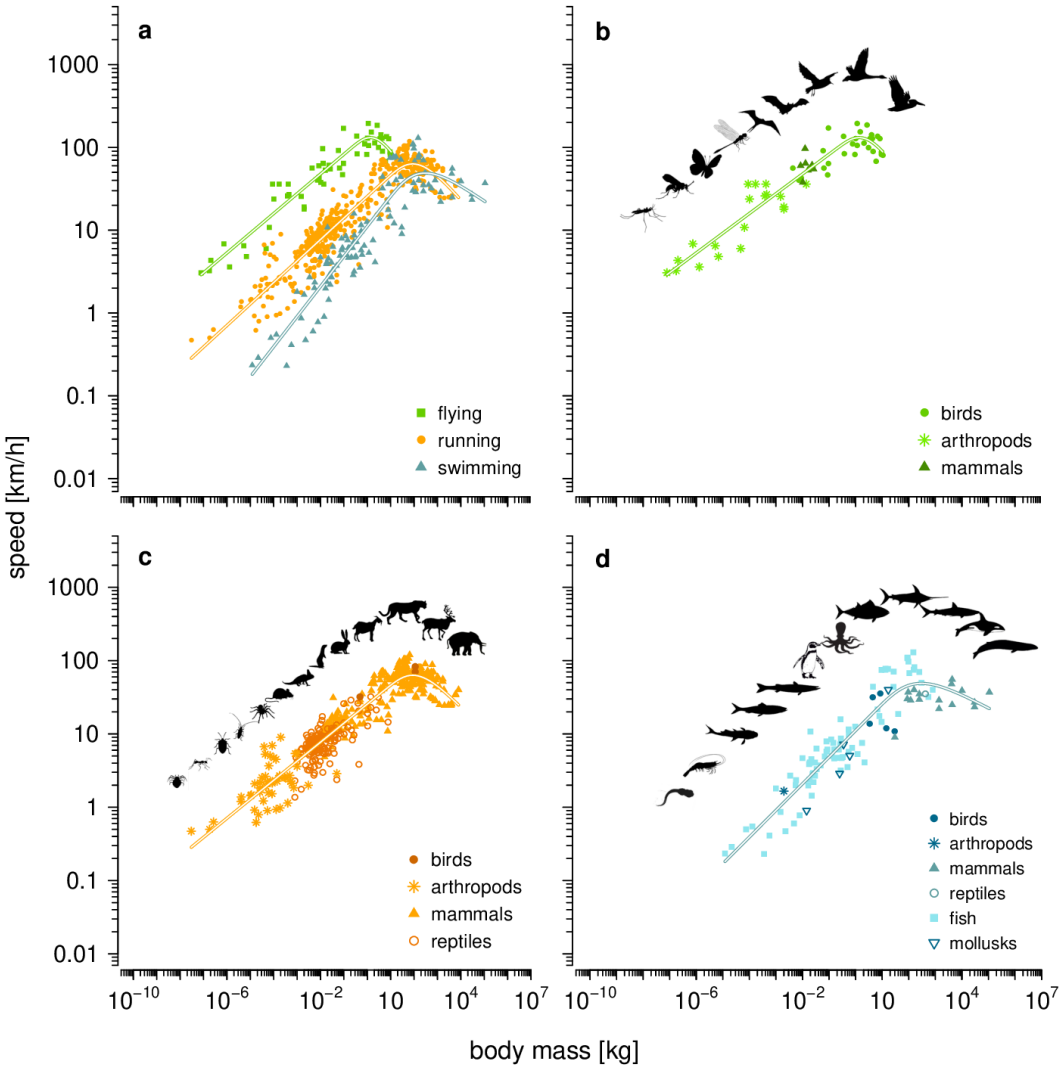

Figure 1.2 | Empirical data and time-dependent model fit on the allometric scaling of maximum speed. (**a**) Scaling for the different locomotion modes (flying, running, swimming) in comparison. Taxonomic differences are illustrated separately for (**b**) flying (n = 55), (**c**) running (n = 459) and (**d**) swimming (n = 109) animals. Overall model fit: $R^2 = 0.893$. The residual variation does not exhibit a signature of taxonomy (only a weak effect of thermoregulation, see Methods).

While the model provides strikingly strong fits with observations (R^2 = 0.893), some unexplained variation remains. This might partially be explained by the fact that our data probably include not only maximum *anaerobic* speeds but also some slightly slower maximum *aerobic* speeds. Moreover, we assessed the robustness of our model by exploring this residual variation with respect to taxonomy (arthropods, birds, fish, mammals, mollusks, and reptiles), primary diet (carnivore, herbivore, omnivore), thermoregulation (ectotherm, endotherm) and locomotion mode (flying, running, swimming). As taxonomy and thermoregulation are highly correlated, we made a first model without taxonomy and a second model without thermoregulation and compared them by their BIC values (see Methods for details). According to this, the model including thermoregulation instead of taxonomy is the most adequate (ΔBIC = 27.37). In this model, the differences between the diet types were not significant. In contrast, combinations of locomotion mode with thermoregulation exhibited significant differences (Figure 1.3). In flying and running animals, endotherms generally tend to be faster than ectotherms (Figure 1.3a and b). Metabolic constraints may enable endotherms to have higher activity levels compared to ectotherms at the low to intermediate temperatures most commonly encountered in nature (Gillooly et al. 2001). This pattern is reversed in aquatic systems where endotherms (mammals and penguins) are significantly slower than ectotherms (mainly fish, Figure 1.3c). We assume that this is due to the transition from a terrestrial to an aquatic lifestyle aquatic endotherms underwent. Semi-aquatic endotherms are adapted to movement in two different media, which reduces swimming efficiency in comparison to wholly marine mammals: they have $2.4x10^5$ times higher costs of transport (Williams 1999). But also in marine mammals, costs of transport are considerably higher than in fish of similar size because they have higher energy expenditures for maintaining their body temperature (Williams 1999). Thus, the effect of thermoregulation on the allometric scaling of maximum speed depends on the locomotion mode and the medium. Future research combining maximum speed and ambient temperature data could provide a more detailed analysis of temperature effects on maximum speed. Overall, the significant effect of thermoregulation explained only ~ 4% of the residual variation suggesting that the vast majority of the variation in speed across locomotion modes, ecosystem types and taxonomic groups is well explained by our maximum speed model.

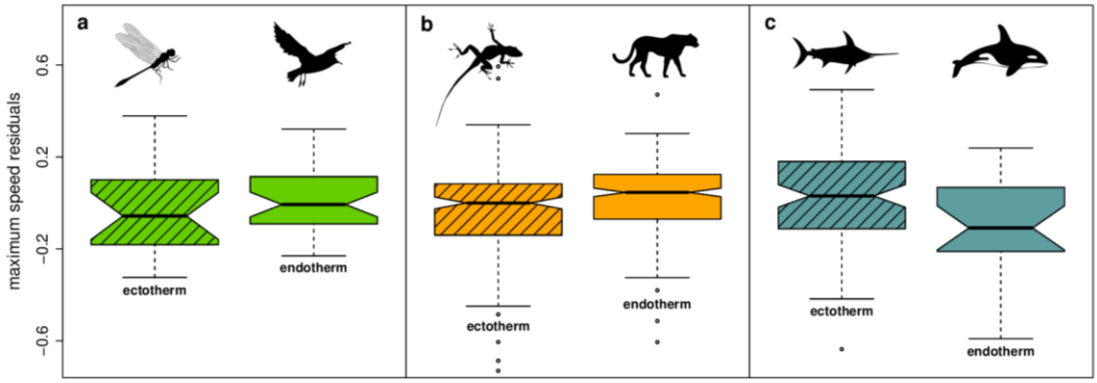

Figure 1.3 | Effect of thermoregulation on the maximum speed of animals (residuals of the relationship in Figure 1.2). In flying (**a**) and running (**b**) animals, endotherms are generally faster than ectotherms. In swimming animals (**c**) this effect is reversed with ectotherms being generally faster than endotherms. Box plots show medians (horizontal line), an approximation of 95% confidence intervals suitable for comparing two medians (notches), 25th and 75th percentiles (boxes), the most extreme values within 1.5 times the length of the box away from the box (whiskers), and outliers (dots).

Discussion

Our findings help solve one of the most challenging questions in movement ecology over the last decades: why are the largest animals not the fastest? Some studies have suggested a threshold beyond which animals run slower than predicted by a power-law relationship due to biomechanical constraints (Garland 1983), thus implying that speed scaling depends on body-mass range (Iriarte-Díaz 2002, Fuentes 2016). Others have invoked morphology, locomotion energetics and biomechanics (Garland 1983, Iriarte-Díaz 2002, Bejan and Marden 2006, Clemente et al. 2009, 2012, Fuentes 2016, Dick and Clemente 2017) to suggest that the maximum speed of running animals is constrained by the ability of muscles and bones to withstand the stress of the locomotor force hitting the ground (Biewener 1982, Clemente et al. 2012, Dick and Clemente 2017). Size-related increases in locomotor stress may thus be mitigated by taxon-specific adaptations of bones, muscles and postures until eventually reaching limits where larger body sizes come at the cost of reduced speed (Dick and Clemente 2017). As these biomechanical concepts were lacking mechanistic predictions, the hump-shaped relationship between maximum speed and body mass has

often been characterized with polynomial functions including linear and quadratic terms. We have thus also used polynomials as the best available alternative to compare against our model predictions. While offering a flexible way to describe non-linear patterns, we find that polynomials do not predict the overall scaling relationship as accurately as our general time-dependent maximum speed model, which provides the single most general capture of patterns and processes across taxa and a larger body mass range. Our speed predictions are thereby only derived from two major species traits: body mass and locomotion mode, which explain almost 90% ($R^2 = 0.893$) of the variation in maximum speed. This general approach allows a species-level prediction of speed, which is crucial for understanding movement patterns, species interactions and animal space use.

However, our model not only allows prediction of the speed of extant but also that of extinct species. For example, paleontologists have long debated potential running speeds of large birds (Blanco and Jones 2005b) and dinosaurs (Thulborn 1982, Sellers and Manning 2007a) roaming past ecosystems. The benchmark of speed predictions is set by detailed morphological models (Thulborn 1982, Sellers and Manning 2007a). Interestingly, our maximum speed model yields similar predictions by only accounting for body mass and locomotion mode (almost 80% of the morphological speed predictions are within the confidence intervals of our model predictions, Table 1.1). For instance, in contrast to a power-law model, the morphological and the time-dependent model predict lower speeds of *Tyrannosaurus* compared to the much smaller *Velociraptor*.

Table 1.1 | Maximum-speed predictions for extant and extinct flightless birds, and bipedal and quadrupedal dinosaurs

Taxa	Body mass (kg)	Speed (km h^{-1})		
		Power law (95% CI)	Morphological models	Time-dependent model (95% CI)
Flightless birds				
Dromaius (extant)	27.2	40.92 (38.58–43.40)	47.88	57.62 (47.65–60.91)
Struthio (extant)	65.3	49.33 (46.27–52.59)	55.44	62.75 (46.71–66.03)
Patagornis (extinct)	45	45.56 (42.83–48.46)	50.40	61.34 (47.39–64.68)
Bipedal dinosaurs				
Velociraptor	20	38.32 (36.19–40.58)	38.88	54.56 (46.89–57.82)
Allosaurus	1,400	94.87 (87.09–103.34)	33.84	40.78 (28.93–44.83)
Tyrannosaurus	6,000	129.41 (117.47–142.57)	28.8	27.05 (17.84–31.52)
Quadrupedal dinosaurs				
Triceratops	8,478	139.32 (126.11–153.91)	26.4	24.36 (15.70–28.83)
Apatosaurus	27,869	179.59 (161.01–200.31)	12.3	16.75 (9.77–21.09)
Brachiosaurus	78,258	223.85 (199.00–251.80)	17.6	11.99 (6.39–16.04)

Model predictions of a simple power law, morphological models and our time-dependent maximum-speed model are compared (references in Supplementary Table 5). Confidence intervals (95% CI) are given for the power law and time-dependent model.

This is consistent with theories claiming that *Tyrannosaurus* was very likely a slow runner (Hutchinson and Garcia 2002). A simple power-law model only yields reasonable results for lower body masses (e.g. flightless birds) while predictions for large species such as giant quadrupedal dinosaurs are unrealistically high. In contrast, our time-dependent model makes adequate predictions for small as well as large species including extinct dinosaurs (Figure 1.4, green triangles). Note that the highly accurate prediction of the dinosaur speeds is achieved without free parameters as the model parameters are only obtained by fits to data of extant species (Figure 1.2 and Figure 1.4 grey points).

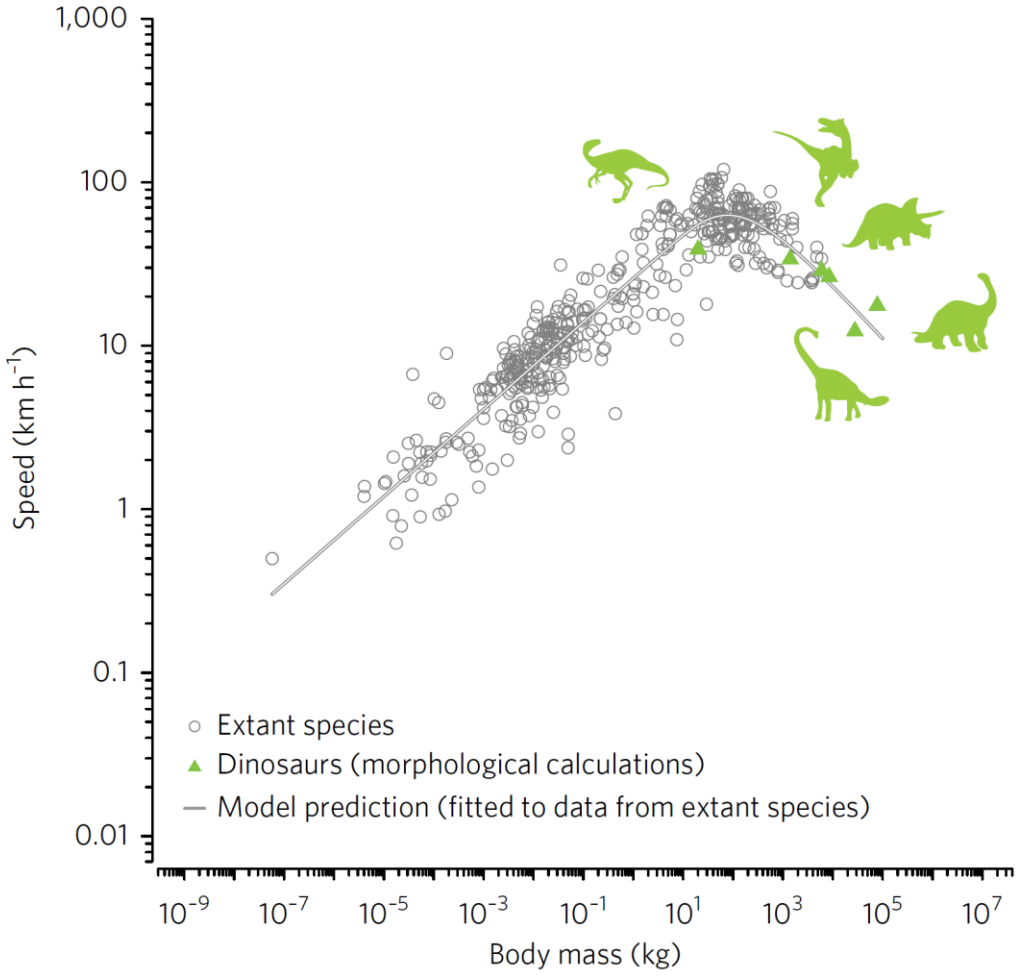

Figure 1.4 | Predicting the maximum speed of extinct species by the time-dependent model. The model prediction (grey line) is just fitted to data of extent species (grey circles) and extended to higher body masses. Speed data for dinosaurs (green circles) come from detailed morphological model calculations (values in Table 1) and were not used to obtain model parameters.

Our model also allows drawing inferences about evolutionary and ecological processes by analyzing the deviations of empirically measured speeds from the model predictions. Higher maximum speeds than predicted indicate evolutionary pressure on optimizing speed capacities that could for instance arise from co-evolution of pursuit predators and their prey.

As many physiological and ecological processes such as metabolism, growth and feeding rates depend on ambient (ectotherms) or body (endotherms) temperature (Brown et al. 2004, Rall et al. 2012), it is not surprising that some variables of movement speed and acceleration also increase with temperature (Dell et al. 2011). In our model, such a temperature dependence could be included as a Boltzmann factor in the constant a (equ. 5). Sufficient ambient temperature measurements at the point in time and space of the animals' maximum speed are currently lacking, but our model offers a framework to formally include temperature effects in future work.

In ecological research, our maximum-speed model provides a mechanistic understanding of the upper limit to animal movement patterns during migration, dispersal or bridging habitat patches. The travelling speed characterizing these movements is the fraction of maximum speed that can be maintained over longer periods of time. It would be interesting to analyze how travel speed scales with body mass on the large body-mass scale and if it also follows a hump-shaped pattern. If so, animals would use an approximately fixed percentage of their maximum speed during travel. If, however, travel speed follows a power-law relationship with body mass, large and small animals would use a higher proportion of their maximum speed during travel than intermediately sized animals. This would also affect different measurements of animal space use as well as migration and dispersal distances. While home ranges (Jetz et al. 2004, Tamburello et al. 2015) and day range s(Carbone et al. 2005) of animals have been shown to follow power-law relationships with body mass, migration distances of flying animals for example follow a curvilinear relationship with body mass (Hein et al. 2012). Our new results call for mechanistic analyses of how the hump-shaped scaling pattern of maximum speed could potentially affect other movement parameters.

The integration of our model as a species-specific scale ("what is physiologically possible") with research on how this fraction is modified by species traits and

environmental parameter such as landscape structure, resource availability and temperature ("what is ecologically realized in nature") can help provide a mechanistic understanding unifying physiological and ecological constraints on animal movement. In addition to generalizing our understanding across species traits and current landscape characteristics, this integrated approach will facilitate the prediction of how species-specific movement and subsequently home ranges and meta-communities may respond to the ongoing landscape fragmentation and environmental change. Thus, our approach may act as a simple and powerful tool for predicting the natural boundaries of animal movement and help gain a more unified understanding of the currently assessed movement data across taxa and ecosystems (Hussey et al. 2015, Kays et al. 2015).

Acknowledgements

M.R.H, W.J., B.C.R., and U.B. gratefully acknowledge the support of the German Centre for integrative Biodiversity Research (iDiv) Halle-Jena-Leipzig funded by the German Research Foundation (FZT 118).

Author Contributions

M.R.H. and U.B. developed the model. M.R.H. gathered the data. M.R.H. and B.C.R. carried out statistical analyses. W.J. was involved in study concept and data analyses. M.R.H. and U.B. wrote the paper. All authors discussed the results and commented on the manuscript.

Ecology, 98(11), 2017, pp. 2751–2757

2

The little things that run: a general scaling of invertebrate exploratory speed with body mass

Myriam R. Hirt, Tobias Lauermann, Ulrich Brose, Lucas P.J.J. Noldus & Anthony I. Dell

Abstract

Speed is a key trait of animal movement, and while much is already known about vertebrate speed and how it scales with body mass, studies on invertebrates are sparse, especially across diverse taxonomic groups. Here, we used automated image-based tracking to characterize the exploratory (voluntary) speed of 173 invertebrates comprising 57 species across 6 taxonomic groups (Arachnida, Chilopoda, Diplopoda, Entognatha, Insecta, Malacostraca) and 4 feeding types (carnivore, detritivore, herbivore, omnivore). Across all individuals, exploratory speed scaled with body mass following a power-law relationship with a scaling exponent of 0.19 (±0.04 standard error) and an intercept of 14.33 (±1.2). These parameters varied substantially with taxonomic group and feeding type. For the first time, we provide general empirically-derived allometric scaling relationships of exploratory speed across broad taxonomic groups of invertebrates. As exploratory speed drives key components of species interactions – such as

encounter and attack rates, or competition – our study contributes to a deeper understanding of the role of individual movement in population and community level processes.

Key words: movement, body size, allometry, behavior, encounter rate, automated tracking, computer vision

Introduction

Relative to their high diversity, invertebrates are often underrepresented in ecology as they are more difficult to study than the much larger vertebrates. Nevertheless, they are "the little things that run the world" (Wilson 1987) not only by sheer abundance and diversity but also by contributing to key ecosystem structure, functions and services (Wilson 1987, Hochkirch 2016). Thus, information on invertebrate ecology is crucial in all ecological fields, including movement ecology. The metabolic rate of animals determines the overall average rates of energy requirements (comprising resource consumption, biomass production and reproduction; Brown et al. 2004, Savage et al. 2004). For mobile animals, the movement in time and space transforms these rates into interactions with their environment, such as finding resources or mating partners, escaping predators, reaching breeding/oviposition sites, or dispersing. Uncovering the factors that constrain animal movement is thus essential for a mechanistic understanding of how animals survive and reproduce in the real world, including species' interaction strengths (Pawar et al. 2012), spatial distributions (With et al. 1997, Fryxell et al. 2004) and meta-community structures (Davies et al. 2001, Massol et al. 2011). While these relationships have partially been identified for vertebrates (Peters 1986, Domenici 2001, Hedenström and Rosén 2001, Hirt et al. 2017a), additional research on invertebrate movement is needed (Kissling et al. 2014, Kalinkat et al. 2015).

The high diversity of invertebrates hinders systematic measurement of the movement of every species, but allometric scaling relationships can be used to generate general predictions based on individual body masses. Similar to many physiological and ecological parameters (Brown et al. 2004), movement speed has also often been shown to follow a power-law relationship with body mass (Peters 1986, Hedenström 2003, Bejan and Marden 2006). Most of these studies focused on vertebrates, especially mammals, reptiles and birds (Pennycuick 1997, Van Damme and Vanhooydonck 2001, Iriarte-Díaz 2002, Bejan and Marden 2006, Clemente et al. 2009)[16,17][16,17]. These studies comprise several types of speed, including movement where the animal is working at maximum or near maximum capacity (e.g. during attack or escape) and where movement is less strenuous (e.g. during habitat exploration, foraging, dispersal or migration). Theory derived from metabolic and

biomechanical first principles assumes that the metabolic power expended for movement ($\propto B_o m^{\beta}$, where B_o is a coefficient that depends upon taxon, metabolic state, and body temperature, and m^{β} represents body mass and its scaling exponent) equals the product of body speed (v) and force (F) applied by the locomotory appendage (leg, wing, tail, etc.) onto the environmental medium yielding $v \propto B_o m^{\beta}/F$. Since force is proportional to the cross-sectional area of body and appendage muscles, it scales with body mass as $F = F_0 M^{\beta_F}$ with β_F typically varying between 0.5 – 0.67 (Schmidt-Nielsen 1984, Peters 1986, Pawar et al. 2012). This results in

$$v = aM^b \quad (1)$$

where $a = B_o/F_o$ and $b = \beta - \beta_F$. Using the scaling of field to maximal metabolic rate (0.8–0.9; Pawar et al. 2012), v should scale with mass to an exponent between 0.13 ($\beta = 0.8$, $\beta_F = 0.67$) and 0.4 ($\beta = 0.9$, $\beta_F = 0.5$; Pawar et al. 2012). Most empirically derived (mostly vertebrate) scaling exponents fall within this range (Peters 1986, Van Damme and Vanhooydonck 2001, Bejan and Marden 2006, Clemente et al. 2009). The few empirical studies that include more than two invertebrate species either do not report allometric equations (Forsythe 1983) or focus on a single taxonomic group (e.g., ants, whose foraging speed scales with mass to an exponent between 0.14 and 0.32 with a central tendency around 0.25; Hurlbert et al. 2008). A general empirical analysis of the allometry of invertebrate speed across broad taxonomic and functional groups is still lacking.

A key contributor to this dearth of comparative empirical studies of invertebrates is probably the technical difficulty of measuring speed for small animals. Here, we used automated image-based tracking (Dell et al. 2014a) to analyze terrestrial invertebrate movement under laboratory conditions across diverse taxonomic groups and feeding types. Our measurements of exploratory speeds for 173 individuals from 57 species across 6 classes spanning 3 orders of magnitude in body mass yielded the largest and most diverse database on invertebrate movement compiled so far. Exploratory (voluntary) speed characterizes an animal exploring landscapes for food or shelter, and so is of key ecological importance. Based on theory and data we describe above, we hypothesized that exploratory speed should follow a general allometric scaling relationship with an exponent between 0.13 and 0.4. Exploratory speed is at least partially fueled by metabolism, and it constrains the

strength of consumer-resource energy flows. As the allometric scaling of both of these parameters differs across phylogenetic groups and feeding types of invertebrate species (Ehnes et al. 2011, Lang et al. 2017), we also tested for similar effects on the allometric scaling of exploratory speed.

Methods

Animal collection

All animals were manually collected in 2014 in deciduous forest litter layers near Göttingen, Lower Saxony, Germany (N 51,5546° E 9,9289°). Animals were housed individually in small plastic containers (with sediment and leaf litter from their habitat) in an environmental chamber at 15°C and ~60% relative humidity. Animals were kept for a maximum of 50 hours prior to experimental trials (see below), with the time spent in captivity prior to filming recorded as a co-variable for statistical analyses. We collected movement and weight data (precision scale with animal weighing mode) from 173 individuals comprising 57 species from 6 classes (Arachnida, Chilopoda, Malacostraca, Diplopoda, Arachnida, Entognatha), which we henceforth refer to as taxonomic groups (Appendix Table S1). These 57 species span 16 orders and 41 families, but replication within these lower taxonomic levels was insufficient for detailed analyses. Each animal was also classified into one of four feeding types: carnivores, detritivores (including microbivores and microbi-detritivores), herbivores and omnivores.

Experimental setup

Animals were filmed individually in the same walk-in environmental chamber in which they were stored after collection (see above), using a custom-designed experimental set-up that allows video recording of movement and behavior of a wide range of taxa (see Barnes et al. 2015 for more detail). Our setup (see Figure 1b in Barnes et al. 2015) used infrared backlighting to maximize contrast between the animal and its background. Light was provided by an infrared LED light panel (850 nm, Smart Vision Lights, Muskegon, MI, USA). Circular glass arenas with three different diameters (543 mm, 293 mm, and 80 mm)

were used depending on the size of the animal (larger animals were filmed in larger arenas). Arena size was used as a co-variable in statistical analyses. The sides of the filming arena were lined with a random grey-scale checkerboard pattern, providing a non-uniform background devoid of directional bias. The top of the filming chamber was made of white cloth, above which four LED bulbs (LifeLite daylight mirror lamp, 5 W at 9.2 V and 0.54 A) were placed to imitate natural twilight in the filming chamber. A CCD camera (Prosilica GX1920) with a 25 mm lens (Fujinon) and an infrared pass filter (850 nm, Midwest Optical) were positioned through a hole in the middle of the cloth. Prior to filming, all animals spent 30 minutes in a small acclimatization chamber within the filming chamber, open only to infrared light from below. Once the acclimation chamber was removed, filming started as soon as the animal moved with a speed of > 1.5 mm/s and continued for a total of 60 minutes. StreamPix (Norpix, Montréal, Canada) was used to record the videos at 15 frames per second and 1936 x 1456 spatial resolution.

Automated tracking

EthoVision 10.1 (Noldus Information Technology, Wageningen, The Netherlands) was used to identify the position (mid-point of the body) of the animal in each video frame. Each frame was individually time-stamped, permitting calculation of body speed. Random variations in brightness or color information (noise) can lead to tracking errors, although EthoVision produced accurate tracks as long as animals were moving. To exclude artificial changes in position and orientation that were registered even when animals were stationary, we defined a true bout of movement to begin when speeds were higher than 0.6 mm/s and to end when speeds were lower than 0.3 mm/s (these thresholds were defined based on pre-experiments with non-moving animals). Every frame that was outside such a period of movement was excluded from the analyses.

Statistical analyses

We excluded 12 tracks in which the animals spent less than 30% of the filming time moving as it is difficult to calculate accurate means of exploratory speed over short periods of movement. For each of the remaining 173 trajectories, we calculated the average speed of

each individual during periods of movement (see above). Subsequently, we used linear models to test for effects of log-10 body mass [g] on log-10 mean exploratory speed [mm/s]. As the body masses were weighed with a precision scale with animal weighing mode, the error was assumed to be marginal, and we used model-1 regressions (Warton et al. 2006). Based on a-priori model choice, we tested for three relationships: (1) the simple allometric speed model without cofactors (speed ~ mass), (2) the taxonomic-allometric speed model (speed ~ mass * taxonomy) with taxonomic group (Arachnida, Chilopoda, Diplopoda, Entognatha, Insecta and Malacostraca) as fixed co-factor and (3) the trophic-allometric speed model (speed ~ mass * feeding type) with feeding type (carnivore, detritivore, herbivore and omnivore) as fixed co-factor. While more complex models with full or partial interactions between these factors are statistically feasible, we refrained from including them in our study as (1) we were lacking explicit hypotheses on their interactions, and (2) many combinations of these factors are not realized in nature (e.g., all Arachnida are carnivores and all Diplopoda are detritivores). Model comparison by AIC suggests that the trophic-allometric model was the most appropriate for predicting the speeds of invertebrates (AIC = 67.096, R^2 = 0.43), whereas the taxonomic-allometric model (AIC = 84.175, R^2 = 0.40) and the simple allometric model (AIC = 128.82, R^2 = 0.13) had lower explanatory power. Additional comparisons with more complex models showed that including either arena size or time spent in captivity as co-factors was unwarranted, thus we did not include these factors in the main analyses. All statistics were performed using R 3.2.3 (R Core Team 2015).

Results

We analyzed the exploratory speed of 173 invertebrates across 6 classes: Arachnida (number of individuals n_i = 52, number of species n_s = 16), Chilopoda (n_i = 12, n_s = 5), Diplopoda (n_i = 26, n_s = 10), Entognatha (n_i = 8, n_s = 5), Insecta (n_i = 55, n_s = 17), and Malacostraca (n_i = 20, n_s = 4) (Table S1). These groups are distributed across 4 feeding types - carnivores, detritivores, herbivores, and omnivores. Across our entire data set, body mass ranged over 3 orders of magnitude from 0.22 mg (*Mesentotoma dollfusi*, Entognatha) to 460 mg (Scarabaeidae indet., Insecta), and mean exploratory speed ranged over almost 2 orders of

magnitude from 0.64 mm/s (*Damaeus onustus*, Arachnida) to 56.6 mm/s (Carabidae indet., Insecta). On average, larger invertebrates moved significantly faster than smaller ones (Figure 2.1a), with exploratory speed (v) following a power-law relationship with body mass (M, equation 1) with a constant a = 14.33 and an exponent b = 0.19 ($p < 10^{-5}$, R^2 = 0.51; Figure 2.1a).

Despite finding a significant relationship between body mass and exploratory speed, substantial unexplained variation remains (Figure 2.1a). Taxonomy partly explains this variation as the mass-speed relationship is significantly affected by taxonomic group (interaction term taxonomic group x body mass: p = 0.01). Arachnida, Chilopoda and Malacostraca have exploratory speeds that are strongly influenced by body mass, with scaling exponents of 0.43 ($CI_{95\%}$ = 0.25-0.61), 0.53 ($CI_{95\%}$ = 0.22-0.83) and 0.47 ($CI_{95\%}$ = 0.33-0.61), respectively (Figure 2.1b, c, g). Moreover, Chilopoda are mostly faster than expected by the overall trend (colored compared to grey regression line, Figure 2.1c) while Malacostraca are on average slower (colored and grey line, Figure 2.1g). In contrast, the body mass dependence of exploratory speed is less strong for Diplopoda and Insecta, with slopes of 0.12 ($CI_{95\%}$ = -0.05-0.28) and 0.19 ($CI_{95\%}$ = 0.06-0.32), respectively (Figure 2.1d, f), and weakest for Entognatha (e.g. collembolans), with a scaling exponent of only 0.07 ($CI_{95\%}$ = -0.06-0.2, Figure 2.1e). However, Insecta are on average faster than the overall trend (colored and grey line, Figure 2.1f) while Diplopoda are generally slower (colored and grey line, Figure 2.1d). Based on 95% confidence intervals, only Malacostraca have a higher slope than Insecta, Entognatha and Diplopoda, and Entognatha a lower slope than Chilopoda and Arachnida.

We also found significant effects of feeding type on the allometric scaling relationship (interaction term with body mass: p = 0.005). The allometric scaling of exploratory speed is steepest for carnivores (b = 0.42, $CI_{95\%}$ = 0.32-0.53, Figure 2.2b), followed by omnivores (b = 0.18, $CI_{95\%}$ = -0.065-0.43, non-significant, Figure 2.2c) and then detritivores (b = 0.1, $CI_{95\%}$ = 0.015-0.19, Figure 2.2d). Surprisingly, herbivores show a negative but non-significant trend (b = -0.19, $CI_{95\%}$ = -0.5-0.12, Figure 2.2d).

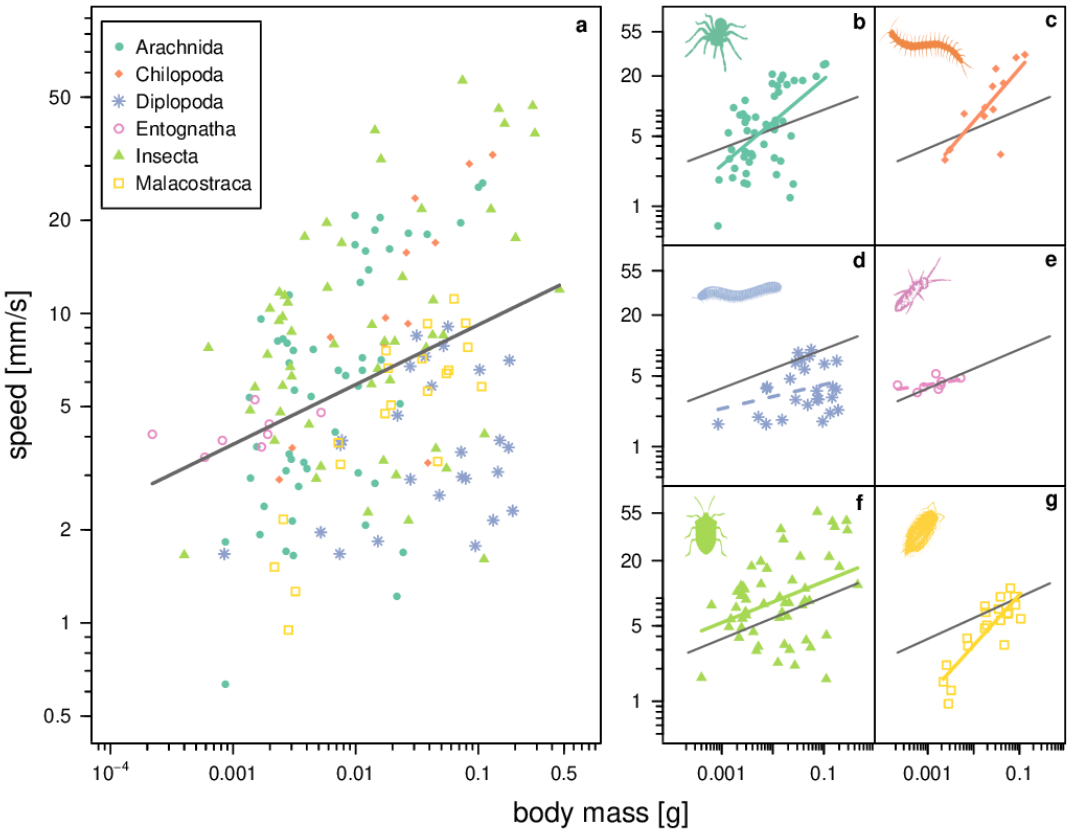

Figure 2.1| Scaling of speed with body mass across phylogenetic groups according to equation (1) for **a)** all species (a = 14.33 ± 1.2 standard error, b = 0.19 ± 0.04, $p < 10^{-5}$), **b)** Arachnida (a = 50.14, b = 0.43 ± 0.09, $p < 10^{-4}$), **c)** Chilopoda (a = 79.85, b = 0.53 ± 0.14, p = 0.003), **d)** Diplopoda (a = 5.40, b = 0.12 ± 0.08, p = 0.15), **e)** Entognatha (a = 6.60, b = 0.07 ± 0.05, p = 0.23), **f)** Insecta (a = 19.83, b = 0.19 ± 0.07, p = 0.005), and **g)** Malacostraca (a = 28.64, b = 0.47 ± 0.07, $p < 10^{-5}$). Note that intercepts a give speeds at body masses of 10^0 = 1 g. Grey line shows the simple allometric scaling relationship, colored lines show the group-specific scaling relationship of the taxonomic-allometric model. Dashed lines indicate non-significant regressions.

As tested by an ancova (speed ~ mass * carnivory, with carnivory separating species in carnivores and non-carnivores) and similar to the 95% confidence intervals, carnivores have a significantly higher slope than the other feeding types ($p < 10^{-6}$). Moreover, carnivores are mostly faster compared to the overall trend (colored and grey line, Figure 2.2b). In contrast, detritivores are on average slower than expected (grey and colored lines, Figure 2.2c).

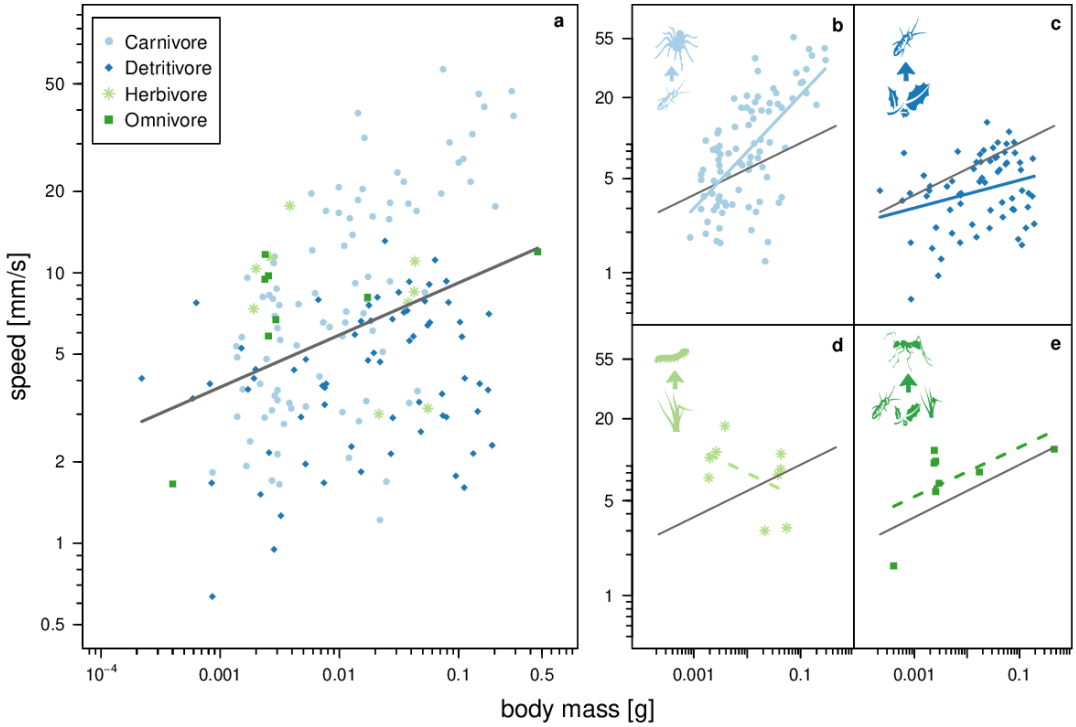

Figure 2.2 | Scaling of speed with body mass across feeding types according to equation (1) for a) all species ($a = 14.33 \pm 1.2$ standard error, $b = 0.19 \pm 0.04$, $p < 10^{-5}$), **b)** carnivores ($a = 55.20$, $b = 0.42 \pm 0.05$, $p < 10^{-11}$), **c)** detritivores ($a = 6.17$, $b = 0.10 \pm 0.04$, $p = 0.02$), **d)** herbivores ($a = 3.32$, $b = -0.19 \pm 0.13$, $p = 0.19$), and **e)** omnivores ($a = 18.75$, $b = 0.18 \pm 0.1$, $p = 0.12$). Note that intercepts a give speeds at body masses of $10^0 = 1$ g. Grey line shows the simple allometric scaling relationship, colored lines show the group-specific scaling relationship of the trophic-allometric model. Dashed lines indicate non-significant regressions.

Discussion

In contrast to vertebrates, little was previously known about general patterns in the allometry of speed in invertebrates, as the few studies that include more than one or two species are restricted to specific taxonomic groups (Forsythe 1983, Hurlbert et al. 2008). We contribute to filling this gap by providing the first general empirical estimates of the scaling of invertebrate exploratory speed with body mass across 173 individuals from 57 species and 6 taxonomic groups. We show that exploratory speeds of invertebrates follow a power law relationship with body mass with a scaling exponent of 0.19 (± 0.04), which is similar to prior estimates for 24 ant species (0.25, Hurlbert et al. 2008). These allometric exponents

of exploratory speed are much lower than those for resting metabolic rates of terrestrial invertebrates (0.69, Ehnes et al. 2011) or field and maximum metabolic rates of vertebrates (0.8-0.9, Pawar et al. 2012 and references therein). Although metabolism provides the fuel for biological activities, these differences among exponents support the assumptions of our theoretical derivations that body morphologies also limit movement capacities. Moreover, our empirical scaling exponent of speed (0.19) is on the lower end of the predicted range (0.13 to 0.4, see Introduction and Pawar et al. 2012), probably because we focused on exploratory speed where the animal is not working at full capacity.

We found substantial variation between groups in their scaling of body speed, which can arise from a number of sources affecting both the intercept and exponent. Most variation should be captured by the normalization factors, which account for the effects of taxon, metabolic state, body temperature, and locomotory type. Thus, difference in the scaling between taxonomic groups probably arises due to differences in body shape and other functional traits related to locomotion. Our results on group-specific scaling relationships facilitate future research on how different morphological characteristics across these groups and their allometric scaling limit invertebrate movement. As most ecological studies, our analyses are slightly biased by phylogenetic effects and the different number of individuals measured across the species groups. Future studies could include additional species groups such as mites, which would allow phylogenetically-controlled analyses of speed, morphology and metabolism. Our study showed striking differences between the allometric scaling relationships of metabolism and speed across taxonomic groups, which indicates a need for more mechanistic research on constraints of invertebrate movement, integrating metabolic, morphological and other phylogenetic factors.

Exploratory speed is also an important component of encounter rates, with higher average speeds generally leading to higher encounter rates, and thus higher attack rates (Mittelbach 1981, Pawar et al. 2012, Polidori et al. 2013, Dell et al. 2014b) and stronger effects of competition (Lang et al. 2012, van Gils et al. 2015). Our allometric exponent of exploratory speed (0.19) is similar to that of terrestrial invertebrate attack rates (0.24, Rall et al. 2012), supporting prior assumptions that attack rates depend more strongly on movement capacities than on metabolic rates alone (Pawar et al. 2012, Rall et al. 2012), which have a much higher allometric exponent (see above). Although differences in the

length of foraging bouts across species also affect realized attack rates, the higher allometric exponent of metabolism compared to exploratory speed and attack rates suggest that with increasing body masses, species become increasingly limited by resource supply. This could explain the higher allometric exponent of carnivore exploratory speed (0.42, Figure 2.2b) in comparison to other feeding types (<0.18, Figure 2.2c-e), as carnivores often depend on attacking active resources. These differences across feeding types may thus represent different evolutionary selection pressures.

Comparison of the group-specific regression lines to the overall trend (colored and grey lines, Figure 2.2) revealed a slower than expected exploratory speed of detritivores (Diplopoda and Malacostraca) relative to the other feeding types. We anticipate three, mutually non-exclusive explanations for this finding. First, detritivores feed on a sessile resource (litter) and, hence, there is no evolutionary pressure on developing high speeds to capture prey, compared to predators that hunt active prey (e.g. spiders). Second, detritivores mainly move within litter and soil, which impedes high-speed movements. Third, the dominant detritivorous groups in our study (Diplopoda and Malacostraca) have evolved strong exoskeletons as defenses against predation, which reduces the need for high speed movements. As none of the three hypotheses alone can explain our finding, a combination of all three factors may be the most suitable explanation for the pattern that detritivores are systematically slower than the other feeding types.

Due to their vast diversity and abundance and important role in ecosystems, invertebrates are indeed "the little things that run the world" (Wilson 1987), yet we know so little about them that we are facing a "scientific insect crisis" (Hochkirch 2016). This crisis starts with characterizing the sheer number and species richness of invertebrates, through to information on their behavior, physiology or movement. In this vein, it is essential that we develop general scaling laws that incorporate the vast diversity of invertebrates. As this diversity inhibits a measurement of speed that is similarly representative as for vertebrates (Kissling et al. 2014, Kissling 2015), the scaling relationships we present here can be used to generally predict the speeds of invertebrates depending on their individual body mass, taxonomic group and feeding type. As exploratory speed should also be a good predictor of the distances that can be covered by animals, gaining a better understanding of invertebrate speed also contributes to

predictions of meta-population structure and network connectivity by providing information on the species-specific movement capacities linking habitat patches. Our study, therefore, represents an important step towards a wider understanding of the ecology of the most diverse group of animals on our planet and how they run the world.

Acknowledgements

M.R.H and U.B. are supported by the German Centre for integrative Biodiversity Research (iDiv) Halle-Jena-Leipzig funded by the German Research Foundation (FZT 118). We thank Lena Rohde and Kristy Udy for laboratory assistance and Alison Iles, Jordi Moya-Laraño and Carl Cloyed for comments.

Author Contributions

M.R.H. and T.L. contributed equally. A.I.D. designed the study. T.L. gathered the data. M.R.H. analyzed the data and wrote the manuscript. M.R.H. and U.B. carried out statistical analyses. All authors discussed the results and commented on the manuscript. * These authors contributed equally.

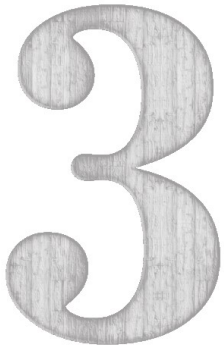

Bridging scales - allometric random walks link movement ecology and biodiversity research

Myriam R. Hirt, Volker Grimm, Yuanheng Li, Björn C. Rall,

Benjamin Rosenbaum & Ulrich Brose

Abstract

Integrating mechanistic models of movement and behavior into large-scale movement ecology and biodiversity research is one of the major challenges in current ecological science. This is mainly due to a large gap between the spatial scales at which these research lines act. Here, we propose to apply trait-based movement models to bridge this gap and generalize movement trajectories across species and ecosystems. We show how to use species traits (e.g. body mass) to generate allometric random walks and illustrate in two worked examples how this facilitates general predictions of species-interaction traits, meta-community structures and biodiversity patterns. Thereby, allometric random walks foster a closer integration of movement ecology and biodiversity research by scaling up from small-scale mechanistic measurements to a predictive understanding of movement and biodiversity patterns in different landscapes.

Key Words: body size, fragmentation, landscape ecology, meta-communities, food webs, dispersal

Movement ecology and biodiversity research: from small-scale mechanisms to large-scale patterns

At the landscape scale, movement has broad implications for virtually all patterns in biodiversity and species communities (Brose et al. 2004, Nathan et al. 2008, Jeltsch et al. 2013) (Figure 3.1). At this spatial scale, new technical advances in tracking have provided big data of unprecedented quality for analyses in vertebrate movement ecology (Kays et al. 2015). While this facilitates studies how movement trajectories and biodiversity patterns are related, it requires a complementary understanding of how the underlying physiological, behavioral and trophic processes drive these patterns and their correlations (Figure 3.1b). In addition, the heavy weight of active tracking tags prevents assessing large-scale movement patterns for most of the invertebrates that dominate natural communities in diversity and abundance (Kissling et al. 2014).

A mechanistic understanding of movement and behavioral processes and their correlations with species traits often takes place at a smaller spatial scale of laboratory or small-scale field experiments (Hirt et al. 2017b). This leaves a large gap between the measurement of movement parameters and landscape patterns in movement and their consequences for meta-communities, food webs, and biodiversity (Figure 3.1a). Here, we propose to bridge these scales by random-walk models that implement mechanistic movement processes to enable predictions of movement and biodiversity patterns at the scale of larger and more heterogeneous landscapes (Figure 3.1b). These models can be individual based to account for individual variation in movement and behavior or employ species averages. So far, their systematic development has been hampered by the need for parametrization for all species or even all individuals across species. We suggest to use the traits body mass and locomotion mode (running, flying, swimming) as predictors of movement capacities to achieve this parameterization of mechanistic walk models. We present a possible way of integrating such traits into random walk models to generate allometric random walks. Furthermore, we demonstrate in two worked examples how to use this approach to predict species-interaction strengths such as attack rates (worked example I) as well as meta-community structures and biodiversity patterns (worked example II, Figure 3.1b).

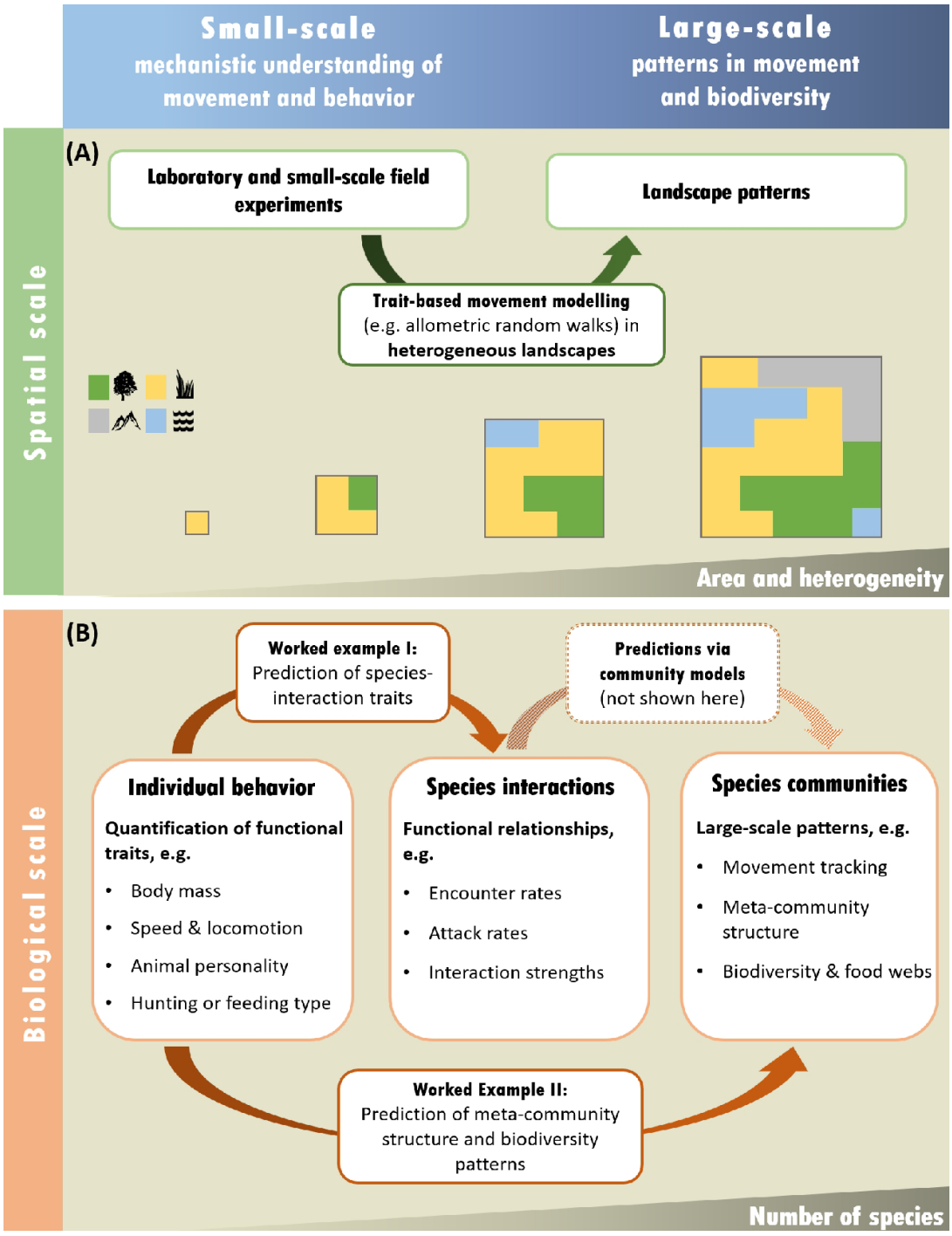

Figure 3.1 | The different scales of movement ecology and biodiversity research. (a) The spatial scale: a mechanistic understanding of movement and behavioral processes takes place at a laboratory or small-scale experimental scale while movement and biodiversity patterns are mainly described at larger scales of heterogeneous landscapes. This gap can be bridged by parameterizing movement models to obtain trait-based models such as allometric random walks, which are introduced in the course of this study. (b) The scale of biological organization: by integrating parameters of individual behavior (e.g. speed) into movement models, species-interaction traits such as attack rates and interaction strengths can be predicted (see worked example I) and possibly scaled up to larger areas

or heterogeneous landscapes to gain a mechanistic understanding of how landscape structures affect predator-prey interactions and consequently community persistence and diversity. Furthermore, parameterized movement models can be used to directly predict meta-community structures and assess the effects of habitat fragmentation and landscape heterogeneity on food webs and biodiversity patterns (see worked example II).

Ecological applicability of state-of-the-art movement models

Currently, there is a large gap between movement models and their ecological applicability to natural movement patterns of many species. Random walk models are conceptually simple and therefore widely used, but in their original form conceptualized animals as more or less featureless particles, whereas real animals have different traits, make adaptive decisions, and respond to landscape features. More recent random walk models have included various features of animal behavior (Codling et al. 2008), and individual-based movement models gain more ecological realism by combining these random walks with an animal's decisions in response to the landscape (Nathan et al. 2008, Jonsen et al. 2013). However, the data needed for developing such models are, despite rapid development in animal tracking technologies (Kays et al. 2015), still lacking and those that are available are species-specific, so that they cannot be generalized for modeling communities comprising species with substantial variation in traits and consequently movement patterns. Developing models for a general mechanistic understanding of animal movement across many species and the resulting biodiversity patterns at larger spatial scales thus requires a novel trait-based approach.

The allometric approach

The widespread ecological implications of body size (Peters 1986) and the Metabolic Theory of Ecology (West et al. 1997) have led to the insight that body size represents a "super trait" determining many other species traits including physiological rates such as metabolism, growth, reproduction (Brown et al. 2004, Savage et al. 2004), interaction strengths with co-existing species (Petchey et al. 2008, Rall et al. 2012), and also behavioral characteristics (Dial et al. 2008). Allometric relationships can thus use one single trait to characterize a species and its other relevant features and can be used to simplify parameterization of

community models that often contain too many parameters and species to allow their direct measurements for all species (Hudson and Reuman 2013). Consequently, recent community models have integrated allometric scaling relationships that predict parameters depending on the population-average body mass (Brose et al. 2006b, Schneider et al. 2016). In addition to providing realistic estimates of population parameters across species, this also avoided, by taking into account trade-offs between traits, the fallacy of unrealistic parameter combinations within species (e.g. species with low feeding rates but high biomass production or metabolic rates) that result from random parametrization (Brose 2010). These allometric approaches have helped tailor trait-based models with empirically testable predictions that hold across ecosystems (Petchey et al. 2008, Boit et al. 2012, Schneider et al. 2016). Despite their predictive success in communities of higher diversity, these population models come at the cost of ignoring (1) variability among the individuals within populations and (2) effects of movement in habitat space including consequences of different landscape structures.

Here, we present a new trait-based framework for movement modeling based on allometric scaling relationships, which helps to achieve a general parameterization across species or even individuals.

A new framework: trait-based movement models generalize across species

Just like physiological and morphological locomotor traits of animals (Biewener 1983, Iriarte-Díaz 2002), movement parameters such as speed (Hirt et al. 2017b, 2017a), migration or dispersal distances (Jenkins et al. 2007, Hein et al. 2012), and home range sizes (Jetz et al. 2004, Tamburello et al. 2015) follow allometric scaling relationships. However, environmental conditions such as resource availability or habitat quality may mask body mass effects, which has for example been shown for dispersal distances (Teitelbaum et al. 2015). Thus, what is realized by animals in nature may differ from the allometric predictions. Nevertheless, the range within which this realized movement occurs has its upper limit at the maximum physiological capacity, meaning that all movement has to be scaled relative to this maximum to allow ecologically meaningful interpretations. This

physiological capacity is defined by the maximum speed, which is the fundamental constraint of movement. Recent research has shown that animal maximum speed follows a hump-shaped relationship with body mass (Hirt et al. 2017a). As this pattern holds across taxa and locomotion modes (running, flying, swimming), it provides a powerful tool for understanding the physiological boundaries of animal movement and will therefore form the basis of our framework.

In classical random walk models, the speeds of each individual step are drawn from pre-defined probability distributions and step lengths are obtained by multiplying this speed by time. These probability distributions have either random parameters (Skellam 1991), or they are based on species-specific movement tracks (Kramer-Schadt et al. 2004). To obtain non-random distributions of step lengths that are general across species, we suggest including two new trait parameters: *body mass* and *locomotion mode*. Empirical allometric scaling relationships thereby quantify increases in speed with individual body masses for each locomotion mode. As maximum speed follows a hump-shaped relationship with body mass, intermediately sized animals have generally higher speeds and can therefore cover longer distances than smaller or larger ones. Moreover, *locomotion mode* accounts for differences in these allometric scaling relationships between running, swimming and flying organisms. This new framework provides real units of movement and therefore allows species-level predictions of movement trajectories.

Applying the framework

Creating allometric random walks by integrating trait-based steps

The advantage of this framework is the flexibility to integrate the trait-based speeds and step lengths into any desired movement model. Speeds can thereby either be calculated for each time period of a behavioral state separately by applying behavior-specific allometric scaling relationships (e.g. foraging, dispersal or migration speeds; *option 1*) or they can be calculated as proportions of the maximum speed (*option 2*). Here, we chose *option 2* to transform a simple random walk into an allometric random walk (aRW), because it is currently difficult to obtain precise allometric scaling relationships for speeds of different behavioral states, whereas data of high quality are available for maximum speed (Hirt et al.

2017a).As many aspects of speed including acceleration and locomotion costs are related to body size (Domenici 2001, Alexander 2005), we anticipate that the simplifying assumption of all speeds being fixed fractions of maximum speed (*option 2*) could be replaced by more detailed, empirically-established scaling relationships for the different speeds (*option 1*) as soon as they are available (see Hirt et al. 2017b or an example of invertebrate foraging speed). All speeds are scaled between 0 (resting) and 1 (maximum speed). Speed values are drawn from a two-parameter beta distribution as it is a continuous probability distribution that is defined on the interval [0, 1] (see Supplementary Material for details). To account for the various behaviors, we defined three different beta distributions from which speeds are drawn: one for low speeds such as foraging or exploratory movement (Figure 3.2a, dashed line), one for intermediate speeds of patch-bridging, dispersal, and migration (travelling speed, Figure 3.2a, solid line) and one for high speeds as they occur during attack or escape in predator-prey interactions (Figure 3.2a, dotted line). Subsequently, the unitless random values drawn from the different beta distributions are multiplied by v_{max}, the species-specific maximum speed, which is derived from the species' body mass and locomotion mode using empirical allometric scaling relationships (Figure 3.2b). For each species, the dimension of speed is thus scaled between zero and its body-mass dependent maximum speed. Within the same locomotion mode (here: running), intermediate body masses lead to higher speeds (here: foraging speeds) and therefore medium-sized animals have larger step lengths and cover more space in the same amount of time (Figure 3.2c, middle row) than smaller (Figure 3.2c, upper row) or larger animals (Figure 3.2c, lower row). In addition, the locomotion mode affects the spatial scale of movement tremendously with flying animals having higher speeds and covering much more space (Figure 3.2, lower row) than running (Figure 3.2d, middle row) or swimming animals (Figure 3.2, upper row) of the same body mass.

Thus, using allometric random walks provide real units of steps and therefore trait-based movement trajectories. In the following, we will demonstrate possible ways of applying these allometric random walks to predict (1) species-interaction strengths in a homogeneous landscape and (2) large-scale biodiversity patterns in a heterogeneous landscape (patch network). Furthermore, possibilities to include more complex aspects of landscape heterogeneity are discussed.

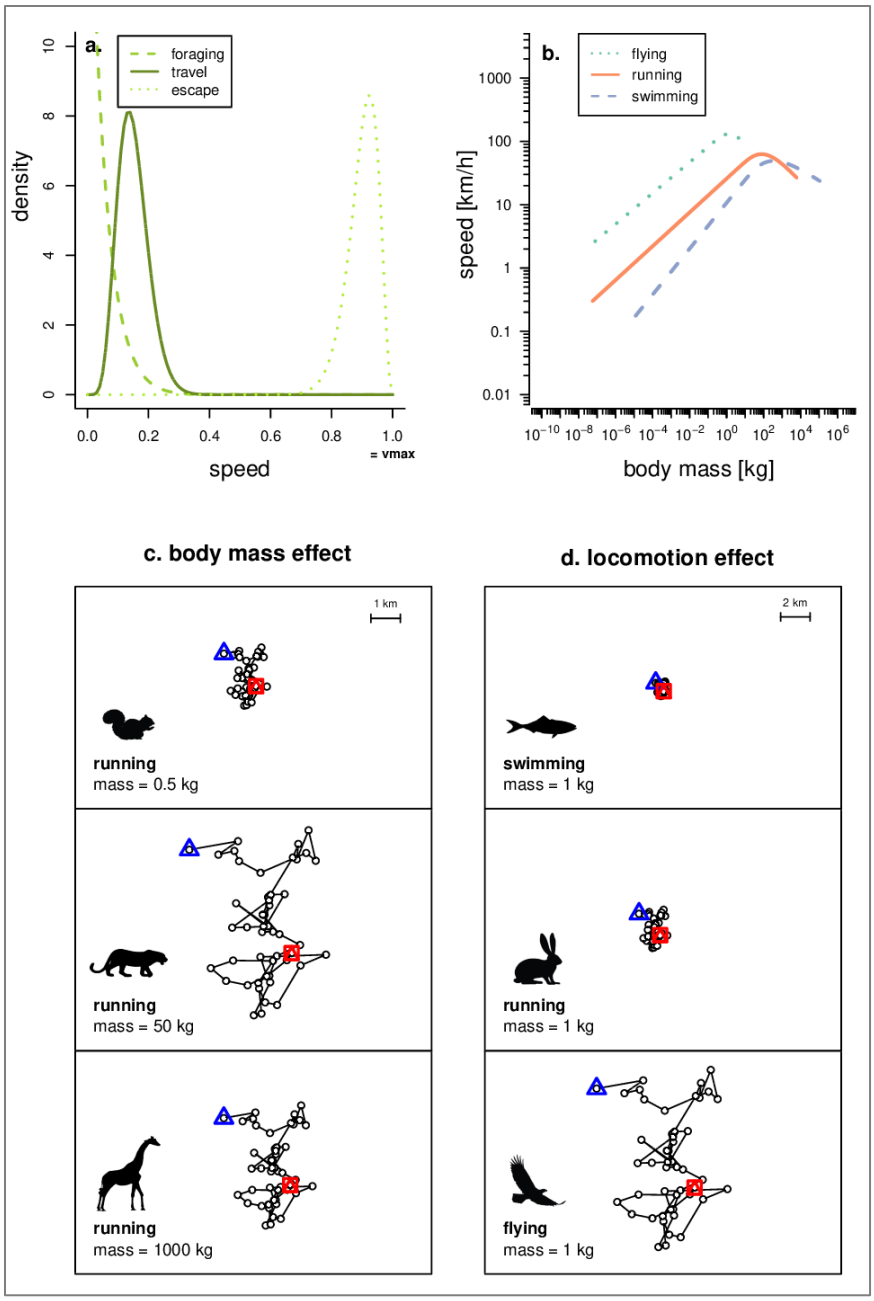

Figure 3.2 | Effects of body mass and locomotion mode on movement trajectories in an allometric random walk. (**a**) The three beta distributions from which speeds are drawn for different behaviors (see Supplementary Material for details). (**b**) Allometric scaling relation-ships of maximum speed (Hirt et al. 2017) for the different locomotion modes. (**c**) Effect of body mass on the movement trajectory of an allometric random walk with foraging speeds. (**d**) Effect of the locomotion mode on the movement trajectory of an allometric random walk with foraging speeds. Note that all triplets of trajectories were generated by using the same seed for random numbers and are projected on the same spatial landscape scale.

Worked example I: Predicting species-interaction traits

Allometric random walks help make realistic predictions of species-interaction parameters such as predator-prey attack rates, competition or pollination, which are mainly based on encounter rates. In the following, we will use the example of attack rates that depend on encounters between predator and prey individuals. As encounter rates depend on the length of the path per unit time that is searched and the predator detection range, higher average speeds of animals generally lead to longer paths and thus higher encounter rates as well as higher attack rates (Pawar et al. 2012, Polidori et al. 2013). Attack rates, in turn, affect interaction strengths and ultimately community attributes such as persistence and stability (May 1972, McCann et al. 1998, Gross et al. 2009) as indicators of local biodiversity. We demonstrate the ability of allometric random walks to predict species-interaction strengths by comparing attack rates generated by individual-based models (IBMs) using a standard (non-allometric) and an allometric random walk. Therefore, we use the model presented by Li et al. 2017 (Li et al. 2017) for a standard IBM and modified it following the above described approach to include allometric step lengths (allometric IBM). Both the standard and the allometric IBM include allometric scaling of other parameters such as detection range, maximum feeding capacity and gut clearance rate. The only difference between the two models is that the allometric IBM uses allometric random walks, whereas the standard IBM uses random step length. To be consistent with the empirical data for comparisons, we simulated 11 invertebrate predator-prey pairs in foraging mode with predator body masses ranging from 0.1 - 500 mg, and a predator-prey body-mass ratio of 100 characterizing typical natural invertebrate communities (Brose et al. 2006a, Kalinkat et al. 2013). Prey abundance was systematically varied, and we fitted functional responses to the data (see (Li et al. 2017) for details). We then analyzed the attack rate in relation to body mass and compared it to published empirical data on attack rates of terrestrial invertebrates (Rall et al. 2012, Li et al. 2017). The allometric IBM generates the realistic pattern of an increase in attack rate with body mass compared to the flat relationship produced by the standard IBM (Figure S1). The allometric scaling exponent of attack rates using the allometric IBM (0.29) predicts the empirical scaling exponent of attack rates of terrestrial invertebrates (0.3 (Li et al. 2017), restricted to empirical data for terrestrial 2D interactions) surprisingly well

considering the fact that no calibration was involved. The standard IBM only generates a marginal increase in attack rate with predator body mass (scaling exponent of 0.05), which is caused by allometric scaling of physiological parameters including that larger predators have larger gut sizes and therefore are able to feed longer compared to smaller predators (a property of the model by Li et al. (Li et al. 2017)). This effect, however, is partially counteracted by the higher prey body size of larger predators.

Overall, this worked example illustrates that IBMs with allometric random walks can accurately predict the strengths of species interactions such as attack rates at the small spatial scales of laboratory experiments. Very similar allometric approaches could be used to model other species interactions such as pollination and competition that also depend on encounter rates. Moreover, this allows scaling up to larger areas or even real landscapes and therefore enables mechanistic research on how landscape structures affect species interactions by changing encounter probabilities in different spatial compartments (e.g. patches, refuges or environmental gradients such as altitude). These simulations require accounting for how behavior and movement decisions of individuals respond to landscape structures. Eventually, incorporating these processes in model simulations will yield landscapes of interaction strengths, attack rates and fear, which would enable a better understanding as well as prediction of movement trajectories (Schmitz et al. 2004, Gallagher et al. 2017). Moreover, as these interaction strengths have knock-on effects on community persistence, this approach will also allow predicting variation in species diversity across landscape structures.

Worked example II: Predicting meta-community structure and biodiversity patterns

The connectivity of a spatial meta-community network (i.e. the percentage of realized dispersal links between pairs of habitat patches) is generally altered via changing the number of habitat patches (network configuration), which profoundly affects the persistence and dynamics of species within these meta-communities (Holland and Hastings 2008). However, the same spatial network configuration can host different species-specific network connectivities that depend on the species' movement abilities (Urban and Keitt

2001, Borthagaray et al. 2012). While prior studies have suggested species- and size-specific meta-community networks (Urban and Keitt 2001, Borthagaray et al. 2012), our approach of allometric random walks offers a novel tool to predict the links in these spatial networks based on mechanistic, trait-based processes. As movement speed strongly depends on body mass, the degree of connectivity of a network should also follow an allometric relationship with medium-sized animals covering longer distances (Jenkins et al. 2007), which leads to connections between more distant patches (Urban and Keitt 2001). Also, the locomotion mode (flying, running or swimming) should have an effect on the species-specific network connectivity with flying animals being able to connect more distant patches than running ones. Consequently, changes in the spatial network configuration will affect species differently. For instance, increasing the degree of fragmentation (leading to higher distances between patches), will have a stronger effect on small and running animals than on larger or flying animals.

We illustrate this concept of species-specific network connectivities in Figure 3.3 using a simplified example of our approach, which applies species-averages of all parameters and thus ignores variation across individuals for the sake of simplicity. Future studies, however, can easily realize this approach with individual-based models in which the parameters such as speed and feeding rates vary according to traits of individuals. In our simplified conceptual example, the dispersal links between the patches can be created by running allometric random walks (here simplified to the mean allometric travelling speeds of the species, Figure 2a) over the maximum travel time through unfavorable habitat. We assume that this maximum travel time should also be body-mass dependent with larger species having lower energetic costs while travelling (lower per unit biomass metabolic rates) and higher energy storage capacities in their body tissue (Peters 1986). Thus, larger animals should have more time available for patch-bridging events than smaller ones before they are exhausted or return to the original patch (Bonte et al. 2012). However, to get accurate quantitative predictions of this scaling relationship, detailed empirical analyses of animal movement between patches and the maximum travel time are needed. In our simplified allometric concept, travelling speeds times maximum travel time yield maximum patch-bridging distances that depend on the body mass of the species. In Figure 3.3, all patches with distances lower than these allometric patch-bridging distances are linked, which

creates species-specific network connectivities (Figure 3.3a) as well as the corresponding link networks (Figure 3.3b) and hypothetical link networks in case of a higher degree of fragmentation with several patches removed from the network (Figure 3.3c). The number of links in the network increases with body mass up to intermediate sizes (Figure 3.3a, b, c from left to right), but it decreases with increasing fragmentation (Figure 3.3b vs. c). Over a larger body mass scale, the network connectivity increases with body mass following a hump-shaped relationship (Figure 3.3d). The exact shape of this scaling relationship, however, depends on the interplay of the allometric scaling of maximum travel time and the hump-shaped scaling relationship of speed. A sensitivity analysis varying the exponents showed that the increase in connectivity with body mass from low to intermediate sizes is generally supported, but the effect at higher body masses strongly depends on the assumed scaling of maximum travel time. Hence, research on the allometric scaling of maximum travel time is urgently needed. With higher fragmentation (i.e. larger distances between patches), the increase of the curve is shifted towards higher body masses, implying that species of the same body mass have a lower connectivity in more fragmented landscapes (Figure 3.3d). This conceptual example is based on two simplifying assumptions. First, we assume that all species regardless of their individual body size use the same type of patches in the spatial network. However, small species might integrate different patches (e.g. also use smaller patches as habitats) in their spatial networks than large species. Hence, an integration of the allometric scaling of required patch size into allometric spatial networks represents an important future step towards realistic trait-based patch networks. Second, we assume that travel speed is a fixed proportion of maximum speed implying that it also follows a hump-shaped relationship with body mass. However, different realized scaling relationships of travel speed could alter the allometry of network connectivity shown in Figure 3.3. Overall, allometric random walks can be an important tool to quantitatively predict how species or individuals connect patch networks depending on their traits and how these networks change with ongoing fragmentation. This allows integrating trait-based movement, behavioral decisions, and responses to different landscape structures into predictions of species-specific patch networks.

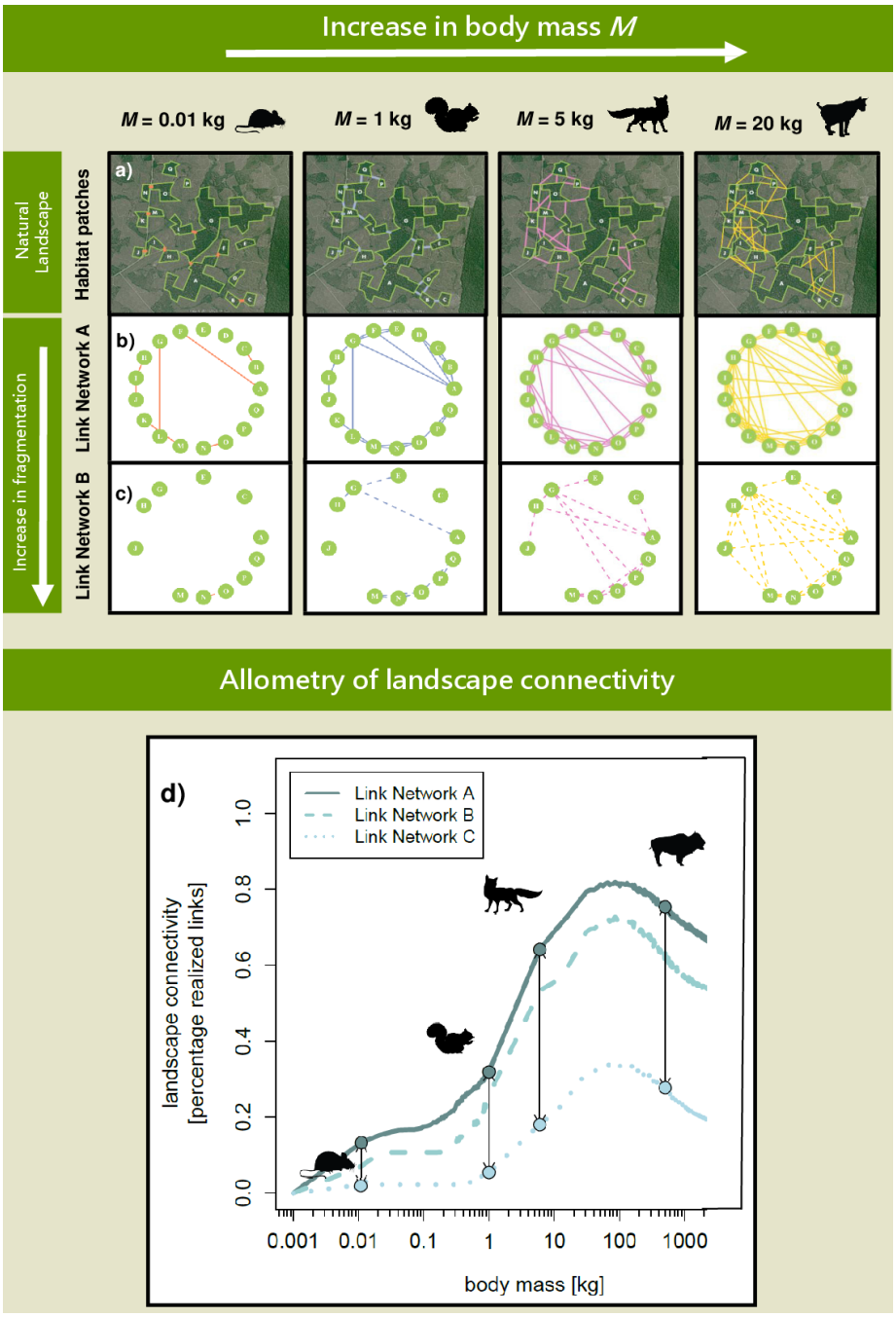

Figure 3.3 | Species-specific landscape connectivity over a fragmentation gradient. (a) An exemplary naturally fragmented landscape with different species-specific connectivities for four example animals of different body masses (low to intermediate). (b) Corresponding link network to the landscape connectivity in a. (c) Link network with a higher degree of fragmentation: patches B, D, F, I, K, and L have been removed from the network. (d) Landscape connectivity over a continuous body mass range (given as the percentage of realized links in the network). The degree of fragmentation increases from link network A to B to C. Link network A and B correspond to the networks in b and c. In the additional link network C, patches A, D, G, I, M, O and Q have been removed.

In the following, we describe a concept how the combination of species-specific patch networks with ecological networks analyses (here: secondary extinction analysis in food webs as an example) could be used for predictions of how strongly biodiversity declines in altered landscapes.

We start with an unfragmented landscape (Figure 3.4, landscape A) and its corresponding features such as biodiversity, body mass-distribution of coexisting species, and food web structure, which can be calculated from the body-mass distribution using feeding kernels for species (Schneider et al. 2016) or individuals as in worked example 1 (Li et al. 2017). In a hypothetical fragmentation scenario, patches are randomly knocked out from the landscape matrix. In this new, fragmented landscape (Figure 3.4, landscape B), the animals of body mass and locomotion mode as given by the body-mass distribution move according to allometric random walks. Based on the allometries of step lengths and travel times included in the random walk and the allometry of population abundances (Reuman et al. 2009), trait-based extinction probabilities can be calculated. Prior secondary extinction studies have employed a variety of different trait-based extinction probabilities (Dunne et al. 2002, Curtsdotter et al. 2011). Here, we chose a simple scenario to illustrate the interplay of one of these traditional scenarios, low abundance, with a spatial extinction scenario, in which animals face extinction depending on the number of habitat patches that are still connected in the network (based on species-averaged random walks as in Figure 3.3). In the simplified spatial extinction scenario, small and large animals will have lower connectivities and a higher probability of extinction in the new landscape than species of intermediate size (Figure 3.4, extinction scenario B_1). However, the higher population density would in turn decrease extinction probabilities of smaller species (Figure 5, extinction scenario B_2). This implies that the largest species have the highest extinction risk, because of their low abundance and the low connectivity of their spatial networks. The relative extinction risks of small species with high abundances and intermediately-sized species with highly connected spatial networks can vary substantially depending on the allometric scaling exponents of abundance (Reuman et al. 2009) and travel speeds.

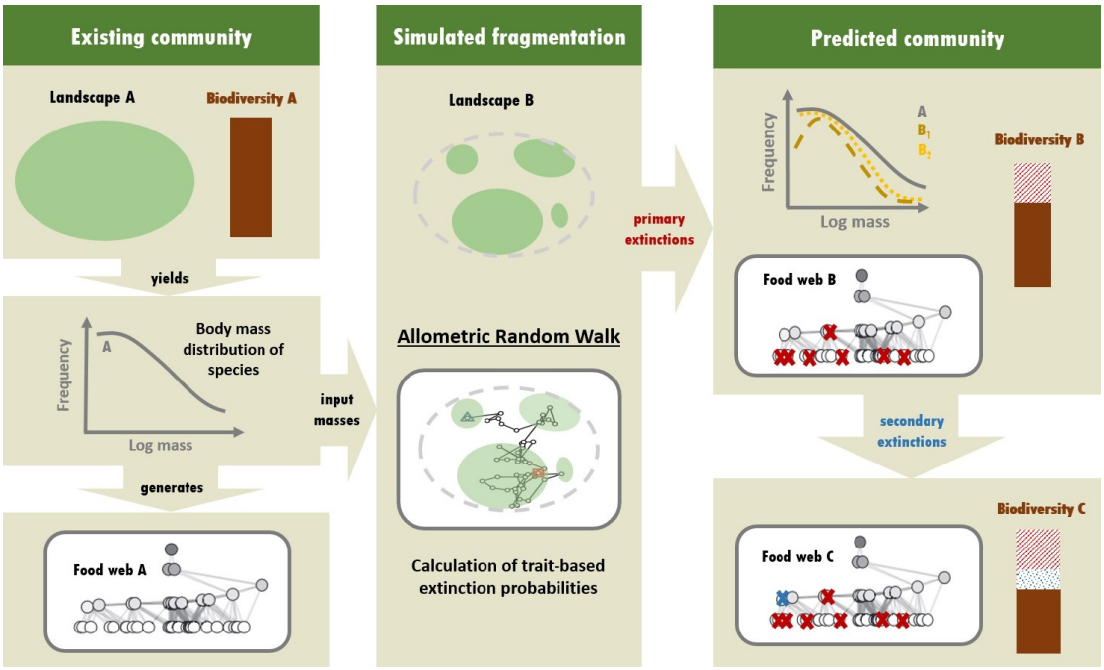

Figure 3.4 | Predicting biodiversity loss due to fragmentation in natural landscapes by applying allometric random walks. An existing community in landscape A with biodiversity A holds a certain body-mass distribution A of species. Using feeding kernels (Schneider et al. 2016), the corresponding food web (food web A) can be generated from this distribution. In a hypothetical fragmented landscape B, species-averaged allometric random walks (body masses are derived from the frequency distribution) allow calculating trait-dependent extinction probabilities in the new landscape. These primary extinctions yield a new community with a different body-mass distribution. B1 illustrates the spatial extinction scenario where intermediately sized animals have the highest connectivity potential and therefore lowest extinction risk; scenario B2 additionally includes abundances, with higher abundances reducing the extinction probability of small species. These new body-mass distributions then yield a new food web structure (food web B) and biodiversity (biodiversity B). Subsequent biodiversity loss can be predicted by simulating secondary extinctions in the food web (food web C and biodiversity C).

Moreover, extinction risks can also be affected by patch size and resource abundance. For instance, small animals might survive in only one patch of the network if it is large enough and the resource availability high enough. Scenarios that are more realistic could also include disturbances, and stochastic extinctions or long-distance dispersals. Ultimately, these features can help dovetail the model to the conditions of specific landscapes and communities.

Following the trait-based probabilities for primary extinctions, a new community with new body-mass distribution, food-web structure and lower biodiversity emerges (Figure

3.4, biodiversity and food web B). Simulations of secondary extinctions will generate a new food web and a community with even lower biodiversity (Figure 3.4, biodiversity and food web C). Together, this multi-step modeling approach (Figure 3.4) helps gain mechanistic insights in landscape-scale biodiversity patterns as well as predicted extinction scenarios following habitat fragmentation. Moreover, this concept can easily be transferred to other ecological networks such as plant-pollinator networks (Rezende et al. 2007).

Outlook & Conclusion

In this conceptual framework, we highlighted the importance of including trait-based step lengths in movement models to make more realistic predictions of movement and biodiversity patterns at the landscape scale. We focused on the basic principle of including body-mass and locomotion-mode dependent speeds in these models, a basis to which important extensions can be added (see Outstanding Questions). These include (1) other important functional and behavioral traits and (2) other aspects of landscape heterogeneity. First, functional traits affecting animal space use such as hunting modes (sit-and-wait vs. cursorial) (Miller et al. 2014) or feeding types (e.g. predator vs. herbivore) (Tamburello et al. 2015, Hirt et al. 2017b) as well as other behavioral facets such as animal personality (e.g. boldness) (Stamps and Groothuis 2010) could be added to this concept. Second, also abiotic conditions and landscape structures play an important role in shaping the space use of animals (Haskell et al. 2002). By supplying different distributions and qualities of resources or by providing refuge places, the landscape structure actively changes movement speeds, detection efficiencies, and ultimately the type and strengths of predator-prey interactions. Moreover, the spatial arrangement of the individual habitat domains (habitat space that predator and prey use while foraging) can alter predator-prey interactions and even shift the direction of predatory effects (Preisser et al. 2007, Schmitz 2007, Schmitz et al. 2017). Schmitz et al. 2017 (Schmitz et al. 2017) develop an elegant approach on how to calculate the overlap between these habitat domains by assessing individual predator and prey movement trajectories. Using allometric random walks could represent an easy way of producing multiple realistic species-specific predator-prey movement scenarios, in which the individuals exhibit behavioral responses to the abiotic (e.g. habitat structure) and biotic

(presence of prey or predators) characteristics of the landscape. This will help make general predictions on predator-prey interactions across landscapes of varying structure and heterogeneity. Moreover, large-scale effects on predator-prey interactions could be assessed on a landscape-complexity gradient. For instance, impacts of movement corridors, barriers, or hiding places on functional responses in simple agricultural vs. more structured landscapes could be identified and finally provide important information on the persistence of species communities. How these additional aspects of landscape heterogeneity (e.g. barriers, environmental gradients) affect the step length distributions of the allometric random walk needs to be explored in future studies, but it is likely that generic trait-based relationships can be devised (see Outstanding Questions). Eventually, all these processes do not only constrain the behavior and interactions between species but indirectly also link to biodiversity patterns of landscapes.

Bridging between the spatial scales of (1) movement and behavioral processes and (2) movement and biodiversity patterns requires the implementation of trait-based movement models, as we cannot determine all relevant movement parameters for all species. We present the new framework of allometric random walks and its potential to fill this gap by being empirically realistic yet general across species. On the one hand, they represent the movement of real species better than random walks with stochastic parameters. On the other hand, they can be generalized more easily across species and communities than walk models based on tedious measurements of species-specific movement parameters. Therefore, this novel approach will provide realistic yet also generalized predictions and critically important mechanistic understanding of large-scale movement and biodiversity patterns.

Acknowledgements

We gratefully acknowledge the support of the German Centre for Integrative Biodiversity Research (iDiv) Halle-Jena-Leipzig funded by the German Research Foundation (FZT 118 and FOR 1748). V.G. was supported by the German Research Foundation in the framework of the BioMove Research Training Group (DFG-GRK 2118/1).

Author Contributions

M.R.H and U.B. developed the overall concept. M.R.H. and B.R. implemented beta distributions in the concept. M.R.H. and V.G. merged the concept with individual-based modelling. Y.L and B.C.R. conducted simulations of worked example I. M.R.H. wrote the manuscript and all authors discussed the results and commented on the manuscript.

4

Rethinking trophic niches: speed and body mass co-limit prey space of mammalian predators

Myriam R. Hirt, Thomas Müller, Benjamin Rosenbaum, Marlee Tucker & Ulrich Brose

Abstract

Realized trophic niches of animals are often characterized by ranges in body-mass ratios between predators and their prey. Here, we extend this prey range to a two-dimensional prey space by incorporating a hump-shaped speed-body mass relation. Thus, prey spaces are not only bounded by an "energy limit", and a "subdue limit" towards small and large prey, respectively, but also by a "speed limit" towards fast prey. We tested predictions of this novel concept using data on body mass and maximum speed of terrestrial mammalian predator-prey pairs. Our results show that these prey spaces are strongly affected by predator hunting styles (i.e., pursuit, group, and ambushing predators) with the pursuit prey-space significantly differing from group and ambush prey-spaces. Pursuit predators only hunt prey that is smaller and slower, whereas group hunters focus on larger but mostly slower prey. Ambushers occupy a similar niche as group hunters but are less restricted by the speed limit at the cost of other constraints such as lower search areas. This indicates that group hunters and ambushers have evolved different strategies to occupy a similar trophic niche that avoids competition with pursuit predators. Moreover, our theory

reveals energetic optima of these hunting strategies along a body-mass axis and thereby provides mechanistic explanations for why there are no small group hunters (micro-lions) or mega-carnivores (mega-cheetahs). Advancing the concept of trophic niches from prey ranges to prey spaces by adding the new dimension of speed thus fosters a new and mechanistic understanding how animals live and interact, which will improve our predictive understanding of predator-prey interactions, food-web structure, species extinctions, and ecosystem functions.

Key Words: ambushing, body-mass ratio, food webs, group hunting, movement, mega-carnivores, predator-prey interactions, prey range, pursuit predation

Introduction

Pursuing and capturing prey is as vital to the predator as it is to the prey to avoid capture. Thus, animals have evolved a variety of morphological traits and behavioral strategies that either maximize capture success or minimize predation risk (Walker et al. 2005, Cortez 2011, Wilson et al. 2018). Predator avoidance strategies of prey have been intensely studied (Lima 1998) but less attention has been paid to the behavior of the predator (Lima 2002). More recent studies have focused on the interplay between predator and prey, and the determinants of predatory success in specific predator-prey pursuits, such as those between lion and zebra, or cheetah and impala (Wilson et al. 2015, 2018). Locomotor abilities such as speed and maneuverability are critical components in these interactions as well as body mass and hunting strategy (Caro 2005, Bailey et al. 2013, Bro-Jørgensen 2013, Wilson et al. 2018). While the determinants and success of specific predator-prey pursuits have thereby been analyzed explicitly, general determinants of predator-prey interactions and trophic niches are not well outlined. From the predator's perspective, this addresses the question: "which prey could possibly be captured and subdued?"

Traditionally, this question on trophic niches was answered by placing predator and prey on a single body-mass axis and setting lower and upper limits to the prey range predators can exploit (Brose 2010, Schneider et al. 2012). Minimum prey size is determined by the "energetic limit": the prey has to be large enough to meet the energy demands of the predator. This means that the energetic costs of hunting and attacking the prey should not exceed the energetic gain (Brose 2010). Maximum prey size is thereby determined by the "subdue limit": the prey has to be small enough to be successfully subdued by the predator (Radloff and Du Toit 2004). For typical terrestrial mammalian predators, these limits imply that prey body masses are between one and four orders of magnitude lower (Figure 4.1a, *typical predator-prey body mass structure,* Brose et al. 2006, Tucker and Rogers 2014). However, there are exceptions to this pattern where predator-prey body-mass ratios are inverted and predators are able to consume much larger prey (Figure 4.1a, *inverse predator-prey body mass structure*), such as lions (~ 200 kg) hunting African buffaloes (~ 650 kg). Lions are able to effectively subdue their larger prey because usually multiple group members are simultaneously attacking it.

Besides body-mass constraints, movement speed as well as acceleration, deceleration, and maneuverability play an important role during the hunting process (Wilson et al. 2018). Primarily, the predator needs to be fast enough to be able to catch its prey, which we refer to as the "speed limit". Under the assumption that maximum speed follows a power-law relationship with body mass (Peters 1986, Hedenström 2003, Bejan and Marden 2006), predators would generally not be able to catch prey that is much larger than they are, since it would always be faster. Therefore, the traditional concept of predator-prey body-mass ranges cannot provide satisfying answers for the questions of (1) how the smaller predators manage to successfully catch their prey if the body-mass structure of the interaction is inverse (Figure 4.1a), and (2) why there are no pursuit predators that are larger than mega-herbivores (e.g. mega-cheetahs). Therefore, a trophic niche concept that goes beyond simple predator-prey body-mass ranges is necessary for a mechanistic understanding of interactions for both typical and inverse body-mass structures (Figure 4.1a). Interestingly, recent research has shown that the maximum speed of animals follows a hump-shaped pattern with body mass (Hirt et al. 2017, Figure 4.1b), enabling medium-sized predators to catch larger and therefore slower prey. This pattern adds a new dimension of speed to predator-prey interactions and generates a two-dimensional "prey space" (across body-mass and speed dimensions, Figure 4.1c-e) instead of a one-dimensional "prey range" based on body mass. When analyzing this prey space, it is critically important to take into account differences in hunting strategies, as they might shift the limits in both dimensions (Bailey et al. 2013, Bro-Jørgensen 2013).

In this study, we analyze the prey space of terrestrial mammalian predators with respect to body mass and maximum speed and assess systematic differences in this prey space according to three different hunting strategies; pursuit predation, group hunting, and ambushing (Table 4.1). We hypothesize that body mass and maximum speed should interactively determine the prey space of predators depending on their hunting strategy. Pursuit predators should not be able to consume prey that is larger (subdue limit) or faster (speed limit) than they are (Figure 4.1c). Group hunters should have a high energetic limit, as prey needs to be shared between the group members. Therefore, they usually need to attack large prey to energetically sustain the whole group. This should be possible as the multiple agents involved in the attack enable them to subdue larger prey (higher subdue

limit) (Bertram 1979; Lamprecht 1981; Packer 1986). Importantly, the novel hump-shaped scaling model of maximum speed illustrates that they are also able to catch this larger (and therefore slower) prey (Figure 4.1d). Ambushers should be the most flexible in terms of these limits. By launching surprise attacks, they should be able to overwhelm larger and faster prey (Figure 4.1e). We test these hypotheses by compiling a new database comprising data on body masses and maximum speeds of predators and their prey. Moreover, we shed light on the question of why there is no evolutionary tendency towards mega-carnivores with a body mass that exceeds that of the mega-herbivores.

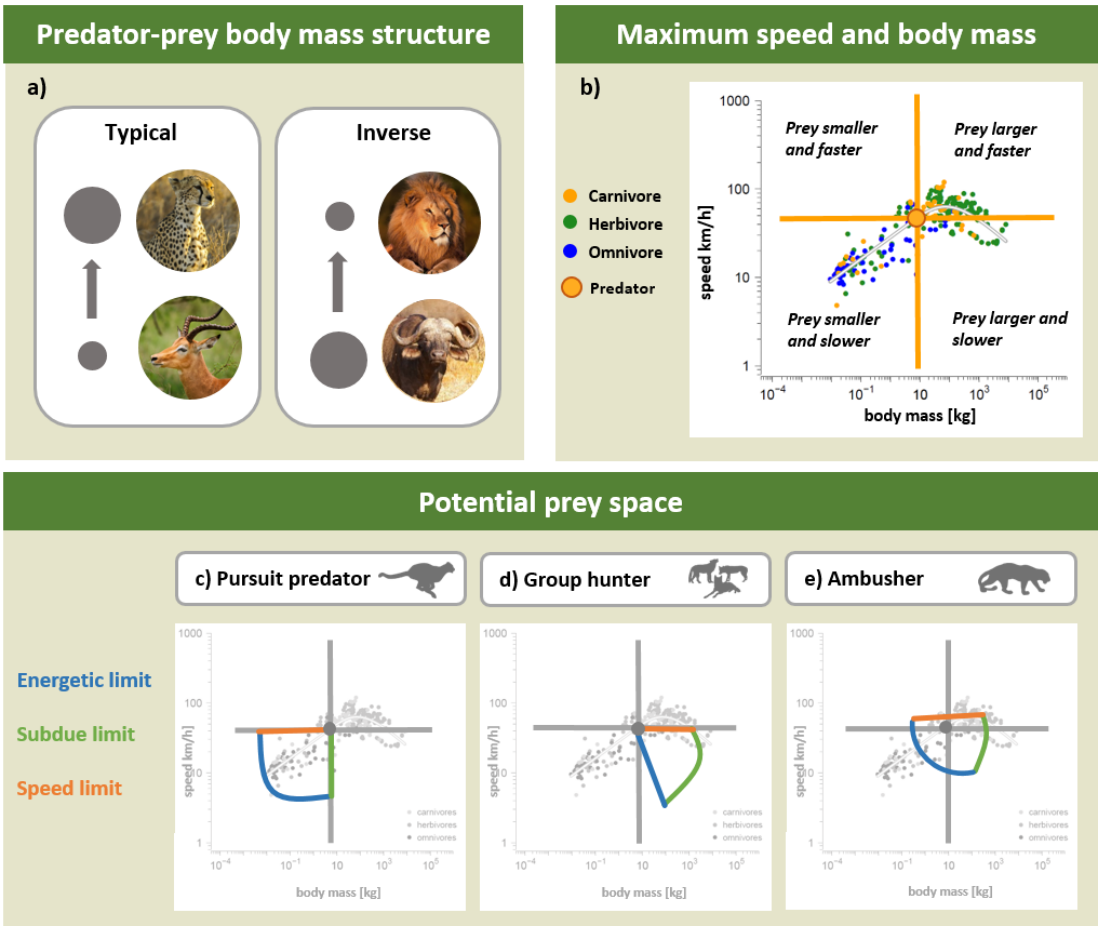

Figure 4.1 | Concept of the prey space of different hunting strategies. (a) Typical and inverse body mass ratio of predators and their prey. (b) Scaling of maximum speed with body mass in terrestrial mammals. (c)-(e) Hypothesized prey space of pursuit predators (c), group hunters (d), and ambushers (e) set by the energetic, subdue, and speed limit.

Methods

We compiled data from the literature on the predominant prey species of 35 terrestrial carnivorous mammal species (see Supplementary Table 4.1). Carnivores were defined as those species with diets compromising of at least 90% meat and only included species that consumed vertebrate prey (Kelt and van Vuren 2001). Prey preference information were obtained using a literature search in Google Scholar using the terms "diet", "prey preference" and each species' name. The predominant prey species consumed was categorized as either 1) the preferred prey, calculated using the Jacob's Index, which standardizes the proportion of the total kills by the carnivore and the proportional availability of the prey species (Hayward and Kerley 2005); or 2) the predominant prey species consumed by the carnivore based on diet analyses. For each species, we noted the top three to five prey species consumed depending on the number of species stated in the literature and their importance based on the percentage of the diet the prey represents. Diet information and preference information were included for both sexes and across populations. We then gathered data on body mass (Myhrvold et al. 2015) and maximum speed (Hirt et al. 2017a) for predator and prey species. This resulted in a database with 32 predator-prey links, mainly restricted by data availability on maximum speed.

We assigned the hunting strategies pursuit predation, group hunting, and ambushing to these links. These hunting strategies comprise several predatory behaviors (Table 4.1). Pursuit predation summarizes "ambush-and-pursuit", which includes an ambush part prior to the chase (e.g. a cheetah stalking a gazelle) and "pounce-and-pursuit", which includes a pouncing part (e.g. a fox jumping to catch a mouse). Although Pounce-and-pursuit is a predatory behavior between pursuit predation and ambushing, we assigned it to the category of pursuit predation because the pounce-and-pursuit predators in our study also show classical pursuit behavior (e.g. a fox preying on a mouse compared to a hare). Cooperative hunting usually occurs in social animals living and hunting in groups (e.g. lions). They actively chase their prey mostly over longer distances. Ambushing means capturing prey by hiding or stalking in dense vegetation and launching a surprise attack (e.g. a cougar jumping on the back of a moose). As we defined the hunting strategy on the link level, a species can have multiple hunting strategies and predatory behaviors. For

example, occasional group hunters such as wild dogs could occur as pursuit predators as well as group hunters or foxes may have pursuit as well as pounce-and-pursuit links.

We then analyzed the predator-prey links in a two-dimensional space of body-mass ratio (prey/predator) and maximum-speed ratio (prey/predator; Figure 4.1). We used Bayesian modeling to estimate the prey space as the kernel of the predator-prey links by assuming a bivariate normal distribution of x = log(*mass ratio*) and y = log(*speed ratio)*. This normal distribution was fitted to the data under the constraint that the axis of largest variation (i.e., the first principal component) crosses the origin. As there is no unidirectional causal relationship between the two variables and because both have measurement errors of the same magnitude, we fitted a major axis regression with a fixed intercept of zero (the predator origin), which makes no assumptions about a causal relationship between the variables. We defined the prey space as the 90% confidence region of the found bivariate normal distribution, which takes the shape of an ellipsis (see Supplement for details of prey space estimation and Bayesian major axis regression). Moreover, we calculated the angles of the predator-prey links relative to the y-axis in clockwise orientation (0°-360°) for each hunting strategy.

Table 4.2 | Overview of the hunting strategies assigned to the predator-prey links. Precise descriptions of the hunting strategies pursuit predation, group hunting, and ambushing, and the predatory behaviors are included.

hunting strategy	predatory behavior	description
Pursuit predation	• pursuit • pounce-and-pursuit • ambush-and-pursuit	Active chase of prey over short or long distances. Sometimes includes stalking prior to a rapid chase.
Group hunting	• pursuit over long distances	Cooperative hunters that actively chase their prey, usually over long distances.
Ambushing	• ambush • stalk-and-ambush	Either ambush and launch a surprise attack or capture prey by stalking followed by a short rush.

Results

In this study, we have analyzed body masses in combination with maximum speeds of mammalian predators and their prey. In the following, we first illustrate the concept of prey *ranges* along these two axes. Predator body mass and maximum speed are expressed relative to the prey values, which yields prey ranges in terms of predator to prey body-mass ratios (hereafter: mass ratio) and predator to prey maximum-speed ratios (hereafter: speed ratio). For illustration purposes, we use the log10 values of these ratios in Figure 4.2. Subsequently, we extend this concept of prey ranges by combining these two axes creating two-dimensional prey *spaces*. Finally, we test our hypotheses on differences in prey spaces according to the hunting strategy of the predator (pursuit predation, group hunting, and ambushing).

The concept of prey ranges can be easily described using the cheetah (*Acinonyx jubatus*) as an example of a pursuit predator. Thomson's gazelle (*Eudorcas thomsonii*) is one of its prey species. In our data, the body masses of the cheetah and the gazelle are 65 kg and 25 kg, respectively, which yields a mass ratio of 2.6 (log10 mass ratio of 0.41, see Supplementary Table 4.2), implying that the cheetah is 2.6 times larger than the gazelle. The impala (*Aepyceros melampus*) with 54 kg is the largest prey of the cheetah in our database implying a mass ratio of 1.19 (log10 = 0.08). Together, this yields a prey range in terms of mass ratios between 1.19 and 2.6 (log10 range of 0.08 to 0.41) for the cheetah. As these mass ratios are normalized to predator mass and thus dimensionless, they can be pooled for all pursuit predators resulting in a prey range of mass ratios between 1.19 (log10 = 0.08, cheetah and impala, see above) and 460 (log10 = 2.66; golden jackal, *Canis aureus*, hunting mice, *Mus musculus*). This implies that pursuit predators typically choose their prey within the range of mass ratios of approximately equally sized (here: ratio of 1.19) to 460 times smaller individuals (mass ratio of 460, Figure 4.2a). Similarly, we can use the mass ratios to characterize the prey range of group hunters (0.05 to 1.6, log10 range of -1.3 to 0.2) and ambushing predators (0.04 to 3.18, log10 range of -1.4 to 0.5), which are significantly lower compared to pursuit predators (Anova, $p < 10^{-5}$, Figure 4.2a). This results in the general pattern that pursuit predators are substantially larger than their prey, whereas ambushers

are equally sized to a bit smaller, and group hunters equally sized to substantially smaller than their prey (Figure 4.2a).

While analyses of prey ranges typically employ body-mass ratios, they can also be carried out using ratios between predator and prey maximum speed. In our database, the maximum speed of the cheetah is 120 km/h, whereas the maximum speed of its prey ranges between 65 km/h (Thomson's gazelle, *Eudorcas thomsonii*) and 97 km/h (springbok, *Antidorcas marsupialis*), which yields speed ratios between 1.24 and 1.85 (log10 range of 0.09 to 0.27, see Supplementary Table 4.2). When pooled for the groups of predator hunting strategies, characteristic patterns emerge: pursuit predators typically have a much higher maximum speed than their prey, whereas group hunters have a similar or slightly higher speed, and ambushers exhibit a wider variety of lower or higher maximum speeds than their prey. These data show that the speed ratio of pursuit predators is significantly higher than those of group hunters or ambushers (Anova, $p < 10^{-4}$, Figure 4.2b).

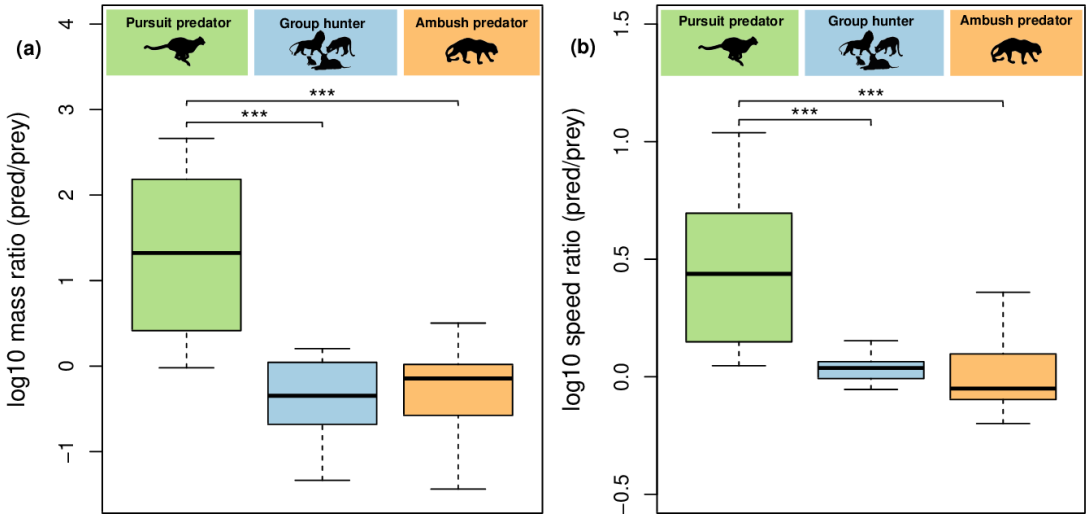

Figure 4.2 | Prey range and niche differentiation of predators of different hunting strategy. (a) Prey range of pursuit predators, group hunters and ambushers defined by body-mass ratios between predator and prey. Body-mass ratios of pursuit predators are significantly higher than those of group hunters or ambushers ($p < 10^{-5}$). (b) Prey range of pursuit predators, group hunters and ambushers defined by maximum-speed ratios between predator and prey. Maximum speed ratio of pursuit predators are significantly higher than those of group hunters or ambushers ($p < 10^{-4}$).

These analyses of the prey ranges in the dimensions of mass ratios (Figure 4.2a) and speed ratios (Figure 4.2b) demonstrate important differences in the niches of predators of different hunting strategies. A more systematic and coherent analysis requires combining the two dimensions of the prey *ranges* described above to create a prey *space* (Figure 4.3a). For illustration purposes, mass and speed ratios are now expressed as prey to predator ratios. Any predator-prey interaction in this prey space is characterized by two values: the mass ratio as the x-value and the speed ratio as the y-value. For instance, the interaction between cheetah and Thomson's gazelle is placed at an x-value of -0.41 (log10 prey to predator mass ratio) and a y-value of -0.27 (log10 prey to predator speed ratio, see Supplementary Table 4.2) in Figure 4.3a. Similar to the analyses of prey ranges, the data of all predator-prey interactions can be pooled in the same diagram as the values are normalized to predator body mass and predator maximum speed. Note that the predators of the interactions are thus positioned at the origin of the plot, as they have no difference in mass and speed to themselves. A feeding link between predator and prey in this prey space can be characterized by the angle of the connection between the origin (representing predator mass and maximum speed) and the data point (representing prey mass and maximum speed relative to the predator values). The quadrants of Figure 4.3a can thus be characterized as: (1) 0° to 90° - the prey is larger and faster (upper right), (2) 90 to 180° - the prey is larger and slower (lower right), (3) 180° to 270° - the prey is smaller and slower (lower left) and (4) 270° to 360° - the prey is smaller and faster than the predator (upper left).

The prey spaces were estimated using a bivariate normal distribution and Bayesian major axis regressions for each of the predator hunting strategies separately (Figure 4.3a). The difference between the prey spaces can be expressed by the differences in slopes and the distribution of data points across the four quadrants (Figure 4.3a). The prey space of pursuit predators is significantly different from the prey spaces of group hunters and ambusher as the slope (b) of the pursuit prey-space is significantly higher than that of group hunters ($P(b_{pursuit} > b_{group}) = 1.00$, Bayesian posterior probability) and ambushers ($P(b_{pursuit} > b_{ambush}) = 0.998$). Moreover, all prey links of pursuit predators occupy the lower left quadrant (main direction of links towards quadrant 3, Figure 4.3a), indicating that they only hunt prey that is smaller and slower. Group hunters focus on prey that is larger and slower than they are

(main direction of links towards quadrant 2, Figure 4.3a), but also have some prey links that are close to the origin but distributed across the other quadrants (prey of roughly similar size and speed). Ambushers mainly hunt equally sized or larger prey that can be slower or faster than they are (Figure 4.3a, small panel on the right). The difference between group hunting and ambushing prey-spaces, however, is not significant ($P(b_{ambush} > b_{group}) = 0.922$), indicating that they occupy similar trophic niches that are clearly separated from pursuit predators.

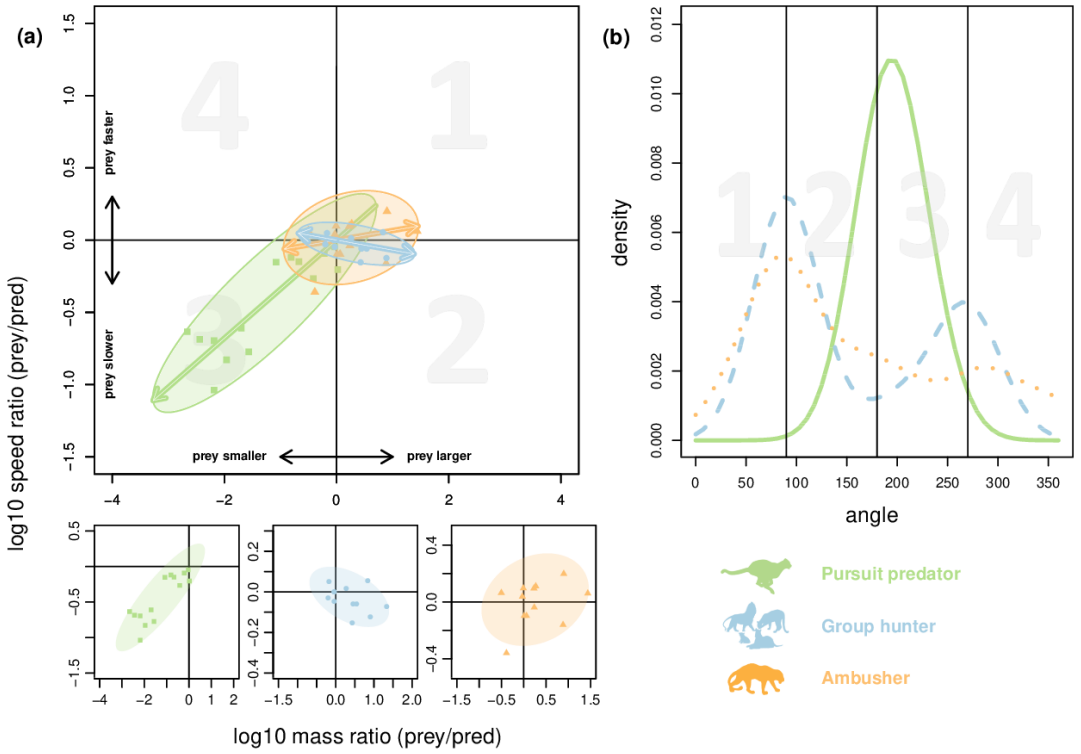

Figure 4.3 | Prey space and niche differentiation of predators of different hunting strategy. (a) Prey spaces of the three different hunting strategies (pursuit predator, group hunter, ambusher) defined by body-mass and maximum-speed ratios of prey to predator. Small panels show prey spaces of pursuit predators, group hunters, and ambushers individually from left to right. Arrows indicate the main direction(s) of the predator-prey links. Slopes calculated by Bayesian major-axis regressions: $b_{pursuit} = 0.348 \pm 0.036$ (slope ± standard deviation, Bayesian posterior probability $P(b > 0) = 1.00$), $b_{group} = -0.076 \pm 0.037$ ($P(b<0) = 0.979$), $b_{ambusher} = 0.048 \pm 0.083$ ($P(b>0) = 0.735$). (b) Niche differentiation by hunting strategy according to a combined effect of body mass and maximum speed. The angles refer to the angles of the feedings links in panel a.

This can also be seen in the subsequent analyzes of the angles of the feeding links and their distributions (Figure 4.3b). The angles are calculated as the angle in degrees of the predator-prey link in Figure 4.3a relative to the y-axis and thus also reflect the main direction(s) of the prey space. There is a clear niche differentiation between pursuit predators and group hunters: while pursuit predators mainly focus on smaller and slower prey (angles around 200°, Figure 4.3b green line), group hunters occupy the surrounding niches with prey that is mostly larger and slower (around 80°, Figure 4.3b, left maximum of the blue line) or slightly smaller and slower (around 260°, Figure 4.3b, right maximum of the blue line). Ambushers occupy similar niches as group hunters but are less distinct.

Discussion

In this study, we have extended the classical concept of prey ranges by integrating the dimensions of prey body-mass and maximum-speed, which defines predator trophic niches in a two-dimensional prey space and found that the prey spaces of ambushers and group hunters are significantly different from that of pursuit predators. Previously, trophic niches were typically expressed as ranges on body-mass axes where the minimum prey sizes consumed by predators are caused by the decreasing energy content of prey individuals making attacks energetically inefficient (Schneider et al. 2012). Maximum prey sizes of predators are constrained by the increasing power that is necessary to subdue the prey (Radloff and Du Toit 2004). In our novel concept of prey spaces, the trophic niches are not only constrained by (1) the energy limit towards smaller prey sizes and (2) the subdue limit towards larger prey sizes but also by (3) the speed limit towards prey of higher speed. Together with a hump-shaped scaling of maximum speed with body mass (Hirt et al. 2017a), this concept yields predictions on the shape of the trophic niches of predators with different hunting strategies (i.e., pursuit predation, group hunting, and ambushing). We tested these hypotheses using a new database combining body mass and maximum speed of various mammalian predators and their prey. Subsequently, we will first discuss the trophic niche differentiation according to the different hunting strategies before we use the three niche limitations to argue why and how these hunting strategies are constrained.

Moreover, we show how our novel prey-space concept provides a mechanistic understanding of how the energy and speed limits prevent the existence of small-bodied group hunters (micro-lions) and larger pursuit predators (mega-cheetahs).

The prey space of pursuit predators fits the concept of a classical predator-prey pair where the predator is larger than its prey (typical body-mass ratio, Figure 4.1a) as well as faster to be able to successfully capture it in a one-to-one chase (Figure 4.2). However, there is an obvious gap within the group of pursuit predators between the categories of classical pursuit and ambush-and-pursuit predators on the one side, and pounce-and-pursuit-predators on the other side (Figure 4.2a, pursuit prey space). In the first category, predator-prey links have lower body mass and speed ratios than in the other categories, implying that classical pursuit predators and their prey are more similar in their morphology. Classical evolutionary theory assumes an arms race between pursuit predator and prey, which drives evolution of high speed in both. In this case, athletic capabilities of predator and prey closely match up (Bro-Jørgensen 2013, Wilson et al. 2018). In contrast, pounce-and-pursuit predators have considerable higher body-mass ratios and therefore higher speed ratios, which implies that they feed on much smaller and slower prey than other pursuit predators. This may be due to a much lower energetic demand of pounce-and-pursuit predation compared to a classical one-to-one-chase, which compensates for the low energetic gain of much smaller prey. Despite the differences between these types of pursuit predation, current limitations in data availability on maximum speed hampered a separation of the two categories. Consistent with our initial hypothesis, pursuit predators are mainly constrained by the speed and subdue limits of the prey space, while the energy limit differs between the categories.

Prey spaces of group hunters and ambushers are significantly different from that of pursuit predators. Interestingly, despite having evolved different hunting strategies, they occupy a similar trophic niche that avoids competition with pursuit predators. Group hunters show an inverse body-mass ratio with the prey mostly being larger than the predator (Figure 4.1a and Figure 4.2). The multiple agents in the group reduce problems of locating and subduing large prey (Bertram 1979; Lamprecht 1981; Packer 1986), and improve the kill efficiency (Schaller 1972; Caraco and Wolf 1975). However, to be able to successfully catch large prey, the prey individual should be equally fast or slower than the

predator. This is only possible because the hump-shaped scaling of maximum speed with body mass opens up a niche of larger and slower prey at intermediate to high body masses (Figure 4.1b). Thus, cooperative hunting is a good strategy for medium-sized mammals to avoid competition within the prey space occupied by pursuit predators. However, group hunters are also able to catch prey that is slightly faster (Figure 4.2). This is probably due to differing individual hunting tactics within the group, which relax the speed pressure compared to a one-to-one chase. These hunting tactics include predator individuals circling prey and others waiting for the prey to capture it while trying to escape (Stander 1992, Bailey et al. 2013). The hunting process also often includes an ambushing part where some group members hide while others chase the prey towards them (Bailey et al. 2013). Hunting in a group thus allows to shift the subdue limit to large prey individuals and relax the speed limit, but it comes at the cost of higher energy limits as the prey is shared within the group.

Ambushers mainly focus on equally-sized to larger prey that can be slower as well as faster. They are able to subdue this larger prey because they launch surprise attacks like, for example, a cougar stalking a moose, leaping onto its back, and killing it by breaking its neck (Husseman et al. 2003, Bartnick et al. 2013). This tactic also enables them to catch faster prey. Thus, they are less restricted by the speed limit than the other hunting strategies, which comes at the cost of other constraints (see detailed discussion below).

Our analysis shows that group hunting and ambushing open up new niches with prey that is not available to classical pursuit predators. However, the hunting strategies are not equally distributed amongst mammalian predators. The vast majority of carnivores are solitary hunters (80-95%, Lührs and Dammhahn 2010) either as pursuit predators (e.g. cheetahs, commonly foxes or lynx) or ambushers (e.g. tigers, jaguars, cougars, and leopards). Only few terrestrial mammalian predators are exclusively group hunters to the extent that all group members hunt simultaneously. This behavior is only found in lions (Stander 1992, Packer et al. 2015), wild dogs (Creel and Creel 1995), and wolves (Mech and Boitani 2003). Many other social animals hunt occasionally in groups such as hyenas, which also scavenge from conspecifics (Kruuk 1972, Packer 1986), chimpanzees (Boesch 1994), and many canid species (Sillero-Zubiri and Gottelli 1995, Muntz and Patterson 2004, Krofel 2008). This poses the question of why group hunting is not more common among mammalian predators. Group hunting has some obvious disadvantages compared to

pursuit predation: group hunters have a lower prey encounter probability and a smaller search area compared to pursuit predators (Scheel 1993, Fryxell et al. 2007). For instance, the total search area of a lion pride consisting of five individuals is similar to the search area of a single lion. If all five individuals were solitary predators, their combined search areas and the resulting prey encounter rates would thus be about fivefold larger. Moreover, the prey needs to be shared between the group members. Thus, cooperative hunting can only evolve when the per capita rate of food intake within a hunting group is higher than that of a solitary individual (Packer and Ruttan 1988). In addition, evolving sociality is a prerequisite of cooperative hunting and highly costly. Being able to exploit the niche of larger prey, therefore, cannot completely counteract the costs of cooperative hunting such as possible inadequacy of food distribution among group members and lower prey availability (Creel 1997).

Ambushers are solitary hunters; however, they have even lower encounter rates with prey and a smaller search area than group hunters or pursuit predators (Werner and Anholt 1993, Crawley 2009, Scharf et al. 2015). Their ambush strategy requires dense vegetation to hide and stalk or wait for prey to come by (Beier et al. 1995). Their encounter rate therefore depends more on the activity of the prey than on their own mobility. Consequently, they invest little energy in searching but much time in waiting for prey (Crawley 2009). This limitation in prey availability makes them less effective in foraging despite their prey space being larger than that of group hunters and more flexible than that of pursuit predators.

Pursuit predators have the largest search area and therefore a higher chance of encountering prey as they hunt individually while moving in open space. Energetically, however, classical pursuit predation is the most costly hunting strategy, as predators need to chase their prey with high speed. Therefore, they need to morphologically evolve high speed capacities and, additionally, a high maneuverability as well as quick acceleration and deceleration capacities (Wilson et al. 2013, 2015). While these aspects are of lower importance to group hunters, endurance speed plays a crucial role in their hunting tactic. For example, wolves often exhaust their prey over long distances (Bailey et al. 2013). Moreover, prey reacts differently to the appearance of predators. Smaller prey mostly tend to flee, while larger prey often stands in a defensive formation (Creel and Creel 1995). The predators then attack from several directions and - if the prey starts to flee - a full-speed

chase begins. Thus, both endurance speed and maximum speed are important for the hunting success of group hunters. Furthermore, group hunters as well as ambushers need to evolve morphological features to be able to successfully kill much larger prey, such as massive jaws and long canines to bite the preys' throat as found in lions or tigers. While group hunters have the additional advantage of a higher number of predator attacks on the prey by the different group members, ambushers mostly have a powerful build that enables them to bring down large prey.

Due to these morphological adaptations, predators should theoretically be able to develop each of the hunting strategies independent of their body mass. However, the hump-shaped scaling of maximum speed with body mass (Figure 4.4a) results in each of the hunting strategies having a specific energetic optimum of its prey space (Figure 4.4b) along the body-mass axis (Figure 4.4c). At lower predator body masses (below the hump), pursuit predation is energetically most effective as all of the prey space is filled (Figure 4.4c). Although the group hunting prey space is partially filled in this area, pursuit predation is the less costly hunting strategy and is therefore likely to be preferred. At intermediate body masses (at the hump), a predator can either evolve morphological adaptations for high-speed movements to optimize its pursuit prey space or hunt cooperatively for larger prey. With increasing body masses above the hump, the pursuit prey-space becomes continuously less filled due to limited availability of smaller and slower prey (Figure 4.4c). Hence, group hunting is energetically more reasonable within this body-mass range (Figure 4.4c). This general distribution of prey spaces might also explain why small group hunting mammals (micro-lions) or large pursuit predators (mega-cheetahs) are energetically unlikely to exist. For small social-living carnivorous mammals, such as mongooses or meerkats, only pursuit predation is energetically reasonable despite their ability to cooperate in a group, because larger and slower prey is not sufficiently available, and their prey space as group hunters would not be filled. Larger social animals, however, are able to develop cooperative hunting strategies, as the hump-shaped scaling of maximum speed makes larger and slower prey available. Predators with larger body masses need to be either group hunters or ambushers, which are mostly smaller than their prey.

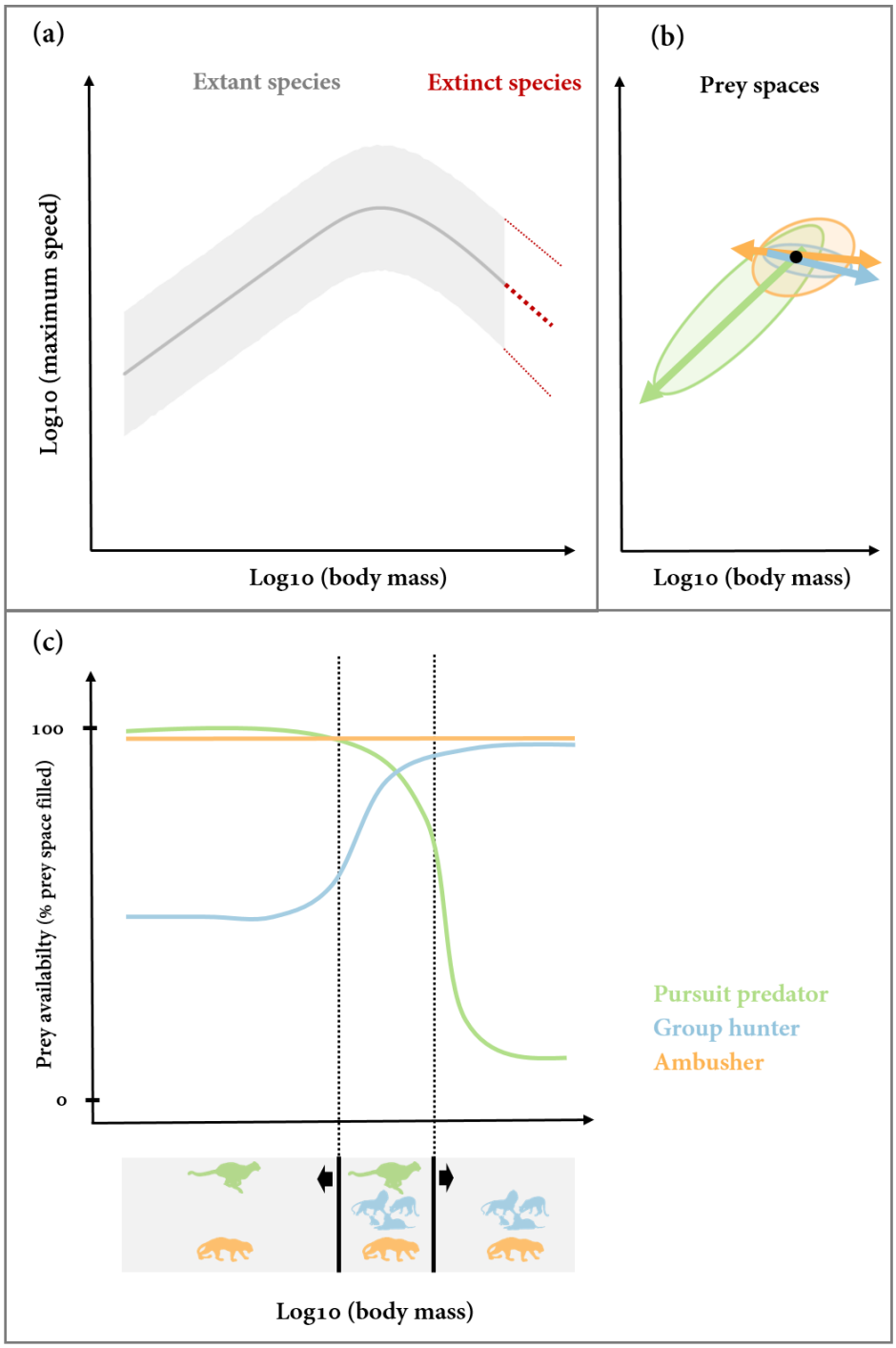

Figure 4.4 | Hypothetical energetic optima of hunting strategies along the body mass axis. Based on the hump-shaped scaling of maximum speed (a) and the prey spaces of the different hunting strategies (pursuit predator, group hunter, ambusher) (b), different energetic optima for each hunting strategy emerge (c). Prey availability is defined as the percentage of prey space that is filled with available prey species. Energetic optima are based on this prey availability combined with additional parameters such as encounter rates, attack success, or energy content of prey.

Alternative theory on maximum body sizes of mammalian carnivores is based on constraints by the increased energy expenditure and intake linked to pursuing and consuming large prey, which should limit maximum carnivore size to approximately one ton (Carbone et al. 2007). However, this prediction only has empirical support for mammal body-masses. For example, extinct carnivorous reptiles had body sizes far beyond this limit (Burness et al. 2001). Our theory is based on the hump-shaped scaling of maximum speed with body mass, which applies to all taxonomic groups, including reptiles, indicating that the same constraints on prey spaces should be in effect.

Here, we only extended trophic niches from one to two dimensions by including body mass and maximum speed in our concept, which are likely to be the key drivers. The speed dimension could further be complemented by endurance speed, which also plays a crucial role during the hunting process. Moreover, there are certainly more dimensions that could be added to this concept, which could either be direct species-related effects (e.g. maneuverability (Wilson et al. 2018), diurnal vs. nocturnal activity (Jaksić 1982, Emmons 1987)) or indirect effects (e.g. habitat structure (Cresswell et al. 2010, Laundré et al. 2010). This is consistent with general analyses across ecosystems showing that trophic niches in complex food webs can be characterized by up to eight dimensions (Eklöf et al. 2013a). The additional dimensions will help further explain or even shift the energetic optima of prey spaces along the body-mass axis. For instance, our theory explains why pursuit hunters with high body-mass ratios can probably not exist above the speed-mass hump, as their prey spaces are not filled (Figure 4.4a). However, decreased maneuverability and acceleration/deceleration capacities impede a classical arms race between predator and prey and could therefore prevent the existence of pursuit predators with low body-mass ratios, whose prey space would still be partially filled. Thus, our theory combined with additional dimensions of trophic niches suggests that large predators should be either group hunters or ambushers instead of pursuit predators.

Overall, empirical tests and natural patterns of predator-prey links support our concept of extending the two body-mass limits ("energy limit" and "subdue limit") by a "speed limit" to define predator trophic niches in a two-dimensional prey space across mammalian hunting strategies. Future extensions of our approach could be generalized across predators of other phylogenetic groups (e.g. reptiles and invertebrates) and other ecosystem types (e.g.

marine and freshwater). In this vein, it will be particularly interesting to include other movement modes (e.g. swimming and flying), as links between species of differing movement modes will yield "speed limits" that are entirely independent of body mass. Moreover, we anticipate that our prey-space concept should be integrated with precise empirical assessments of the maximum speed and body mass of the predator and prey individuals that interact (Wilson et al. 2018), which will yield an unprecedented theory-driven understanding of natural trophic niches.

Advancing the concept of prey ranges to prey spaces certainly deepens our mechanistic understanding of realized trophic niches in the wild. This is particularly important for predicting food-web structures and the impacts of extinctions on predator-prey relationships. So far, body-mass ratios helped comprehend the niche structure of natural communities (Woodward et al. 2005) and enabled predictions of food-web structure by applying allometric diet breadth (Petchey et al. 2008) or allometric niche models (Schneider et al. 2016). This approach also successfully predicted effects of species loss on secondary extinctions and ecosystem functions (Schneider et al. 2012, Brose et al. 2017). The new concept of prey spaces illustrated here calls for a similar extension of one-dimensional to two-dimensional trophic niche models to improve our understanding of natural communities and better predict the consequences of extinctions for predator-prey interactions, food web structure, and ultimately ecosystem functions.

Acknowledgements

M.R.H and U.B gratefully acknowledge the support of the German Centre for Integrative Biodiversity Research (iDiv) Halle-Jena-Leipzig funded by the German Research Foundation (FZT 118). TM and MT were funded by the Robert Bosch foundation.

Author Contributions

M.R.H, T.M., M.T. and U.B. developed the concept. M.R.H. and M.T. established the database. M.R.H. and B.R. carried out statistics. M.R.H. wrote the manuscript and all authors discussed the results and commented on the manuscript.

General Discussion

Discussion

Holistic movement research requires a basic understanding of movement mechanisms to evaluate the vast amount of data on animal movement patterns in terms of their implications for species interactions and communities, and consequently biodiversity patterns. Movement speed, thereby, plays a fundamental role as it provides essential information on the movement capacity and thus has substantial predictive power for space use capacities and interactions rates and strengths. Therefore, a general understanding of how movement speed depends on species traits such as body mass and movement mode is crucial. This is particularly important for the maximum speed of animals as it sets the upper limit of the movement capacity to which all realized movement needs to be scaled. The phenomenon that the largest running animals are not the fastest is a well-known pattern, but a mechanistic model describing it has long been lacking. Most attempts to describe and explain this pattern included morphology, locomotion energetics, and biomechanics as main drivers (Garland 1983, Iriarte-Díaz 2002, Bejan and Marden 2006, Clemente et al. 2009, 2012, Fuentes 2016, Dick and Clemente 2017). This implies that the maximum speed of running animals is constrained by the ability of muscles and bones to withstand the stress of the locomotor force hitting the ground (Biewener 1982, Clemente et al. 2012, Dick and Clemente 2017). However, these biomechanical concepts were lacking mechanistic predictions across phylogenetic groups of animals that exhibit substantial variation in their body morphology.

In **Chapter 1**, I developed a mechanistic model that predicts the large-scale pattern of maximum speed across all taxonomic groups, ecosystem types and movement modes (running, flying, swimming). The model is based on two simple assumptions. First, animals accelerate over a short period of time, after which the energy stored in the muscles is

exhausted. As large animals have more muscle tissue and therefore more energy available, they can theoretically reach higher speeds. Second, due to mass-dependent inertia, smaller animals can accelerate more quickly than larger ones. During acceleration, the largest species' energy requirements soon exceed their available energy reserves, which reduces their realized maximum speed. Taken together, this leads to the pattern that medium-sized animals are the fastest. The model only needs two major species traits as input parameters: body mass and movement mode. I tested this model by an extensive empirical database comprising 474 species over a body mass range from $3x10^{-8}$ to 108,400 kg and found that it explains almost 90% ($R^2 = 0.893$) of the variation in maximum speed. Moreover, the hump-shaped scaling pattern of maximum speed with body mass does not only apply to running animals, but also to flying and swimming animals across phylogenetic groups. This general model approach allows a species-level prediction of speed not only for extant but also for extinct species. The running speeds of dinosaurs, for example, have long been debated and detailed analyses have been performed to answer this question. Either by using anatomical information on bone scaling and strength or by developing musculoskeletal models of the animal (Thulborn 1982, Sellers and Manning 2007a). We used our model to predict the speeds of six dinosaur species, for which accepted maximum speed values were available. Interestingly, our model yields similar predictions by only accounting for body mass and movement mode and approves that large dinosaurs such as *Tyrannosaurus* were slow runners. Hence, this model enhances our understanding of the main physiological drivers of maximum speed and, moreover, acts as a simple and powerful tool for predicting the upper movement capacity of extant and extinct animals. These results have not only solved a long-standing question in movement ecology, but also provide the basis for systematic scaling analyses of movement patterns.

When working on the maximum speed database, I realized how much more difficult it was to get speed data on invertebrates compared to vertebrates. Ultimately, the database contained 412 vertebrate species compared to only 62 invertebrates. This mismatch in data availability is mainly accounted for by difficulties in tracking small-bodied organisms. However, due to their vast diversity and abundance as well as their major contribution to key ecosystem structure, functions, and services (Wilson 1987, Hochkirch 2016), information on invertebrate ecology is crucial in all ecological fields, including movement

ecology. Little was previously known about general patterns in the allometry of invertebrate speed, as the few studies that include more than one or two species are restricted to specific taxonomic groups (Forsythe 1983, Hurlbert et al. 2008).

In **Chapter 2**, I contribute to filling this gap by providing the first general empirical estimates of the scaling of invertebrate exploratory (voluntary) speed with body mass. We tracked 173 individuals of 57 forest litter invertebrate species in the laboratory using automated image-based tracking. These data cover six taxonomic groups (Arachnida, Chilopoda, Malacostraca, Diplopoda, Arachnida, Entognatha) and four feeding types (carnivore, detritivore, herbivore, omnivore). I show that exploratory speed of invertebrates follows a power-law relationship with body mass with a scaling exponent of 0.19 (± 0.04 SE), which is similar to prior estimates for 24 ant species (0.25, Hurlbert et al. 2008). Moreover, there is substantial variation in the allometric scaling of speed between taxonomic groups, which probably arises from differences in body shape and other functional traits related to locomotion. How exactly different morphological characteristics across these groups affect invertebrate movement has to be disentangled in future studies. A closer look at the different feeding types reveals that detritivores (Diplopoda and Malacostraca) have generally lower speeds relative to the other feeding types. A reason for this could be that detritivores mainly feed on a sessile resource (litter), which means that there is a much lower evolutionary pressure on developing high speeds to capture prey compared to active hunters such as spiders. The fact that they move through litter and soil additionally impedes high-speed movements. Another explanation could be that the detritivorous groups in this study (Diplopoda and Malacostraca) have evolved strong exoskeletons as defenses against predation rendering high-speed escape behavior unnecessary. The overall allometric scaling exponent of 0.19 is much lower than those for resting metabolic rates of terrestrial invertebrates (0.69, Ehnes et al. 2011) or field and maximum metabolic rates of vertebrates (0.8-0.9, Pawar et al. 2012 and references therein). This implies that although metabolism fuels movement, body morphologies set constraints that determine the movement capacities across orders of magnitude variation in body mass. In consequence, the metabolic power increases more strongly with body mass than the realized movement speeds, which implies that larger species are particularly limited by morphological factors in their movement speed. However, the allometric exponent of

exploratory speed is similar to that of terrestrial invertebrate attack rates (0.24, Rall et al. 2012), which approves that attack rates depend more strongly on movement capacities than on metabolic rates alone (Pawar et al. 2012, Rall et al. 2012). This is because higher average speeds generally lead to higher encounter rates, and thus higher attack rates between predator and prey (Mittelbach 1981, Pawar et al. 2012, Polidori et al. 2013, Dell et al. 2014b). Thus, this study highlights the importance of speed for species interactions by determining encounter and thereby attack rates. Overall, this research chapter has provided the largest database on invertebrate movement speeds compiled so far, and filled a conceptual missing link between metabolic scaling and interaction rates as they are realized in nature.

The implications of speed not only for species interactions but also for space use capacities in terms of habitat use, and dispersal and migration behavior, made me aware of the widespread importance of this parameter in all movement ecology fields, including movement modelling. In **Chapter 3**, I demonstrate how movement speed can be integrated into movement models to improve the accuracy and predictive power of modelling approaches. State-of-the-art movement models often lack ecological applicability to natural movement patterns. For instance, the traditional random walk models conceptualize animals as more or less featureless particles, thereby neglecting an animal's decisions and its reactions to its environment. More advanced random walk models or individual-based models include these behavioral aspects but are highly specific and thus cannot be generalized (Codling et al. 2008, Nathan et al. 2008, Jonsen et al. 2013). Hence, it is essential to develop models that are, on the one hand, more realistic by taking into account species traits and, on the other hand, easily generalizable for modelling communities comprising species with considerable variation in traits. To achieve this, I propose to integrate allometric scaling of movement parameters into movement models. The main idea is to calculate species-specific and behavior-specific step lengths based on movement speed. Therefore, I use the allometric scaling relationship of maximum speed developed in **Chapter 1.** Movement speeds are thus species-specific as they are calculated from a species' body mass and movement mode. Moreover, they are behavior-specific as the speeds of different movement behaviors (e.g. foraging or dispersal) are calculated as proportions of the maximum speed. To illustrate this concept, I chose a simple random walk and transformed it into a so-called *allometric random walk*. I demonstrate how such a trait-

based movement model can be used to predict (1) predator-prey attack rates in a homogeneous landscape and (2) large-scale biodiversity patterns in a heterogeneous landscape. First, I simulate predator-prey attack rates using a standard (non-allometric) and an allometric random walk and compare the results to published empirical data on terrestrial invertebrates. Thereby, I show that only the allometric random walk generates the realistic pattern of an increase in attack rate with body mass, which can be observed in natural communities (Rall et al. 2012, Li et al. 2018). Interestingly, applying the allometric random walk predicts the empirical scaling exponent of attack rates surprisingly well considering the fact that no calibration was involved (0.29 in the simulations compared to 0.3 in the empirical data). With this worked example, I illustrate how using trait-based movement models can help accurately predict the strengths of species interactions such as attack rates at the small spatial scale of laboratory experiments. Certainly, this approach could also be scaled up to larger areas or even landscapes. For instance, different spatial compartments, such as habitat patches, refuges or environmental gradients, significantly affect the encounter probabilities and thereby the strength of interactions between animals and incorporating these processes in model simulations will yield landscapes of interaction strengths, attack rates and fear (Schmitz et al. 2004, Gallagher et al. 2017). Thus, applying this approach at a larger spatial scale could enable mechanistic research on how landscape structures affect species interactions. In a second example, I show how spatial network connectivities and large-scale biodiversity patterns can be predicted by allometric random walks. The connectivity of a spatial network (i.e. the percentage of realized dispersal links between pairs of habitat patches) depends on the movement capacity of an animal with medium-sized animals being able to cover longer distances and therefore connecting more distant patches. Thus, animals will be differently affected by changes in the landscape structure (e.g. an increase in the degree of fragmentation) depending on their body mass. I use an allometric random walk to predict the maximum patch-bridging distance and thereby the ultimate network connectivity of different species in a fragmented landscape. Over a large body mass scale, the network connectivity increases with increasing body mass following a hump-shaped curve. In more fragmented landscapes, species of the same body mass generally have a lower connectivity. Similar effects can be expected when additionally implementing the movement mode with flying animals being able to connect more distant

patches than running ones. Furthermore, I demonstrate how combining this approach with food web analyses can be used to predict biodiversity declines in altered landscapes. Therefore, I use a hypothetical fragmentation scenario, in which patches are randomly knocked out, and predict the extinction risk of species depending on the number of habitat patches that are still connected in the network and the body-mass dependent population density. Following these trait-based probabilities for primary extinction, a new community with a new body-mass distribution and food-web structure emerges, which will have a lower biodiversity and altered network characteristics. Additionally, secondary extinctions in the food web could be calculated by structural algorithms (e.g. a species goes secondarily extinct when it loses all its resources) or dynamic simulations (e.g. species also go secondarily extinct by top down pressure or unstable dynamics) (Dunne et al. 2002, Curtsdotter et al. 2011, Eklöf et al. 2013b). This exemplary modelling approach shows how allometric random walks can help gain mechanistic insights in how species connect patch networks depending on their traits, how these networks change with ongoing fragmentation, and how this may affect landscape-scale biodiversity patterns. Besides the allometric scaling of movement speed, more important aspects could be added to this framework in the future. These include other functional traits such as hunting modes (sit-and-wait vs. cursorial) (Miller et al. 2014) or feeding types (e.g. predator vs. herbivore) (Tamburello et al. 2015, Hirt et al. 2017b) as well as other behavioral aspects such as animal personality (Stamps and Groothuis 2010). Moreover, landscape features such as the distribution and quality of resources or the provision of refuge places, affect movement speeds and thereby the type and strengths of predator-prey interactions (McIntyre and Wiens 1999, Avgar et al. 2012). Overall, this conceptual framework represents a novel modelling approach to provide realistic and generalizable predictions of movement patterns and their consequences for species interactions, spatial networks, and large-scale biodiversity patterns.

The results of **Chapter 3** clearly emphasize the importance of movement speed for predator-prey interactions by affecting encounter and thereby attack rates. However, speed is not only important for the encounter between predator and prey but also for the outcome of the hunt. Traditionally, trophic niches of predators were expressed on a single body mass axis: the prey has to be large enough to meet the energetic demands of the predator but small enough to be effectively subdued (Radloff and Du Toit 2004, Brose 2010). Thus,

vertebrate predators are typically one to four orders of magnitude larger than their prey (Brose et al. 2006a, Tucker and Rogers 2014). However, exceptions to this pattern exist with predators hunting much larger prey, such as lions hunting African buffaloes. Additional important aspects during the hunting process are maximum speed itself as well as acceleration, deceleration, and maneuverability (Wilson et al. 2015, 2018). Primarily the maximum speed of both decides if a predator is able to catch its prey. In **Chapter 4,** I explored the role of maximum speed as a general determinant in predator-prey interactions and paid special attention to the implications of the hump-shaped scaling of maximum speed with body mass as presented in **Chapter 1**. I redefined the concept of a *prey range*, which only depends on body masses of predator and prey, to a two-dimensional *prey space* by adding maximum speed as a second constraint. Thus, besides the body-mass dependent "energy and subdue limits", the "speed limit" determines if the predator is fast enough to successfully catch its prey. These three limits form the exploitable prey space of predators depending on their hunting strategy. I successfully tested this theory by empirical data on maximum speed and body mass of 32 mammalian predator-prey pairs of different hunting strategy (pursuit predation, group hunting, and ambushing).The prey space of pursuit predators significantly differs from those of group hunters and ambushers, indicating that they have evolved new hunting strategies that enable them to exploit a new trophic niche that avoids the prey space occupied by pursuit predators.

Pursuit predators fit the classical predator-prey pair where the predator is larger as well as faster than its prey (e.g. cheetah hunting gazelle). Group hunters show an inverse body-mass ratio with the predator usually being smaller than its prey (e.g. lions hunting buffalos). The higher number of group members yields higher energetic requirements that have to be fulfilled by hunting large prey. However, the prey still needs to be slower or equally fast as the predator. This is only possible due to the hump-shaped scaling of maximum speed with body mass, which opens up a new niche of larger and slower prey at intermediate predator body masses. Ambushers mainly focus on equally sized or larger prey, which can be slower but also faster than they are. Their hunting tactic includes a surprise attack, which enables them to subdue this larger as well as sometimes faster prey. However, this higher flexibility in terms of the speed limit comes at the cost of reduced search areas and encounter rates with prey. Moreover, as dense vegetation is required to hide and wait for prey, ambushing

only makes sense in habitats with highly structured vegetation. Similarly, the search area of group hunters needs to be divided by the number of group members, yielding a much lower search area and encounter probability with prey compared to pursuit predators. Moreover, possible inadequacy of food distribution among group members as well as the costly evolution of sociality as a prerequisite of cooperative hunting causes a paucity of exclusively group hunting mammals. Pursuit predation, on the contrary, requires the evolution of morphological adaptations to high-speed movement and, additionally, a high maneuverability as well as quick acceleration and deceleration capacities (Wilson et al. 2013, 2015). While every hunting strategy has its advantages and disadvantages, they all have a specific energetic optimum along the body-mass axis caused by the hump-shaped allometric scaling of maximum speed. Pursuit predation is energetically most reasonable at low to intermediate body masses (below the hump) as the prey space is well filled with available smaller and slower prey. At intermediate body masses, the pursuit prey space becomes continuously less filled due to limited availability of smaller and slower prey, making group hunting or ambushing the better strategy (above the hump). This pattern also explains why there are no small group hunting mammals ("micro-lions") or large pursuit predators ("mega-cheetahs"). Moreover, it has important implications for the maximum body mass of predators, explaining why there are no mega-carnivores exceeding the size of mega-herbivores: at high body masses, predators need to be either group hunters or ambushers, which are usually smaller than their prey. Thus, this new concept of two-dimensional prey spaces offers essential mechanistic insight into the trophic niches of mammalian predators and the distribution of hunting strategies among differently sized predators. Moreover, it calls for future approaches that similarly extend one-dimensional to two-dimensional trophic niche models (Petchey et al. 2008, Schneider et al. 2016) to help improve our predictive understanding of natural communities and the consequences of extinctions for predator-prey interactions, food web structure, and ultimately ecosystem functions.

Overall, this thesis provides a comprehensive approach how to scale movement ecology from a mechanistic understanding of movement–related species traits to generalized predictions of species interactions, communities, and biodiversity patterns on a large spatial scale.

Outlook

This thesis analyzes the general determinants of individual movement, their consequences for species interactions and, thereby, finally scales movement ecology from species traits to communities. In this vein, it also raises new exciting research questions that I would like to address in the future. As I have outlined in the introduction, there is a clear need for advances in invertebrate and microbial movement tracking, which can be realized by several methods. One of these methods is the so-called radio-frequency identification (RFID), a passive transmitting system. Thereby, a passive tag is attached to the animal, which does not need a battery but uses energy emitted by the reader. The reader records the animal whenever it enters the detection range. As each tag is unique, individuals can be accurately identified. The passive tag is much lighter than a GPS tag and is therefore ideal for tracking small animals such as invertebrates. We are currently developing an RFID tracking system for invertebrates and I plan to use this method to track Carabid beetles in a meta-community system. Due to a trade-off between tag size and distance to the reader, the minimum tag size we can currently use is 30 mg. Consequently, we need beetles weighing a minimum of ~500 mg, which we catch continuously over the vegetation period of the year by pitfall traps. However, tags weighing less than 2mg generally exist and open up new possibilities of tracking smaller species as soon as the reader technology will be advanced. The experimental design comprises a fragmented landscape consisting of several planted pots as habitat patches within a continuous area of plain earth as landscape matrix (Figure D.1). Each plant pot is surrounded by several readers, which detect each individual entering or leaving the patch. These data are recorded by the RFID tracking device and saved to a server, which yields a dynamic real-time meta-community database. This experimental design provides a good basis for addressing questions of dispersal abilities,

species-specific network connectivities, and predator-prey dynamics. For instance, I could test one of the hypotheses made in **Chapter 3**, that the network connectivity (i.e. the percentage of realized dispersal links between pairs of habitat patches) increases with body mass. Therefore, I would simply track beetles over a body-mass range in a fragmented landscape with varying patch size and distance. In addition, an island biogeography experiment could be designed by installing a large patch as the mainland and implementing smaller patches as islands in varying distances from the mainland. By introducing the beetle community in the mainland, the colonization of the patch islands could be tracked and effects of island size and the degree of isolation could be tested. Based on classical island biogeography theory, I would expect higher colonization rates for larger and less isolated islands. The lower the distance to the mainland, the higher the proportion of animals that are able to cover the distance. The larger the island, the higher the statistical chance of an animal to encounter it (MacArthur and Wilson 2016). Additionally, the interactive movements of predator and prey species could be tracked either in a spatial network or in a continuous landscape. Thereby, the effects of predator presence on prey behavior and space use could be generalized from few species (Schmitz et al. 1997, Schmitz 2008) to whole communities.

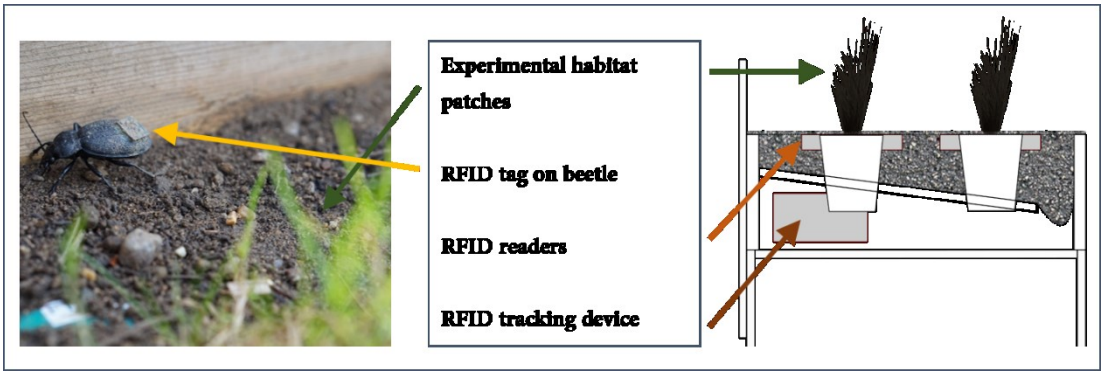

Figure D.1 | Experimental design for tracking invertebrate movement by RFID. The study system consists of several habitat patches (planted pots) within an area of plain earth as unfavorable habitat. The patches are surrounded by readers, which detect all individuals entering or leaving the patch. These events are recorded by the RFID tracking device and saved on an USB storage device.

The metabolism is the most basic physiological process of an animal and therefore affects all other related processes including movement. According to the Metabolic Theory of Ecology, metabolism is not only a function of body mass but also of temperature. This implies that larger animals have a higher metabolic rate than smaller animals, and animals at high body temperatures have higher metabolic rates than animals at low body temperatures. This effect of temperature on metabolism must have implications for movement rates as well. For example, invertebrates should have higher movement speeds in hot than in cold environments. In **Chapter 2**, I tracked invertebrate movement speed in the laboratory by filming. This experimental setup could be ideally used to also test effects of temperature on invertebrate movement speed. Therefore, the experiment could be repeated in environmental chambers at different, controlled temperatures. I would expect that the movement speed increases with increasing temperature in the chamber. Similar tests on network connectivity and temperature could also be performed on microbes or unicells in microcosm experiments with automated tracking systems. Moreover, using microbial systems would enable testing evolutionary effects on movement behavior.

Answering all of these questions is particularly important in the light of global change. First, due to increasing temperatures and human land-use change, habitats are continuously fragmented and modified. Either habitats are completely destroyed forcing animals to disperse in search of new suitable habitat or habitats get fragmented demanding from animals to cover short to long distances across unfavorable or even dangerous areas. Thus, it is crucial to understand how animals connect spatial networks depending on their movement capacity. Second, increasing temperatures directly affect movement rates of ectotherms by affecting their metabolism (Bennett 1990, Abram et al. 2017). Thus, with increasing temperatures, encounter and attack rates of ectotherms will increase (Dell et al. 2011, Gilbert et al. 2014). While the impacts of temperature on the physiology of ectotherms have been extensively studied (Abram et al. 2017), much less is known about how the movement capacity of endotherms reacts to changes in temperature or other environmental conditions. This question could be generally addressed by synthesizing and analyzing global movement tracking data. Therefore, information on vertebrate movement speed could be extracted from global movement databases (Dodge et al. 2013) and be combined with information on former and current environmental conditions such as temperature. Such

an approach would offer a great framework to study endotherm movement in response to temperature on a macro-ecological scale.

Hence, on the basis of this thesis, future research in this field should focus both on further aspects of movement mechanisms ("what is behind it") as well as on advancing our understanding of current natural movement patterns at larger spatial scales by synthesizing global movement and environmental data (big data, "what we see"). Unifying these two research scales will open up new possibilities to predict the implications of future global change for patterns in movement, meta-communities, and biodiversity ("what it tells us"). Such an integrated approach towards understanding and predicting global movement patterns is vital for conserving biodiversity in a changing world.

Appendix

Bibliography

Abram, P. K., G. Boivin, J. Moiroux, and J. Brodeur. 2017. Behavioural effects of temperature on ectothermic animals: unifying thermal physiology and behavioural plasticity. Biological Reviews 92:1859–1876.

Aguzzi, J., V. Sbragaglia, D. Sarriá, J. A. García, C. Costa, J. del Río, A. Mànuel, P. Menesatti, and F. Sardà. 2011. A New Laboratory Radio Frequency Identification (RFID) System for Behavioural Tracking of Marine Organisms. Sensors 11:9532–9548.

Alexander, R. M. 2003. Principles of animal locomotion. Princeton University Press.

Alexander, R. M. 2005. Models and the scaling of energy costs for locomotion. Journal of Experimental Biology 208:1645–1652.

Alexander, R.M., A. S. Jayes, G. M. O. Maloiy, and E. M. Wathuta. 1981. Allometry of the leg muscles of mammals. Journal of Zoology 194:539–552.

Altermatt, F., E. A. Fronhofer, A. Garnier, A. Giometto, F. Hammes, J. Klecka, D. Legrand, E. Mächler, T. M. Massie, F. Pennekamp, M. Plebani, M. Pontarp, N. Schtickzelle, V. Thuillier, and O. L. Petchey. 2015. Big answers from small worlds: a user's guide for protist microcosms as a model system in ecology and evolution. Methods in Ecology and Evolution 6:218–231.

Avgar, T., A. Mosser, G. S. Brown, and J. M. Fryxell. 2012. Environmental and individual drivers of animal movement patterns across a wide geographical gradient. Journal of Animal Ecology 82:96–106.

Bailey, I., J. P. Myatt, and A. M. Wilson. 2013. Group hunting within the Carnivora: physiological, cognitive and environmental influences on strategy and cooperation. Behavioral Ecology and Sociobiology 67:1–17.

Barnes, A. D., I.-K. Spey, L. Rohde, U. Brose, and A. I. Dell. 2015. Individual behaviour mediates effects of warming on movement across a fragmented landscape. Functional Ecology 29:1543–1552.

Bartnick, T. D., T. R. Van Deelen, H. B. Quigley, and D. Craighead. 2013. Variation in cougar (*Puma concolor*) predation habits during wolf (*Canis lupus*) recovery in the southern Greater Yellowstone Ecosystem. Canadian Journal of Zoology 91:82–93.

Bauer, S., and B. J. Hoye. 2014. Migratory animals couple biodiversity and ecosystem functioning worldwide. Science 344:1242552.

Beier, P., D. Choate, and R. Barrett. 1995. Movement Patterns of Mountain Lions During Different Behaviors. Journal of Mammalogy 76:1056–1070.

Bejan, A., and J. H. Marden. 2006. Unifying constructal theory for

scale effects in running, swimming and flying. Journal of Experimental Biology 209:238–248.

Bennett, A. F. 1990. Thermal dependence of locomotor capacity. American Journal of Physiology-Regulatory, Integrative and Comparative Physiology 259:R253–R258.

Bennett, M. B. 1996. Allometry of the leg muscles of birds. Journal of Zoology 238:435–443.

Biewener, A. A. 1982. Bone strength in small mammals and bipedal birds: do safety factors change with body size? Journal of Experimental Biology 98:289–301.

Biewener, A. A. 1983. Allometry of quadrupedal locomotion: the scaling of duty factor, bone curvature and limb orientation to body size. Journal of Experimental Biology 105:147–171.

Biewener, A. A. 2005. Biomechanical consequences of scaling. Journal of Experimental Biology 208:1665–1676.

Blanco, R. E., and W. W. Jones. 2005a. Terror birds on the run: a mechanical model to estimate its maximum running speed. Proceedings of the Royal Society of London B: Biological Sciences 272:1769–1773.

Blanco, R. E., and W. W. Jones. 2005b. Terror birds on the run: a mechanical model to estimate its maximum running speed. Proceedings of the Royal Society B: Biological Sciences 272:1769–1773.

Boesch, C. 1994. Cooperative hunting in wild chimpanzees. Animal Behaviour 48:653–667.

Boit, A., N. D. Martinez, R. J. Williams, and U. Gaedke. 2012. Mechanistic theory and modelling of complex food-web dynamics in Lake Constance. Ecology letters 15:594–602.

Bonte, D., H. Van Dyck, J. M. Bullock, A. Coulon, M. Delgado, M. Gibbs, V. Lehouck, E. Matthysen, K. Mustin, and M. Saastamoinen. 2012. Costs of dispersal. Biological Reviews 87:290–312.

Borthagaray, A. I., M. Arim, and P. A. Marquet. 2012. Connecting landscape structure and patterns in body size distributions. Oikos 121:697–710.

Bro-Jørgensen, J. 2013. Evolution Of Sprint Speed In African Savannah Herbivores In Relation To Predation. Evolution 67:3371–3376.

Brose, U. 2010. Body-mass constraints on foraging behaviour determine population and food-web dynamics. Functional Ecology 24:28–34.

Brose, U., J. L. Blanchard, A. Eklöf, N. Galiana, M. Hartvig, M. R. Hirt, G. Kalinkat, M. C. Nordström, E. J. O'Gorman, B. C. Rall, F. D. Schneider, E. Thébault, and U. Jacob. 2017. Predicting the

consequences of species loss using size-structured biodiversity approaches. Biological Reviews 92:684–697.

Brose, U., T. Jonsson, E. L. Berlow, P. Warren, C. Banasek-Richter, L.-F. Bersier, J. L. Blanchard, T. Brey, S. R. Carpenter, M.-F. C. Blandenier, L. Cushing, H. A. Dawah, T. Dell, F. Edwards, S. Harper-Smith, U. Jacob, M. E. Ledger, N. D. Martinez, J. Memmott, K. Mintenbeck, J. K. Pinnegar, B. C. Rall, T. S. Rayner, D. C. Reuman, L. Ruess, W. Ulrich, R. J. Williams, G. Woodward, and J. E. Cohen. 2006a. Consumer–Resource Body-Size Relationships In Natural Food Webs. Ecology 87:2411–2417.

Brose, U., A. Ostling, K. Harrison, and N. D. Martinez. 2004. Unified spatial scaling of species and their trophic interactions. Nature 428:167–171.

Brose, U., R. J. Williams, and N. D. Martinez. 2006b. Allometric scaling enhances stability in complex food webs. Ecology letters 9:1228–1236.

Brown, D. D., R. Kays, M. Wikelski, R. Wilson, and A. P. Klimley. 2013. Observing the unwatchable through acceleration logging of animal behavior. Animal Biotelemetry 1:20.

Brown, J. H., J. F. Gillooly, A. P. Allen, V. M. Savage, and G. B. West. 2004. Toward a metabolic theory of ecology. Ecology 85:1771–1789.

Burness, G. P., J. Diamond, and T. Flannery. 2001. Dinosaurs, dragons, and dwarfs: The evolution of maximal body size. Proceedings of the National Academy of Sciences 98:14518–14523.

Capellini, I., C. Venditti, and R. A. Barton. 2010. Phylogeny and metabolic scaling in mammals. Ecology 91:2783–2793.

Carbone, C., G. Cowlishaw, N. J. B. Isaac, and J. M. Rowcliffe. 2005. How Far Do Animals Go? Determinants of Day Range in Mammals. The American Naturalist 165:290–297.

Carbone, C., A. Teacher, and J. M. Rowcliffe. 2007. The costs of carnivory. PLoS biology 5:e22.

Caro, T. 2005. Antipredator Defenses in Birds and Mammals. University of Chicago Press.

Clemente, C. J., and C. Richards. 2013. Muscle function and hydrodynamics limit power and speed in swimming frogs. Nature communications 4.

Clemente, C. J., G. G. Thompson, and P. C. Withers. 2009. Evolutionary relationships of sprint speed in Australian varanid lizards. Journal of Zoology 278:270–280.

Clemente, C. J., P. C. Withers, and G. Thompson. 2012. Optimal body size with respect to maximal speed for the yellow-spotted monitor lizard *(Varanus panoptes*; Varanidae).

Physiological and Biochemical Zoology 85:265–273.

Codling, E. A., M. J. Plank, and S. Benhamou. 2008. Random walk models in biology. Journal of the Royal Society Interface 5:813–834.

Colwell, R. K., G. Brehm, C. L. Cardelús, A. C. Gilman, and J. T. Longino. 2008. Global warming, elevational range shifts, and lowland biotic attrition in the wet tropics. science 322:258–261.

Cortez, M. H. 2011. Comparing the qualitatively different effects rapidly evolving and rapidly induced defences have on predator–prey interactions. Ecology Letters 14:202–209.

Crawley, M. J. 2009. Natural Enemies: The Population Biology of Predators, Parasites and Diseases. John Wiley & Sons.

Creel, S. 1997. Cooperative hunting and group size: assumptions and currencies. Elsevier.

Creel, S., and N. M. Creel. 1995. Communal hunting and pack size in African wild dogs, Lycaon pictus. Animal Behaviour 50:1325–1339.

Cresswell, W., J. Lind, and J. L. Quinn. 2010. Predator-hunting success and prey vulnerability: quantifying the spatial scale over which lethal and non-lethal effects of predation occur. Journal of Animal Ecology 79:556–562.

Curtsdotter, A., A. Binzer, U. Brose, F. de Castro, B. Ebenman, A. Eklöf, J. O. Riede, A. Thierry, and B. C. Rall. 2011. Robustness to secondary extinctions: Comparing trait-based sequential deletions in static and dynamic food webs. Basic and Applied Ecology 12:571–580.

Davies, K. F., B. A. Melbourne, and C. R. Margules. 2001. Effects of within-and between-patch processes on community dynamics in a fragmentation experiment. Ecology 82:1830–1846.

Dejours, P. 1987. Comparative physiology: life in water and on land. Springer Science & Business Media.

Dell, A. I., J. A. Bender, K. Branson, I. D. Couzin, G. G. de Polavieja, L. P. Noldus, A. Pérez-Escudero, P. Perona, A. D. Straw, M. Wikelski, and others. 2014a. Automated image-based tracking and its application in ecology. Trends in Ecology & Evolution 29:417–428.

Dell, A. I., S. Pawar, and V. M. Savage. 2011. Systematic variation in the temperature dependence of physiological and ecological traits. Proceedings of the National Academy of Sciences 108:10591–10596.

Dell, A. I., S. Pawar, and V. M. Savage. 2014b. Temperature dependence of trophic interactions are driven by asymmetry of species

responses and foraging strategy. Journal of Animal Ecology 83:70–84.

Dial, K. P., E. Greene, and D. J. Irschick. 2008. Allometry of behavior. Trends in ecology & evolution 23:394–401.

Dick, T. J., and C. J. Clemente. 2017. Where Have All the Giants Gone? How Animals Deal with the Problem of Size. PLoS biology 15:e2000473.

Dodge, S., G. Bohrer, R. Weinzierl, S. C. Davidson, R. Kays, D. Douglas, S. Cruz, J. Han, D. Brandes, and M. Wikelski. 2013. The environmental-data automated track annotation (Env-DATA) system: linking animal tracks with environmental data. Movement Ecology 1:3.

Domenici, P. 2001. The scaling of locomotor performance in predator–prey encounters: from fish to killer whales. Comparative Biochemistry and Physiology Part A: Molecular & Integrative Physiology 131:169–182.

Domenici, P., J. M. Blagburn, and J. P. Bacon. 2011. Animal escapology II: escape trajectory case studies. Journal of Experimental Biology 214:2474–2494.

Domenici, P., D. Booth, J. M. Blagburn, and J. P. Bacon. 2008. Cockroaches Keep Predators Guessing by Using Preferred Escape Trajectories. Current Biology 18:1792–1796.

Dunne, J. A., R. J. Williams, and N. D. Martinez. 2002. Network structure and biodiversity loss in food webs: robustness increases with connectance. Ecology letters 5:558–567.

Ehnes, R. B., B. C. Rall, and U. Brose. 2011. Phylogenetic grouping, curvature and metabolic scaling in terrestrial invertebrates. Ecology Letters 14:993–1000.

Eklöf, A., U. Jacob, J. Kopp, J. Bosch, R. Castro-Urgal, N. P. Chacoff, B. Dalsgaard, C. Sassi, M. Galetti, and P. R. Guimaraes. 2013a. The dimensionality of ecological networks. Ecology letters 16:577–583.

Eklöf, A., S. Tang, and S. Allesina. 2013b. Secondary extinctions in food webs: a Bayesian network approach. Methods in Ecology and Evolution 4:760–770.

Elliott, J. P., I. M. Cowan, and C. S. Holling. 1977. Prey capture by the African lion. Canadian Journal of Zoology 55:1811–1828.

Emmons, L. H. 1987. Comparative feeding ecology of felids in a neotropical rainforest. Behavioral Ecology and Sociobiology 20:271–283.

Forsythe, T. G. 1983. Locomotion in ground beetles (Coleoptera Carabidae): an interpretation of leg structure in functional terms. Journal of Zoology 200:493–507.

Fryxell, J. M., A. Mosser, A. R. E. Sinclair, and C. Packer. 2007. Group formation stabilizes

predator–prey dynamics. Nature 449:1041–1043.

Fryxell, J. M., J. F. Wilmshurst, and A. R. E. Sinclair. 2004. Predictive models of movement by serengeti grazers. Ecology 85:2429–2435.

Fuentes, M. A. 2016. Theoretical considerations on maximum running speeds for large and small animals. Journal of theoretical biology 390:127–135.

Gallagher, A. J., S. Creel, R. P. Wilson, and S. J. Cooke. 2017. Energy landscapes and the landscape of fear. Trends in ecology & evolution 32:88–96.

Garcia, G. J., and J. K. da Silva. 2004. On the scaling of mammalian long bones. Journal of Experimental Biology 207:1577–1584.

Garland, T. 1983. The relation between maximal running speed and body mass in terrestrial mammals. Journal of Zoology 199:157–170.

Gelman, A., and J. Hill. 2007. Data analysis using regression and multilevelhierarchical models. Cambridge University Press New York, NY, USA.

Gilbert, B., T. D. Tunney, K. S. McCann, J. P. DeLong, D. A. Vasseur, V. Savage, J. B. Shurin, A. I. Dell, B. T. Barton, C. D. G. Harley, H. M. Kharouba, P. Kratina, J. L. Blanchard, C. Clements, M. Winder, H. S. Greig, and M. I. O'Connor. 2014. A bioenergetic framework for the temperature dependence of trophic interactions. Ecology Letters 17:902–914.

Gillooly, J. F., J. H. Brown, G. B. West, V. M. Savage, and E. L. Charnov. 2001. Effects of Size and Temperature on Metabolic Rate. Science 293:2248–2251.

van Gils, J. A., M. van der Geest, B. De Meulenaer, H. Gillis, T. Piersma, and E. O. Folmer. 2015. Moving on with foraging theory: incorporating movement decisions into the functional response of a gregarious shorebird. Journal of Animal Ecology 84:554–564.

Gross, T., L. Rudolf, S. A. Levin, and U. Dieckmann. 2009. Generalized models reveal stabilizing factors in food webs. Science 325:747–750.

Haddad, N. M., L. A. Brudvig, J. Clobert, K. F. Davies, A. Gonzalez, R. D. Holt, T. E. Lovejoy, J. O. Sexton, M. P. Austin, C. D. Collins, W. M. Cook, E. I. Damschen, R. M. Ewers, B. L. Foster, C. N. Jenkins, A. J. King, W. F. Laurance, D. J. Levey, C. R. Margules, B. A. Melbourne, A. O. Nicholls, J. L. Orrock, D.-X. Song, and J. R. Townshend. 2015. Habitat fragmentation and its lasting impact on Earth's ecosystems. Science Advances 1:e1500052.

Hamilton, W. D., and R. M. May. 1977. Dispersal in stable habitats. Nature 269:578–581.

Haskell, J. P., M. E. Ritchie, and H. Olff. 2002. Fractal geometry predicts varying body size scaling relationships for mammal and bird home ranges. Nature 418:527.

Hayward, M. W., and G. I. H. Kerley. 2005. Prey preferences of the lion (*Panthera leo*). Journal of Zoology 267:309–322.

Hedenström, A. 2003. Scaling migration speed in animals that run, swim and fly. Journal of Zoology 259:155–160.

Hedenström, A., and M. Rosén. 2001. Predator versus prey: on aerial hunting and escape strategies in birds. Behavioral Ecology 12:150–156.

Hein, A. M., C. Hou, and J. F. Gillooly. 2012. Energetic and biomechanical constraints on animal migration distance. Ecology letters 15:104–110.

Hirt, M. R., W. Jetz, B. C. Rall, and U. Brose. 2017a. A general scaling law reveals why the largest animals are not the fastest. Nature ecology & evolution 1:1116–1122.

Hirt, M. R., T. Lauermann, U. Brose, L. P. Noldus, and A. I. Dell. 2017b. The little things that run: a general scaling of invertebrate exploratory speed with body mass. Ecology 98:2751–2757.

Hochkirch, A. 2016. The insect crisis we can't ignore. Nature 539:141.

Holland, M. D., and A. Hastings. 2008. Strong effect of dispersal network structure on ecological dynamics. Nature 456:792.

Huang, J., H. Yu, X. Guan, G. Wang, and R. Guo. 2016. Accelerated dryland expansion under climate change. Nature Climate Change 6:166–171.

Hubbell, S. P. 2001. The Unified Neutral Theory of Biodiversity and Biogeography. Princeton University Press, Princeton, NJ.

Hudson, L. N., and D. C. Reuman. 2013. A cure for the plague of parameters: constraining models of complex population dynamics with allometries. Page 20131901 Proc. R. Soc. B. The Royal Society.

Huey, R. B., and P. E. Hertz. 1984. Effects of body size and slope on acceleration of a lizard (*Stellio stellio*). Journal of Experimental Biology 110:113–123.

Hurlbert, A. H., F. Ballantyne, and S. Powell. 2008. Shaking a leg and hot to trot: the effects of body size and temperature on running speed in ants. Ecological Entomology 33:144–154.

Husseman, J. S., D. L. Murray, G. Power, C. Mack, C. R. Wenger, and H. Quigley. 2003. Assessing differential prey selection patterns between two sympatric large carnivores. Oikos 101:591–601.

Hussey, N. E., S. T. Kessel, K. Aarestrup, S. J. Cooke, P. D. Cowley, A. T. Fisk, R. G. Harcourt, K. N. Holland, S. J. Iverson, J. F. Kocik, J. E. Mills Flemming, and F. G.

Whoriskey. 2015. Aquatic animal telemetry: A panoramic window into the underwater world. Science 348:1255642–1255642.

Hutchinson, J. R., and M. Garcia. 2002. Tyrannosaurus was not a fast runner. Nature 415:1018–1021.

Iriarte-Díaz, J. 2002. Differential scaling of locomotor performance in small and large terrestrial mammals. Journal of Experimental Biology 205:2897–2908.

Jaksić, F. M. 1982. Inadequacy of activity time as a niche difference: the case of diurnal and nocturnal raptors. Oecologia 52:171–175.

Jeltsch, F., D. Bonte, G. Pe'er, B. Reineking, P. Leimgruber, N. Balkenhol, B. Schröder, C. M. Buchmann, T. Mueller, and N. Blaum. 2013. Integrating movement ecology with biodiversity research-exploring new avenues to address spatiotemporal biodiversity dynamics. Movement Ecology 1:6.

Jenkins, D. G., C. R. Brescacin, C. V. Duxbury, J. A. Elliott, J. A. Evans, K. R. Grablow, M. Hillegass, B. N. Lyon, G. A. Metzger, and M. L. Olandese. 2007. Does size matter for dispersal distance? Global Ecology and Biogeography 16:415–425.

Jessup, C. M., R. Kassen, S. E. Forde, B. Kerr, A. Buckling, P. B. Rainey, and B. J. M. Bohannan. 2004. Big questions, small worlds: microbial model systems in ecology. Trends in Ecology & Evolution 19:189–197.

Jetz, W., C. Carbone, J. Fulford, and J. H. Brown. 2004. The scaling of animal space use. Science 306:266–268.

Jones, J. H., and S. L. Lindstedt. 1993. Limits to maximal performance. Annual Review of Physiology 55:547–569.

Jonsen, I. D., M. Basson, S. Bestley, M. V. Bravington, T. A. Patterson, M. W. ever Pedersen, R. Thomson, U. H. Thygesen, and S. J. Wotherspoon. 2013. State-space models for bio-loggers: A methodological road map. Deep Sea Research Part II: Topical Studies in Oceanography 88:34–46.

Kalinkat, G., M. Jochum, U. Brose, and A. I. Dell. 2015. Body size and the behavioral ecology of insects: linking individuals to ecological communities. Current Opinion in Insect Science 9:24–30.

Kalinkat, G., F. D. Schneider, C. Digel, C. Guill, B. C. Rall, and U. Brose. 2013. Body masses, functional responses and predator–prey stability. Ecology letters 16:1126–1134.

Kays, R., M. C. Crofoot, W. Jetz, and M. Wikelski. 2015. Terrestrial animal tracking as an eye on life and planet. Science 348:aaa2478–aaa2478.

Kelt, D. A., and D. H. van Vuren. 2001. The Ecology and Macroecology of Mammalian Home Range Area. The American Naturalist 157:637–645.

Kissling, W. D. 2015. Animal telemetry: Follow the insects. Science 349:597–597.

Kissling, W. D., D. E. Pattemore, and M. Hagen. 2014. Challenges and prospects in the telemetry of insects. Biological Reviews 89:511–530.

Kolokotrones, T., V. Savage, E. J. Deeds, and W. Fontana. 2010. Curvature in metabolic scaling. Nature 464:753–756.

Kramer-Schadt, S., E. Revilla, T. Wiegand, and U. R. S. Breitenmoser. 2004. Fragmented landscapes, road mortality and patch connectivity: modelling influences on the dispersal of Eurasian lynx. Journal of Applied Ecology 41:711–723.

Krofel, M. 2008. Survey of golden jackals (*Canis aureus* L.) in Northern Dalmatia, Croatia: preliminary results. Natura Croatica 17:259–264.

Kruuk, H. 1972. The spotted hyena: a study of predation and social behavior.

Lang, B., R. B. Ehnes, U. Brose, and B. C. Rall. 2017. Temperature and consumer type dependencies of energy flows in natural communities. Oikos.

Lang, B., B. C. Rall, and U. Brose. 2012. Warming effects on consumption and intraspecific interference competition depend on predator metabolism. Journal of Animal Ecology 81:516–523.

Laundré, J. W., L. Hernández, and W. J. Ripple. 2010. The landscape of fear: ecological implications of being afraid. Open Ecology Journal 3:1–7.

Leibold, M. A., and J. M. Chase. 2017. Metacommunity Ecology. Princeton University Press.

Li, Y., U. Brose, K. Meyer, and B. C. Rall. 2017. How patch size and refuge availability change interaction strength and population dynamics: a combined individual-and population-based modeling experiment. PeerJ 5:e2993.

Li, Y., B. C. Rall, and G. Kalinkat. 2018. Experimental duration and predator satiation levels systematically affect functional response parameters. Oikos 127:590–598.

Lima, S. L. 1998. Stress and Decision Making under the Risk of Predation: Recent Developments from Behavioral, Reproductive, and Ecological Perspectives. Pages 215–290 *in* A. P. Møller, M. Milinski, and P. J. B. Slater, editors. Advances in the Study of Behavior. Academic Press.

Lima, S. L. 2002. Putting predators back into behavioral predator–prey interactions. Trends in Ecology & Evolution 17:70–75.

Lührs, M.-L., and M. Dammhahn. 2010. An unusual case of cooperative

hunting in a solitary carnivore. Journal of Ethology 28:379–383.

MacArthur, R. H., and E. O. Wilson. 1963. An equilibrium theory of insular zoogeography. Evolution 17:373–387.

MacArthur, R. H., and E. O. Wilson. 2016. The Theory of Island Biogeography. Princeton University Press.

Maloiy, G. M. O., R. Alexander, R. Njau, and A. S. Jayes. 1979. Allometry of the legs of running birds. Journal of Zoology 187:161–167.

Massol, F., D. Gravel, N. Mouquet, M. W. Cadotte, T. Fukami, and M. A. Leibold. 2011. Linking community and ecosystem dynamics through spatial ecology. Ecology Letters 14:313–323.

May, R. M. 1972. Will a large complex system be stable? Nature 238:413.

McCann, K., A. Hastings, and G. R. Huxel. 1998. Weak trophic interactions and the balance of nature. Nature 395:794.

McIntyre, N. E., and J. A. Wiens. 1999. Interactions between landscape structure and animal behavior: the roles of heterogeneously distributed resources and food deprivation on movement patterns. Landscape Ecology 14:437–447.

Mech, L. D., and L. Boitani. 2003. Wolf social ecology.

Miller, J. R., J. M. Ament, and O. J. Schmitz. 2014. Fear on the move: predator hunting mode predicts variation in prey mortality and plasticity in prey spatial response. Journal of Animal Ecology 83:214–222.

Mitchell, W. A., and S. L. Lima. 2002. Predator-prey shell games: large-scale movement and its implications for decision-making by prey. Oikos 99:249–259.

Mittelbach, G. G. 1981. Foraging efficiency and body size: a study of optimal diet and habitat use by bluegills. Ecology 62:1370–1386.

Muntz, E. M., and B. R. Patterson. 2004. Evidence for the use of vocalization to coordinate the killing of a white-tailed deer, *Odocoileus virginianus*, by coyotes, *Canis latrans*. The Canadian Field-Naturalist 118:278–280.

Myhrvold, N. P., E. Baldridge, B. Chan, D. Sivam, D. L. Freeman, and S. K. Ernest. 2015. An amniote life-history database to perform comparative analyses with birds, mammals, and reptiles. Ecology 96:3109–3109.

Nathan, R., W. M. Getz, E. Revilla, M. Holyoak, R. Kadmon, D. Saltz, and P. E. Smouse. 2008. A movement ecology paradigm for unifying organismal movement research. Proceedings of the National Academy of Sciences 105:19052–19059.

Neutel, A.-M., J. A. P. Heesterbeek, J. van de Koppel, G.

Hoenderboom, A. Vos, C. Kaldeway, F. Berendse, and P. C. de Ruiter. 2007. Reconciling complexity with stability in naturally assembling food webs. Nature 449:599–602.

Newbold, T., L. N. Hudson, S. L. L. Hill, S. Contu, I. Lysenko, R. A. Senior, L. Börger, D. J. Bennett, A. Choimes, B. Collen, J. Day, A. D. Palma, S. Díaz, S. Echeverria-Londoño, M. J. Edgar, A. Feldman, M. Garon, M. L. K. Harrison, T. Alhusseini, D. J. Ingram, Y. Itescu, J. Kattge, V. Kemp, L. Kirkpatrick, M. Kleyer, D. L. P. Correia, C. D. Martin, S. Meiri, M. Novosolov, Y. Pan, H. R. P. Phillips, D. W. Purves, A. Robinson, J. Simpson, S. L. Tuck, E. Weiher, H. J. White, R. M. Ewers, G. M. Mace, J. P. W. Scharlemann, and A. Purvis. 2015. Global effects of land use on local terrestrial biodiversity. Nature 520:45–50.

Norberg, J., M. C. Urban, M. Vellend, C. A. Klausmeier, and N. Loeuille. 2012. Eco-evolutionary responses of biodiversity to climate change. Nature Climate Change 2:747.

Packer, C. 1986. The ecology of sociality in felids. Ecological aspects of social evolution:429–451.

Packer, C., and L. Ruttan. 1988. The Evolution of Cooperative Hunting. The American Naturalist 132:159–198.

Packer, C., D. Scheel, and A. E. Pusey. 2015. Why Lions Form Groups: Food is Not Enough. The American Naturalist.

Parmesan, C., N. Ryrholm, C. Stefanescu, J. K. Hill, C. D. Thomas, H. Descimon, B. Huntley, L. Kaila, J. Kullberg, T. Tammaru, W. J. Tennent, J. A. Thomas, and M. Warren. 1999. Poleward shifts in geographical ranges of butterfly species associated with regional warming. Nature 399:579–583.

Parmesan, C., and G. Yohe. 2003. A globally coherent fingerprint of climate change impacts across natural systems. Nature 421:37–42.

Pawar, S., A. I. Dell, and V. M. Savage. 2012. Dimensionality of consumer search space drives trophic interaction strengths. Nature 486:485–489.

Pennekamp, F., J. I. Griffiths, E. A. Fronhofer, A. Garnier, M. Seymour, F. Altermatt, and O. L. Petchey. 2017. Dynamic species classification of microorganisms across time, abiotic and biotic environments—A sliding window approach. PLOS ONE 12:e0176682.

Pennekamp, F., and N. Schtickzelle. 2013. Implementing image analysis in laboratory-based experimental systems for ecology and evolution: a hands-on guide. Methods in Ecology and Evolution 4:483–492.

Pennycuick, C. 1997. Actual and "optimum" flight speeds: field data reassessed. The Journal of

Experimental Biology 200:2355–2361.

Petchey, O. L., A. P. Beckerman, J. O. Riede, and P. H. Warren. 2008. Size, foraging, and food web structure. Proceedings of the National Academy of Sciences 105:4191–4196.

Peters, R. H. 1986. The ecological implications of body size. Cambridge University Press, Cambridge.

Polidori, C., D. Santoro, and N. Blüthgen. 2013. Does prey mobility affect niche width and individual specialization in hunting wasps? A network-based analysis. Oikos 122:385–394.

Pollock, C. M., and R. E. Shadwick. 1994. Allometry of muscle, tendon, and elastic energy storage capacity in mammals. American Journal of Physiology-Regulatory, Integrative and Comparative Physiology 266:R1022–R1031.

Preisser, E. L., J. L. Orrock, and O. J. Schmitz. 2007. Predator hunting mode and habitat domain alter nonconsumptive effects in predator–prey interactions. Ecology 88:2744–2751.

R Core Team. 2015. R: A language and environment for statistical computing. R Foundation for Statistical Computing, Vienna, Austria.

Radloff, F. G., and J. T. Du Toit. 2004. Large predators and their prey in a southern African savanna: a predator's size determines its prey size range. Journal of Animal Ecology 73:410–423.

Rall, B. C., U. Brose, M. Hartvig, G. Kalinkat, F. Schwarzmüller, O. Vucic-Pestic, and O. L. Petchey. 2012. Universal temperature and body-mass scaling of feeding rates. Philosophical Transactions of the Royal Society of London B: Biological Sciences 367:2923–2934.

Rattenborg, N. C., B. Voirin, A. L. Vyssotski, R. W. Kays, K. Spoelstra, F. Kuemmeth, W. Heidrich, and M. Wikelski. 2008. Sleeping outside the box: electroencephalographic measures of sleep in sloths inhabiting a rainforest. Biology Letters 4:402–405.

Reed, M. S., and L. C. Stringer. 2016. Land Degradation, Desertification and Climate Change: Anticipating, assessing and adapting to future change. Routledge.

Reuman, D. C., C. Mulder, C. Banašek-Richter, M.-F. C. Blandenier, A. M. Breure, H. Den Hollander, J. M. Kneitel, D. Raffaelli, G. Woodward, and J. E. Cohen. 2009. Allometry of body size and abundance in 166 food webs. Advances in Ecological Research 41:1–44.

Rezende, E. L., J. E. Lavabre, P. R. Guimarães, P. Jordano, and J. Bascompte. 2007. Non-random coextinctions in phylogenetically

structured mutualistic networks. Nature 448:925.

Ripple, W. J., and R. L. Beschta. 2004. Wolves and the ecology of fear: can predation risk structure ecosystems? AIBS Bulletin 54:755–766.

Ripple, W. J., E. J. Larsen, R. A. Renkin, and D. W. Smith. 2001. Trophic cascades among wolves, elk and aspen on Yellowstone National Park's northern range. Biological Conservation 102:227–234.

Ropert-Coudert, Y., and R. P. Wilson. 2005. Trends and perspectives in animal-attached remote sensing. Frontiers in Ecology and the Environment 3:437–444.

Savage, V. M., J. F. Gillooly, J. H. Brown, G. B. West, and E. L. Charnov. 2004. Effects of Body Size and Temperature on Population Growth. The American Naturalist 163:429–441.

Scharf, I., E. Nulman, O. Ovadia, and A. Bouskila. 2015. Efficiency Evaluation of Two Competing Foraging Modes under Different Conditions. The American Naturalist.

Scheel, D. 1993. Profitability, encounter rates, and prey choice of African lions. Behavioral Ecology 4:90–97.

Schmidt-Nielsen, K. 1984. Scaling: why is animal size so important? Cambridge University Press.

Schmitz, O. J. 2007. Predator diversity and trophic interactions. Ecology 88:2415–2426.

Schmitz, O. J. 2008. Effects of Predator Hunting Mode on Grassland Ecosystem Function. Science 319:952–954.

Schmitz, O. J., Beckerman Andrew P., and O'Brien Kathleen M. 1997. Behaviorally mediated trophic cascades: effects of predation risk on food web interactions. Ecology 78:1388–1399.

Schmitz, O. J., V. Krivan, and O. Ovadia. 2004. Trophic cascades: the primacy of trait-mediated indirect interactions. Ecology Letters 7:153–163.

Schmitz, O. J., J. R. B. Miller, A. M. Trainor, and B. Abrahms. 2017. Toward a community ecology of landscapes: predicting multiple predator–prey interactions across geographic space. Ecology 98:2281–2292.

Schneider, F. D., U. Brose, B. C. Rall, and C. Guill. 2016. Animal diversity and ecosystem functioning in dynamic food webs. Nature Communications 7.

Schneider, F. D., S. Scheu, and U. Brose. 2012. Body mass constraints on feeding rates determine the consequences of predator loss. Ecology Letters 15:436–443.

Sellers, W. I., and P. L. Manning. 2007a. Estimating dinosaur maximum running speeds using evolutionary robotics. Proceedings of the Royal Society of London B: Biological Sciences 274:2711–2716.

Sellers, W. I., and P. L. Manning. 2007b. Estimating dinosaur maximum

running speeds using evolutionary robotics. Proceedings of the Royal Society of London B: Biological Sciences 274:2711–2716.

Signer, C., T. Ruf, F. Schober, G. Fluch, T. Paumann, and W. Arnold. 2010. A versatile telemetry system for continuous measurement of heart rate, body temperature and locomotor activity in free-ranging ruminants. Methods in Ecology and Evolution 1:75–85.

Sillero-Zubiri, C., and D. Gottelli. 1995. Diet and Feeding Behavior of Ethiopian Wolves (*Canis simensis*). Journal of Mammalogy 76:531–541.

Skellam, J. G. 1991. Random dispersal in theoretical populations. Bulletin of Mathematical Biology 53:135–165.

Stamps, J., and T. G. G. Groothuis. 2010. The development of animal personality: relevance, concepts and perspectives. Biological Reviews 85:301–325.

Stan Development Team. 2017. RStan: the R interface to Stan. R package version 2.16.2. http://mc-stan.org.

Stander, P. E. 1992. Cooperative hunting in lions: the role of the individual. Behavioral ecology and sociobiology 29:445–454.

Sutherland, G. D., A. S. Harestad, K. Price, and K. P. Lertzman. 2000. Scaling of natal dispersal distances in terrestrial birds and mammals. Conservation ecology 4:16.

Tamburello, N., I. M. Côté, and N. K. Dulvy. 2015. Energy and the scaling of animal space use. The American Naturalist 186:196–211.

Teitelbaum, C. S., W. F. Fagan, C. H. Fleming, G. Dressler, J. M. Calabrese, P. Leimgruber, and T. Mueller. 2015. How far to go? Determinants of migration distance in land mammals. Ecology Letters 18:545–552.

Thuiller, W., T. Münkemüller, S. Lavergne, D. Mouillot, N. Mouquet, K. Schiffers, and D. Gravel. 2013. A road map for integrating eco-evolutionary processes into biodiversity models. Ecology letters 16:94–105.

Thulborn, R. A. 1982. Speeds and gaits of dinosaurs. Palaeogeography, Palaeoclimatology, Palaeoecology 38:227–256.

Tucker, M. A., and T. L. Rogers. 2014. Examining predator–prey body size, trophic level and body mass across marine and terrestrial mammals. Proceedings of the Royal Society of London B: Biological Sciences 281:20142103.

Urban, D., and T. Keitt. 2001. Landscape connectivity: a graph-theoretic perspective. Ecology 82:1205–1218.

Urbano, F., F. Cagnacci, C. Calenge, H. Dettki, A. Cameron, and M.

Neteler. 2010. Wildlife tracking data management: a new vision. Philosophical Transactions of the Royal Society B: Biological Sciences 365:2177–2185.

Van Damme, R., and B. Vanhooydonck. 2001. Origins of interspecific variation in lizard sprint capacity. Functional Ecology 15:186–202.

Van Moorter, B., N. Bunnefeld, M. Panzacchi, C. M. Rolandsen, E. J. Solberg, and B.-E. Sæther. 2013. Understanding scales of movement: animals ride waves and ripples of environmental change. Journal of Animal Ecology 82:770–780.

Walker, J. A., C. K. Ghalambor, O. L. Griset, D. McKenney, and D. N. Reznick. 2005. Do faster starts increase the probability of evading predators? Functional Ecology 19:808–815.

Warton, D. I., I. J. Wright, D. S. Falster, and M. Westoby. 2006. Bivariate line-fitting methods for allometry. Biological Reviews 81:259–291.

Werner, E. E., and B. R. Anholt. 1993. Ecological consequences of the trade-off between growth and mortality rates mediated by foraging activity. The American Naturalist 142:242–272.

West, G. B., J. H. Brown, and B. J. Enquist. 1997. A General Model for the Origin of Allometric Scaling Laws in Biology. Science 276:122–126.

Weyand, P. G., and M. W. Bundle. 2005. Energetics of high-speed running: integrating classical theory and contemporary observations. American Journal of Physiology - Regulatory, Integrative and Comparative Physiology 288:R956–R965.

White, C. R. 2010. Physiology: There is no single *p*. Nature 464:691–693.

Wikelski, M., R. W. Kays, N. J. Kasdin, K. Thorup, J. A. Smith, and G. W. Swenson. 2007. Going wild: what a global small-animal tracking system could do for experimental biologists. Journal of Experimental Biology 210:181–186.

Williams, T. M. 1999. The evolution of cost efficient swimming in marine mammals: limits to energetic optimization. Philosophical Transactions of the Royal Society of London B: Biological Sciences 354:193–201.

Wilson, A. M., T. Y. Hubel, S. D. Wilshin, J. C. Lowe, M. Lorenc, O. P. Dewhirst, H. L. Bartlam-Brooks, R. Diack, E. Bennitt, and K. A. Golabek. 2018. Biomechanics of predator–prey arms race in lion, zebra, cheetah and impala. Nature 554:183.

Wilson, A. M., J. C. Lowe, K. Roskilly, P. E. Hudson, K. A. Golabek, and J. W. McNutt. 2013. Locomotion dynamics of hunting in wild cheetahs. Nature 498:185.

Wilson, E. O. 1987. The Little Things That Run the World (The Importance and Conservation of

Invertebrates). Conservation Biology 1:344–346.

Wilson, R. P., I. W. Griffiths, M. G. Mills, C. Carbone, J. W. Wilson, and D. M. Scantlebury. 2015. Mass enhances speed but diminishes turn capacity in terrestrial pursuit predators. Elife 4.

With, K. A., R. H. Gardner, and M. G. Turner. 1997. Landscape connectivity and population distributions in heterogeneous environments. Oikos:151–169.

Woodward, G., B. Ebenman, M. Emmerson, J. M. Montoya, J. M. Olesen, A. Valido, and P. H. Warren. 2005. Body size in ecological networks. Trends in ecology & evolution 20:402–409.

Supplementary Information for Research Chapter 1

Hirt, M. R., W. Jetz, B. C. Rall, and U. Brose. 2017. “A general scaling law reveals why the largest animals are not the fastest”. Nature Ecology & Evolution 1:1116 –1122.

Supplementary Table 1.1 | Distribution of data across movement types and taxa.

movement mode	taxonomic group	n data points
running	arthropods	50
	birds	3
	mammals	261
	reptiles	144
flying	arthropods	19
	birds	29
	mammals	7
swimming	arthropods	1
	birds	5
	fish	81
	mammals	16
	mollusks	5
	reptiles	1

Supplementary Table 1.2 | Distribution of data across study and publication types.

study type	nbr. of data points
field study	33
laboratory study	119
meta-study	404
unclear	66

Supplementary Table 1.3 | ΔBIC values for comparing the seven speed models. Taxonomic groups comprise arthropods, birds, fish, mammals, mollusks, reptiles.

models	Δ BIC		
	flying	running	swimming
time-dependent model	0	0	0
polynomial	6.79	118.20	19.51
polynomial (* taxon)	17.96	15.97	24.90
polynomial (+ taxon)	8.03	78.60	18.81
power law (* taxon)	12.90	122.57	8.82
power law (+ taxon)	13.52	112.38	25.55
power law	11.95	191.66	46.48

Note that for the time-dependent model, taxon could not be directly included because of the complexity of fitting a non-linear model with four free parameters. Therefore, we conducted a residual analysis (see main text).

Supplementary Table 1.4 | Fitted values of the time-dependent maximum speed model: parameters a, b, h and i (from Eq. 5) with standard errors and resulting equations for the different movement modes (flying, running, swimming). Body mass M in kg and speed v in km h^{-1}.

movement mode	a	b	h	i	equation ($v_{real} =$)
flying	142.8 ± 16.7	0.24 ± 0.01	2.4 ± 1.4	-0.72 ± 0.26	$142.8\ M^{0.24}(1 - e^{-2.4\ M^{-0.72}})$
running	25.5 ± 0.84	0.26 ± 0.006	22 ± 7.6	-0.6 ± 0.05	$25.5\ M^{0.26}(1 - e^{-22\ M^{-0.6}})$
swimming	11.2 ± 0.91	0.36 ± 0.02	19.5 ± 13.6	-0.56 ± 0.07	$11.2\ M^{0.36}(1 - e^{-19.5\ M^{-0.56}})$

Supplementary Table 1.5 | References for the masses and speed predictions of Table 1 in the main text.

species	mass	reference		
		power law	morphological model	time-dependent model
Dromaius	Blanco & Jones 2005	*	Blanco & Jones 2005	+
Struthio	Blanco & Jones 2005	*	Blanco & Jones 2005	+
Patagornis	Sellers & Manning 2007	*	Sellers & Manning 2007	+
Velociraptor	Blanco & Jones 2005	*	Blanco and Jones 2005	+
Allosaurus	Blanco and Jones 2005	*	Blanco & Jones 2005	+
Tyrannosaurus	Blanco &Jones 2005	*	Blanco & Jones 2005	+
Triceratops	Thulborn 1982	*	Thulborn 1982	+
Apatosaurus	Thulborn 1982	*	Thulborn 1982	+
Brachiosaurus	Thulborn 1982	*	Thulborn 1982	+

* prediction from a power law (equ. 1); + prediction from our model (equ. 5)

Supplementary Table 1.6 | Body mass and maximum speed of running, flying, and swimming animals.

species	taxonomic group	locomotion mode	thermoregulation	body mass [kg]	mass ref.	max. speed [km/h]	speed ref.	primary diet
Aeshna cyanea	arthropod	flying	ectotherm	4.22E-04	*28*	36	*70*	carnivore
Anax junius	arthropod	flying	ectotherm	4.50E-04	*28*	27	*70*	carnivore
Anax parthenope julius	arthropod	flying	ectotherm	3.90E-04	*28*	25.92	*4*	carnivore
Anax sp.	arthropod	flying	ectotherm	0.0138	*11*	36	*11*	carnivore
Anopheles ziemanni	arthropod	flying	ectotherm	5.22E-06	*92*	6.48	*36*	carnivore
Anthonomus grandis	arthropod	flying	ectotherm	6.86E-06	*94*	4.8	*55*	herbivore
Culex pipiens	arthropod	flying	ectotherm	1.30E-06	*51*	3.6	*19*	carnivore
Drosophila hydei	arthropod	flying	ectotherm	1.76E-07	*64*	3.24	*25*	herbivore
Drosophila melanogaster	arthropod	flying	ectotherm	7.47E-07	*11*	6.84	*11*	herbivore
Drosophila melanogaster	arthropod	flying	ectotherm	7.89E-08	*64*	3.06	*52*	herbivore
Drosophila virilis	arthropod	flying	ectotherm	2.05E-07	*64*	4.32	*81*	herbivore
Eristalis sp.	arthropod	flying	ectotherm	9.00E-05	*37*	36	*20*	herbivore
Volucella pellucens	arthropod	flying	ectotherm	1.70E-04	*37*	36	*20*	herbivore
Euglossa imperialis	arthropod	flying	ectotherm	0.0015	*29*	25.56	*21*	herbivore
Leptocorisa chinensis	arthropod	flying	ectotherm	4.73E-05	*42*	6	*77*	herbivore
Manduca sexta	arthropod	flying	ectotherm	0.002	*29*	19.08	*75*	herbivore
Manduca sexta	arthropod	flying	ectotherm	0.002	*29*	18	*86*	herbivore
Riptortus pedestris	arthropod	flying	ectotherm	6.52E-05	*47*	10.8	*77*	herbivore
Tabanus affinis	arthropod	flying	ectotherm	1.01E-04	*11*	23.76	*11*	carnivore
Accipiter striatus	bird	flying	endotherm	0.0965	*30*	64	*12*	carnivore
Anas acuta	bird	flying	endotherm	0.947	*30*	82.08	*11*	omnivore
Anas platyrhynchos	bird	flying	endotherm	1.14	*30*	105	*101*	omnivore
Apus apus	bird	flying	endotherm	0.058	*11*	91.8	*11*	carnivore
Aquila chrysaetos	bird	flying	endotherm	4.2635	*30*	129	*93*	carnivore
Archilochus colubris	bird	flying	endotherm	0.0075	*11*	40.32	*11*	herbivore
Buteo jamaicensis	bird	flying	endotherm	1.11	*30*	65	*46*	carnivore
Calypte anna	bird	flying	endotherm	0.0044	*56*	56.16	*17*	herbivore
Chen caerulescens	bird	flying	endotherm	2.641	*30*	80	*104*	herbivore

Columba livia	bird	flying	endotherm	0.3545	*30*	59	*101*	herbivore
Cygnus columbianus	bird	flying	endotherm	6.75	*30*	135	*31*	omnivore
Cygnus columbianus bewickii	bird	flying	endotherm	6.05	*11*	67.68	*11*	omnivore
Cygnus cygnus	bird	flying	endotherm	9.35	*30*	88	*39*	omnivore
Diomedea exulans	bird	flying	endotherm	8.19	*30*	127	*71*	carnivore
Falco peregrinus	bird	flying	endotherm	0.78	*30*	110	*96*	carnivore
Fregata aquila	bird	flying	endotherm	1.5	*101*	153	*101*	carnivore
Gymnogyps californianus	bird	flying	endotherm	4.49	*30*	90	*101*	carnivore
Hirundapus caudacutus	bird	flying	endotherm	0.096	*30*	170	*101*	carnivore
Mergus serrator	bird	flying	endotherm	1.02	*30*	129	*101*	carnivore
Morus bassanus	bird	flying	endotherm	3	*30*	100	*101*	carnivore
Numenius phaeopus	bird	flying	endotherm	0.366	*30*	83.52	*11*	carnivore
Nymphicus hollandicus	bird	flying	endotherm	0.088	*30*	46.8	*41*	herbivore
Otis tarda	bird	flying	endotherm	10.55	*30*	80	*43*	herbivore
Pelecanus onocrotalus	bird	flying	endotherm	9.52	*30*	82.08	*11*	carnivore
Phylloscopus trochilus	bird	flying	endotherm	0.0087	*30*	43.2	*11*	carnivore
Plectropterus gambensis	bird	flying	endotherm	3.869	*30*	142	*101*	omnivore
Somateria mollissima	bird	flying	endotherm	2.07	*30*	113	*101*	carnivore
Thalassarche chrysostoma	bird	flying	endotherm	3.51	*30*	127	*14*	carnivore
Xanthocephalus xanthocephalus	bird	flying	endotherm	0.0646	*30*	56.33	*23*	omnivore
Chalinolobus tuberculatus	mammal	flying	endotherm	0.0085	*60*	60	*60*	carnivore
Euderma maculatum	mammal	flying	endotherm	0.0162	*56*	53	*15*	carnivore
Glossophaga soricina	mammal	flying	endotherm	0.0103	*56*	37.8	*88*	herbivore
Lasiurus borealis	mammal	flying	endotherm	0.013	*56*	64	*62*	carnivore
Lasiurus semotus	mammal	flying	endotherm	0.02603	*56*	54.72	*62*	carnivore
Nyctinomops macrotis	mammal	flying	endotherm	0.023	*56*	61	*22*	carnivore
Tadarida brasiliensis	mammal	flying	endotherm	0.0125	*56*	96.5	*26*	carnivore
Agelenopsis aperta	arthropod	running	ectotherm	1.28E-04	*3*	0.933	*66*	carnivore
Argiope keyserlingi	arthropod	running	ectotherm	4.02E-06	*65*	1.2	*65*	carnivore
Blaberus discoidalis	arthropod	running	ectotherm	0.003	*76*	1.998	*76*	omnivore
Carabinae	arthropod	running	ectotherm	8.68E-05	*32*	2.14	*32*	carnivore
Carabinae	arthropod	running	ectotherm	8.85E-05	*32*	2.24	*32*	carnivore
Carabinae	arthropod	running	ectotherm	7.28E-05	*32*	2.25	*32*	carnivore

Carabinae	arthropod	running	ectotherm	1.40E-04	*32*	2.27	*32*	carnivore
Cataglyphis sp.	arthropod	running	ectotherm	1.55E-05	*83*	2.088	*40*	carnivore
Cicindela eburneola	arthropod	running	ectotherm	3.89E-05	*45*	6.696	*45*	carnivore
Cicindela hudsoni	arthropod	running	ectotherm	2.00E-04	*45*	9	*45*	carnivore
Cicindela leucothrix	arthropod	running	ectotherm	6.20E-05	*45*	3.67	*45*	carnivore
Cicindela repanda	arthropod	running	ectotherm	4.76E-05	*87*	1.91	*35*	carnivore
Cicindela saetigera	arthropod	running	ectotherm	7.08E-05	*45*	5.04	*45*	carnivore
Cicindela salicursoria	arthropod	running	ectotherm	4.36E-05	*45*	5.29	*45*	carnivore
Cicindela velox	arthropod	running	ectotherm	8.60E-05	*45*	6.95	*45*	carnivore
Dolomedes fimbriatus	arthropod	running	ectotherm	1.87E-04	*9*	0.976	*9*	carnivore
Dolomedes plantarius	arthropod	running	ectotherm	1.79E-04	*67*	2.7	*38*	carnivore
Dolomedes triton	arthropod	running	ectotherm	4.00E-04	*9*	1.14	*9*	carnivore
Hogna carolinensis (female)	arthropod	running	ectotherm	1.26E-04	*57*	4.50	*57*	carnivore
Hogna carolinensis (male)	arthropod	running	ectotherm	1.02E-04	*57*	4.73	*57*	carnivore
Hololena adnexa	arthropod	running	ectotherm	2.64E-05	*74*	2.16	*74*	carnivore
Hololena curta	arthropod	running	ectotherm	2.64E-05	*74*	1.83	*74*	carnivore
insect	arthropod	running	ectotherm	0.001	*7*	3.6	*7*	herbivore
insect	arthropod	running	ectotherm	0.001	*7*	5.4	*7*	herbivore
insect	arthropod	running	ectotherm	0.05	*7*	2.88	*7*	herbivore
Ocymyrmex barbiger	arthropod	running	ectotherm	4.10E-06	*53*	1.38	*53*	omnivore
Paratarsotomus macropalpis	arthropod	running	ectotherm	1.82E-07	*89*	0.5	*89*	carnivore
Paratarsotomus macropalpis	arthropod	running	ectotherm	2.68E-07	*69*	0.63	*69*	carnivore
Parateneriffia spp.	arthropod	running	ectotherm	3.00E-08	*89*	0.4716	*89*	carnivore
Pardosa amentata	arthropod	running	ectotherm	1.10E-05	*67*	1.476	*24*	carnivore
Pardosa lugubris	arthropod	running	ectotherm	1.03E-05	*67*	1.44	*13*	carnivore
Pardosa valens	arthropod	running	ectotherm	8.50E-05	*1*	1.53	*1*	carnivore
Periplaneta americana	arthropod	running	ectotherm	8.30E-04	*33*	5.4	*33*	omnivore
Pirata sedentarius (Size class 1)	arthropod	running	ectotherm	1.52E-05	*2*	0.915	*2*	carnivore
Pirata sedentarius (Size class 2)	arthropod	running	ectotherm	2.25E-05	*2*	0.791	*2*	carnivore
Pirata sedentarius (Size class 3)	arthropod	running	ectotherm	3.62E-05	*2*	1.22	*2*	carnivore
Pirata sedentarius (Size class 4)	arthropod	running	ectotherm	5.85E-05	*2*	1.57	*2*	carnivore
Schizocosa ocreata (Size class 1)	arthropod	running	ectotherm	1.78E-05	*24*	0.621	*24*	carnivore
Schizocosa ocreata (Size class 2)	arthropod	running	ectotherm	2.56E-05	*24*	1.60	*24*	carnivore

Schizocosa ocreata (Size class 3)	arthropod	running	ectotherm	3.11E-05	*24*	2.53	*24*	carnivore
Schizocosa ocreata (Size class 4)	arthropod	running	ectotherm	4.49E-05	*24*	2.64	*24*	carnivore
Schizocosa ocreata (Size class 5)	arthropod	running	ectotherm	5.30E-05	*24*	2.23	*24*	carnivore
Servaea incana	arthropod	running	ectotherm	5.36E-05	*54*	0.9	*54*	carnivore
Varacosa terricola (Size class 1)	arthropod	running	ectotherm	1.76E-04	*24*	2.57	*24*	carnivore
Varacosa terricola (Size class 2)	arthropod	running	ectotherm	2.87E-04	*24*	2.57	*24*	carnivore
Varacosa terricola (Size class 3)	arthropod	running	ectotherm	3.20E-04	*24*	2.50	*24*	carnivore
Varacosa terricola (Size class 4)	arthropod	running	ectotherm	4.87E-04	*24*	2.72	*24*	carnivore
Varacosa terricola (Size class 5)	arthropod	running	ectotherm	5.28E-04	*24*	2.24	*24*	carnivore
Varacosa terricola (Size class 6)	arthropod	running	ectotherm	6.01E-04	*24*	2.11	*24*	carnivore
Varacosa terricola (Size class 7)	arthropod	running	ectotherm	7.17E-04	*24*	1.84	*24*	carnivore
Geococcyx californianus	bird	running	endotherm	0.5	*101*	32	*101*	omnivore
Struthio camelus	bird	running	endotherm	111	*30*	70	*101*	herbivore
Struthio camelus	bird	running	endotherm	111	*30*	82.8	*11*	herbivore
Acinonyx jubatus	mammal	running	endotherm	39	*16*	104.95	*16*	carnivore
Acinonyx jubatus	mammal	running	endotherm	65	*101*	120	*101*	carnivore
Acinonyx jubatus	mammal	running	endotherm	58.8	*44*	106.91	*44*	carnivore
Acinonyx jubatus	mammal	running	endotherm	44.87	*11*	104.4	*11*	carnivore
Aepyceros melampus	mammal	running	endotherm	50	*16*	74.99	*16*	herbivore
Aepyceros melampus	mammal	running	endotherm	50	*34*	47	*34*	herbivore
Aepyceros melampus	mammal	running	endotherm	53.25	*7*	45.68	*7*	herbivore
Alcelaphus buselaphus	mammal	running	endotherm	150	*16*	69.98	*16*	herbivore
Alcelaphus buselaphus	mammal	running	endotherm	170	*34*	80	*34*	herbivore
Alcelaphus buselaphus	mammal	running	endotherm	136	*7*	77.98	*7*	herbivore
Alces alces	mammal	running	endotherm	410.2	*16*	55.98	*16*	herbivore
Alces alces	mammal	running	endotherm	384	*7*	54.55	*7*	herbivore
Ammospermophilus leucurus	mammal	running	endotherm	0.0759	*44*	16.77	*44*	omnivore
Antechinomys laniger	mammal	running	endotherm	0.025	*44*	14.51	*44*	carnivore
Antechinus flavipes	mammal	running	endotherm	0.052	*44*	16.20	*44*	carnivore
Antechinus stuartii	mammal	running	endotherm	0.0315	*44*	17.38	*44*	carnivore
Antidorcas marsupialis	mammal	running	endotherm	21.18	*16*	87.90	*16*	herbivore
Antidorcas marsupialis	mammal	running	endotherm	34	*34*	97	*34*	herbivore
Antidorcas marsupialis	mammal	running	endotherm	34	*7*	94.302	*7*	herbivore

Antilocapra americana	mammal	running	endotherm	46.03	*16*	87.10	*16*	herbivore
Antilocapra americana	mammal	running	endotherm	50	*101*	98	*101*	herbivore
Antilope cervicapra	mammal	running	endotherm	37	*34*	105	*34*	herbivore
Antilope cervicapra	mammal	running	endotherm	34.99	*16*	94.84	*16*	herbivore
Antilope cervicapra	mammal	running	endotherm	37.5	*7*	102.08	*7*	herbivore
Axis axis	mammal	running	endotherm	45.5	*56*	65	*102*	herbivore
Bettongia penicillata	mammal	running	endotherm	1.1	*44*	24.11	*44*	herbivore
Bison bison	mammal	running	endotherm	624.58	*56*	52.00	*16*	herbivore
Bison bison	mammal	running	endotherm	865	*7*	54.43	*7*	herbivore
Bison bonasus	mammal	running	endotherm	225	*16*	55.98	*16*	herbivore
Bos sauveli	mammal	running	endotherm	800	*34*	29	*34*	herbivore
Bos sauveli	mammal	running	endotherm	800	*7*	28.15	*7*	herbivore
Boselaphus tragocamelus	mammal	running	endotherm	200	*16*	47.97	*16*	herbivore
Camelus bactrianus	mammal	running	endotherm	549.54	*16*	59.98	*16*	herbivore
Camelus dromedarius	mammal	running	endotherm	500	*34*	32	*34*	herbivore
Camelus dromedarius	mammal	running	endotherm	414.95	*16*	52.00	*16*	herbivore
Camelus dromedarius	mammal	running	endotherm	550	*7*	31.09	*7*	herbivore
Canis aureus	mammal	running	endotherm	9.2	*16*	55.98	*16*	carnivore
Canis aureus	mammal	running	endotherm	8.8	*44*	54.44	*44*	carnivore
Canis familiaris	mammal	running	endotherm	17	*34*	54.95	*16*	carnivore
Canis familiaris	mammal	running	endotherm	25	*44*	65.14	*44*	carnivore
Canis latrans	mammal	running	endotherm	12.3	*16*	55.98	*16*	carnivore
Canis latrans	mammal	running	endotherm	18	*101*	69.04	*101*	carnivore
Canis latrans	mammal	running	endotherm	13.3	*44*	63.19	*44*	carnivore
Canis lupus	mammal	running	endotherm	40	*34*	63.97	*16*	carnivore
Canis lupus	mammal	running	endotherm	35.3	*44*	62.06	*44*	carnivore
Canis mesomelas	mammal	running	endotherm	7.6	*16*	59.98	*16*	carnivore
Canis mesomelas	mammal	running	endotherm	7	*44*	58.29	*44*	carnivore
Capra aegaerus	mammal	running	endotherm	46	*16*	44.98	*16*	herbivore
Capra aegagrus	mammal	running	endotherm	30	*7*	43.75	*7*	herbivore
Capra aegagrus	mammal	running	endotherm	30	*7*	78.09	*7*	herbivore
Capra caucasica	mammal	running	endotherm	55	*16*	44.98	*16*	herbivore
Capreolus capreolus	mammal	running	endotherm	25	*16*	59.98	*16*	herbivore

Ceratotherium simum	mammal	running	endotherm	2000	*7*	24.36	*7*	herbivore
Ceratotherium simum	mammal	running	endotherm	1901	*16*	39.99	*16*	herbivore
Ceratotherium simum	mammal	running	endotherm	3000	*34*	25	*34*	herbivore
Cercartetus concinnus	mammal	running	endotherm	0.015	*44*	4.84	*44*	carnivore
Cervus canadensis	mammal	running	endotherm	382	*101*	72.4	*101*	herbivore
Cervus elaphus	mammal	running	endotherm	84.92	*16*	71.94	*16*	herbivore
Chaetodipus baileyi	mammal	running	endotherm	0.0391	*44*	12.09	*44*	herbivore
Chaetodipus fallax	mammal	running	endotherm	0.018	*44*	12.45	*44*	herbivore
Connochaetes gnou	mammal	running	endotherm	157	*16*	79.98	*16*	herbivore
Connochaetes gnou	mammal	running	endotherm	250	*101*	64	*101*	herbivore
Connochaetes gnou	mammal	running	endotherm	300	*34*	90	*34*	herbivore
Connochaetes gnou	mammal	running	endotherm	132.25	*56*	62.18	*7*	herbivore
Connochaetes gnou	mammal	running	endotherm	132.25	*56*	69.97	*7*	herbivore
Connochaetes taurinus	mammal	running	endotherm	180	*34*	79.98	*16*	herbivore
Crocuta crocuta	mammal	running	endotherm	65.01	*16*	59.98	*16*	carnivore
Crocuta crocuta	mammal	running	endotherm	50	*101*	64	*101*	carnivore
Crocuta crocuta	mammal	running	endotherm	52	*44*	62.99	*44*	carnivore
Dama dama	mammal	running	endotherm	45	*16*	65.01	*16*	herbivore
Dama dama	mammal	running	endotherm	55	*7*	63.40	*7*	herbivore
Damaliscus dorcas	mammal	running	endotherm	43.45	*16*	69.98	*16*	herbivore
Damaliscus hunteri	mammal	running	endotherm	158.85	*16*	69.98	*16*	herbivore
Damaliscus lunatus	mammal	running	endotherm	125.89	*16*	69.98	*16*	herbivore
Damaliscus lunatus	mammal	running	endotherm	130	*7*	68.24	*7*	herbivore
Dasyuroides byrnei	mammal	running	endotherm	0.12	*44*	25.66	*44*	carnivore
Diceros bicornis	mammal	running	endotherm	875	*16*	44.98	*16*	herbivore
Diceros bicornis	mammal	running	endotherm	1200	*7*	43.80	*7*	herbivore
Dipodomys deserti	mammal	running	endotherm	0.0976	*44*	14.63	*44*	herbivore
Dipodomys merriami	mammal	running	endotherm	0.035	*44*	31.22	*44*	herbivore
Dipodomys microps	mammal	running	endotherm	0.056	*44*	20.43	*44*	herbivore
Dipodomys ordii	mammal	running	endotherm	0.0478	*44*	13.66	*44*	herbivore
Elephas maximus	mammal	running	endotherm	4000	*34*	26	*34*	herbivore
Elephas maximus	mammal	running	endotherm	4000	*7*	25.28	*7*	herbivore
Equus asinus	mammal	running	endotherm	165.2	*16*	54.95	*16*	herbivore

Equus burchelli	mammal	running	endotherm	136.14	*16*	69.98	*16*	herbivore
Equus burchelli	mammal	running	endotherm	235	*7*	68.15	*7*	herbivore
Equus caballus	mammal	running	endotherm	529.66	*16*	63.97	*16*	herbivore
Equus caballus	mammal	running	endotherm	350	*7*	68.04	*7*	herbivore
Equus caballus	mammal	running	endotherm	600	*101*	88	*101*	herbivore
Equus hemionus	mammal	running	endotherm	220.8	*16*	63.97	*16*	herbivore
Equus hemionus	mammal	running	endotherm	220.8	*16*	63.97	*16*	herbivore
Equus hemionus	mammal	running	endotherm	230	*101*	64	*101*	herbivore
Equus hemionus	mammal	running	endotherm	200	*7*	68.04	*7*	herbivore
Equus hemionus	mammal	running	endotherm	200	*7*	68.04	*7*	herbivore
Equus zebra	mammal	running	endotherm	276.06	*16*	63.97	*16*	herbivore
Equus zebra	mammal	running	endotherm	328	*101*	64.4	*101*	herbivore
Eudorcas thomsonii	mammal	running	endotherm	20	*101*	65	*101*	herbivore
Felis catus	mammal	running	endotherm	6	*101*	48	*101*	carnivore
Gazella dorcas	mammal	running	endotherm	19	*16*	79.98	*16*	herbivore
Gazella granti	mammal	running	endotherm	50	*16*	80.91	*16*	herbivore
Gazella subgutturosa	mammal	running	endotherm	24	*16*	97.05	*16*	herbivore
Gazella thomsoni	mammal	running	endotherm	19	*16*	79.98	*16*	herbivore
Giraffa camelopardalis	mammal	running	endotherm	1700	*16*	55.98	*16*	herbivore
Giraffa camelopardalis	mammal	running	endotherm	1700	*101*	52	*101*	herbivore
Giraffa camelopardalis	mammal	running	endotherm	1000	*34*	60	*34*	herbivore
Giraffa cameolopardalis	mammal	running	endotherm	1075	*7*	58.41	*7*	herbivore
Gorilla gorilla	mammal	running	endotherm	127	*44*	31.08	*44*	herbivore
Heteromys desmarestianus	mammal	running	endotherm	0.05	*44*	12.19	*44*	herbivore
Hippopotamus amphibius	mammal	running	endotherm	1210.60	*16*	25.00	*16*	herbivore
Hippopotamus amphibius	mammal	running	endotherm	3800	*7*	24.36	*7*	herbivore
Hippotragus equinus	mammal	running	endotherm	224.91	*16*	55.98	*16*	herbivore
Hippotragus equinus	mammal	running	endotherm	226.5	*7*	54.58	*7*	herbivore
Hippotragus niger	mammal	running	endotherm	181.13	*16*	57.02	*16*	herbivore
Homo sapiens	mammal	running	endotherm	70	*44*	38.83	*44*	omnivore
Homo sapiens	mammal	running	endotherm	70	*7*	43.85	*7*	omnivore
Hyaena hyaena	mammal	running	endotherm	31.99	*16*	50.00	*16*	carnivore
Hyaena hyaena	mammal	running	endotherm	26.8	*44*	48.47	*44*	carnivore

Isoodon obesulus	mammal	running	endotherm	0.718	*44*	13.90	*44*	omnivore
Lama guanicoe	mammal	running	endotherm	89.95	*16*	55.98	*16*	herbivore
Lama guanicoe	mammal	running	endotherm	95	*7*	54.62	*7*	herbivore
Leggadina forresti	mammal	running	endotherm	0.0155	*44*	12.25	*44*	omnivore
Lepus alleni	mammal	running	endotherm	4.4	*44*	70.04	*44*	herbivore
Lepus americanus	mammal	running	endotherm	1.5	*44*	48.55	*44*	herbivore
Lepus arcticus	mammal	running	endotherm	4.6	*44*	62.24	*44*	herbivore
Lepus californicus	mammal	running	endotherm	2	*44*	62.14	*44*	herbivore
Lepus europaeus	mammal	running	endotherm	4	*44*	70.02	*44*	herbivore
Lepus townsendii	mammal	running	endotherm	3.5	*44*	54.45	*44*	herbivore
Liomys pictus	mammal	running	endotherm	0.042	*44*	16.72	*44*	omnivore
Lontra canadensis	mammal	running	endotherm	8.09	*56*	18	*85*	carnivore
Loxodonta africana	mammal	running	endotherm	8000	*101*	40.07	*101*	herbivore
Loxodonta africana	mammal	running	endotherm	6000	*34*	35	*34*	herbivore
Loxodonta africana	mammal	running	endotherm	6000	*7*	34.02	*7*	herbivore
Lycaon pictus	mammal	running	endotherm	21.98	*16*	66.07	*16*	carnivore
Lycaon pictus	mammal	running	endotherm	30	*101*	72.42	*101*	carnivore
Lycaon pictus	mammal	running	endotherm	20	*44*	68.05	*44*	carnivore
Macropus eugenii	mammal	running	endotherm	4	*44*	38.88	*44*	herbivore
Macropus rufus	mammal	running	endotherm	80	*101*	70	*101*	herbivore
Macropus spp	mammal	running	endotherm	50	*7*	38.89	*7*	herbivore
Macropus spp	mammal	running	endotherm	50	*7*	58.32	*7*	herbivore
Macropus spp	mammal	running	endotherm	50	*7*	97.2	*7*	herbivore
Macropus spp.	mammal	running	endotherm	50	*44*	63.33	*44*	herbivore
Madoqua kirki	mammal	running	endotherm	5.11	*16*	41.98	*16*	herbivore
Madoqua kirki	mammal	running	endotherm	5	*7*	40.82	*7*	herbivore
Marmota monax	mammal	running	endotherm	4	*44*	15.55	*44*	herbivore
Meles meles	mammal	running	endotherm	11.6	*44*	29.17	*44*	carnivore
Mephitis mephitis	mammal	running	endotherm	2.5	*44*	15.55	*44*	omnivore
Mesocricetus brandti	mammal	running	endotherm	0.11	*44*	8.75	*44*	herbivore
Microdipodops megacephalus	mammal	running	endotherm	0.0123	*44*	10.60	*44*	omnivore
Microtus pennsylvanicus	mammal	running	endotherm	0.05	*44*	10.68	*44*	herbivore
Microtus pinetorum	mammal	running	endotherm	0.03	*44*	6.60	*44*	herbivore

Monodelphis brevicaudata	mammal	running	endotherm	0.0745	*44*	11.37	*44*	carnivore
Mus musculus	mammal	running	endotherm	0.019	*101*	13	*101*	omnivore
Mus musculus	mammal	running	endotherm	0.016	*44*	12.64	*44*	omnivore
Myrmecobius fasciatus	mammal	running	endotherm	0.48	*44*	13.54	*44*	carnivore
Napaeozapus insignis	mammal	running	endotherm	0.025	*44*	8.36	*44*	omnivore
Nasua narica	mammal	running	endotherm	4.4	*44*	26.24	*44*	omnivore
Nasua nasua	mammal	running	endotherm	3.40	*16*	26.98	*16*	omnivore
Neotoma lepida	mammal	running	endotherm	0.1106	*44*	16.62	*44*	herbivore
Notomys alexis	mammal	running	endotherm	0.0245	*44*	12.73	*44*	omnivore
Notomys cervinus	mammal	running	endotherm	0.035	*44*	13.66	*44*	omnivore
Odocoileus hemionus	mammal	running	endotherm	54.95	*16*	63.97	*16*	herbivore
Odocoileus hemionus	mammal	running	endotherm	120	*34*	61	*34*	herbivore
Odocoileus virginianus	mammal	running	endotherm	61.94	*16*	63.97	*16*	herbivore
Odocoileus virginianus	mammal	running	endotherm	80	*101*	48.2	*101*	herbivore
Onychomys torridus	mammal	running	endotherm	0.0193	*44*	10.06	*44*	omnivore
Oreamnos americanus	mammal	running	endotherm	119.95	*16*	33.04	*16*	herbivore
Oreamnos americanus	mammal	running	endotherm	113.5	*7*	32.05	*7*	herbivore
Oryctolagus cuniculus	mammal	running	endotherm	1.9	*44*	54.432	*44*	herbivore
Ourebia ourebi	mammal	running	endotherm	14.49	*16*	50.00	*16*	herbivore
Ovibos moschatus	mammal	running	endotherm	209.89	*16*	39.99	*16*	herbivore
Ovis ammon	mammal	running	endotherm	114.02	*16*	59.98	*16*	herbivore
Ovis ammon	mammal	running	endotherm	65	*7*	58.32	*7*	herbivore
Ovis canadensis	mammal	running	endotherm	95.06	*16*	47.97	*16*	herbivore
Panthera leo	mammal	running	endotherm	169.82	*16*	54.95	*16*	carnivore
Panthera leo	mammal	running	endotherm	200	*101*	80	*101*	carnivore
Panthera leo	mammal	running	endotherm	155.80	*7*	57.35	*7*	carnivore
Panthera pardus	mammal	running	endotherm	51.05	*16*	59.98	*16*	carnivore
Panthera pardus	mammal	running	endotherm	52.4	*44*	58.32	*44*	carnivore
Panthera tigris	mammal	running	endotherm	144.88	*16*	55.98	*16*	carnivore
Panthera tigris	mammal	running	endotherm	161	*7*	54.43	*7*	carnivore
Pecari tajacu	mammal	running	endotherm	21.98	*16*	34.99	*16*	omnivore
Perognathus longimembris	mammal	running	endotherm	0.0089	*44*	9.62	*44*	omnivore
Perognathus parvus	mammal	running	endotherm	0.0244	*44*	12.15	*44*	herbivore

Peromyscus crinitus	mammal	running	endotherm	0.0137	*44*	11.08	*44*	omnivore
Peromyscus eremicus	mammal	running	endotherm	0.0198	*44*	12.73	*44*	omnivore
Peromyscus leucopus	mammal	running	endotherm	0.025	*44*	10.69	*44*	omnivore
Peromyscus maniculatus	mammal	running	endotherm	0.0182	*44*	13.03	*44*	omnivore
Peromyscus maniculatus	mammal	running	endotherm	0.022	*11*	9	*11*	omnivore
Peromyscus truei	mammal	running	endotherm	0.0193	*44*	13.90	*44*	herbivore
Phacochoerus aethiopicus	mammal	running	endotherm	87.90	*16*	54.95	*16*	herbivore
Phacochoerus aethiopicus	mammal	running	endotherm	85	*7*	46.77	*7*	herbivore
Phacochoerus aethiopicus	mammal	running	endotherm	85	*7*	53.48	*7*	herbivore
Potorous tridactylus	mammal	running	endotherm	0.998	*44*	20.80	*44*	omnivore
Potorous tridactylus	mammal	running	endotherm	0.998	*7*	20.80	*7*	omnivore
Presbytis	mammal	running	endotherm	13	*44*	35.97	*44*	herbivore
Procyon lotor	mammal	running	endotherm	7.50	*16*	10.91	*16*	omnivore
Procyon lotor	mammal	running	endotherm	7	*44*	23.35	*44*	omnivore
Pseudomys australis	mammal	running	endotherm	0.05	*44*	15.92	*44*	omnivore
Pseudomys hermannsburgensis	mammal	running	endotherm	0.018	*44*	12.25	*44*	omnivore
Pseudomys nanus	mammal	running	endotherm	0.061	*44*	14.05	*44*	herbivore
Rangifer tarandus	mammal	running	endotherm	159.96	*16*	69.98	*16*	herbivore
Rangifer tarandus	mammal	running	endotherm	120	*34*	80	*34*	herbivore
Rangifer tarandus	mammal	running	endotherm	100	*7*	77.79	*7*	herbivore
Rattus	mammal	running	endotherm	0.25	*44*	9.43	*44*	omnivore
Rupicapra pyrenaica	mammal	running	endotherm	33.96	*16*	50.00	*16*	herbivore
Rupicapra rupicapra	mammal	running	endotherm	38.02	*16*	50.00	*16*	herbivore
Rupicapra rupicapra	mammal	running	endotherm	50	*34*	50	*34*	herbivore
Saiga tatarica	mammal	running	endotherm	26.18	*16*	74.99	*16*	herbivore
Saiga tatarica	mammal	running	endotherm	35	*34*	80	*34*	herbivore
Saiga tatarica	mammal	running	endotherm	35	*7*	77.76	*7*	herbivore
Sciurus carolinensis	mammal	running	endotherm	0.5	*44*	29.11	*44*	herbivore
Sciurus carolinensis	mammal	running	endotherm	0.133	*101*	20	*101*	omnivore
Sciurus carolinensis	mammal	running	endotherm	0.479	*11*	27.36	*11*	omnivore
Sciurus niger	mammal	running	endotherm	1.078	*44*	23.33	*44*	omnivore
Sciurus vulgaris	mammal	running	endotherm	0.4	*44*	19.46	*44*	herbivore
Sminthopsis crassicaudata	mammal	running	endotherm	0.017	*44*	11.18	*44*	carnivore

Sminthopsis macroura	mammal	running	endotherm	0.02	*44*	14.03	*44*	carnivore
Spermophilopsis leptodactylus	mammal	running	endotherm	0.6	*44*	35.01	*44*	omnivore
Spermophilus citellus	mammal	running	endotherm	0.5	*44*	17.47	*44*	herbivore
Spermophilus saturatus	mammal	running	endotherm	0.222	*44*	21.53	*44*	herbivore
Spermophilus tereticaudus	mammal	running	endotherm	0.1126	*44*	14.78	*44*	omnivore
Spermophilus tridecemlineatus	mammal	running	endotherm	0.125	*44*	11.82	*44*	omnivore
Spermophilus undulatus	mammal	running	endotherm	0.6	*44*	19.45	*44*	omnivore
Sus scrofa	mammal	running	endotherm	135	*56*	56	*98*	omnivore
Sylvilagus	mammal	running	endotherm	1.5	*44*	38.88	*44*	herbivore
Sylvilagus	mammal	running	endotherm	1.5	*7*	48.55	*7*	herbivore
Sylvilagus floridanus	mammal	running	endotherm	2	*101*	48	*101*	herbivore
Syncerus caffer	mammal	running	endotherm	439.54	*16*	57.02	*16*	herbivore
Syncerus caffer	mammal	running	endotherm	620	*7*	55.44	*7*	herbivore
Tamias amoenus	mammal	running	endotherm	0.051	*44*	18.86	*44*	omnivore
Tamias minimus	mammal	running	endotherm	0.0293	*44*	16.27	*44*	herbivore
Tamias striatus	mammal	running	endotherm	0.1	*44*	16.52	*44*	herbivore
Tamias striatus	mammal	running	endotherm	0.125	*11*	17.28	*11*	herbivore
Tamiasciurus hudsonicus	mammal	running	endotherm	0.22	*44*	14.62	*44*	herbivore
Tamiasciurus hudsonicus	mammal	running	endotherm	0.22	*7*	14.62	*7*	herbivore
Tapirus terrestris	mammal	running	endotherm	172.98	*16*	39.99	*16*	herbivore
Taurotragus derbianus	mammal	running	endotherm	680.77	*16*	69.98	*16*	herbivore
Taurotragus oryx	mammal	running	endotherm	559.76	*16*	69.98	*16*	herbivore
Taurotragus oryx	mammal	running	endotherm	511	*7*	68.17	*7*	herbivore
Tayassu pecari	mammal	running	endotherm	33.04	*16*	34.99	*16*	omnivore
Urocitellus beldingi	mammal	running	endotherm	0.3	*44*	12.61	*44*	herbivore
Urocyon cinereoargenteus	mammal	running	endotherm	5.8	*101*	67.6	*101*	omnivore
Urocyon cinereoargenteus	mammal	running	endotherm	3.7	*44*	62.21	*44*	omnivore
Urocyon cineroargenteus	mammal	running	endotherm	3.80	*16*	41.98	*16*	omnivore
Uromys caudimaculatus	mammal	running	endotherm	1.18	*44*	16.16	*44*	omnivore
Ursus americanus	mammal	running	endotherm	104.95	*16*	47.97	*16*	carnivore
Ursus americanus	mammal	running	endotherm	93.4	*44*	46.63	*44*	carnivore
Ursus arctos	mammal	running	endotherm	250	*101*	35	*101*	carnivore
Ursus arctos	mammal	running	endotherm	251.3	*7*	46.66	*7*	carnivore

Ursus arctos horribilis	mammal	running	endotherm	154.88	*16*	47.97	*16*	carnivore
Ursus maritimus	mammal	running	endotherm	174.98	*16*	50	*16*	carnivore
Ursus maritimus	mammal	running	endotherm	650	*101*	30	*101*	carnivore
Ursus maritimus	mammal	running	endotherm	265	*7*	38.92	*7*	carnivore
Vicugna vicugna	mammal	running	endotherm	44.98	*16*	46.99	*16*	herbivore
Vulpes vulpes	mammal	running	endotherm	5.50	*16*	47.97	*16*	carnivore
Vulpes vulpes	mammal	running	endotherm	4.8	*44*	70.03	*44*	carnivore
Vulpes vulpes	mammal	running	endotherm	4.59	*11*	72	*11*	carnivore
Zapus hudsonicus	mammal	running	endotherm	0.018	*44*	8.65	*44*	omnivore
Zapus trinotatus	mammal	running	endotherm	0.0285	*44*	13.84	*44*	omnivore
Zyzomys argurus	mammal	running	endotherm	0.0605	*44*	12.05	*44*	omnivore
Acanthodactylus erythrurus	reptile	running	ectotherm	0.0089	*80*	11.27	*80*	carnivore
Acanthodactylus pardalis	reptile	running	ectotherm	0.0067	*80*	9.42	*80*	carnivore
Acanthodactylus scutellatus	reptile	running	ectotherm	0.00784	*27*	11.95	*27*	carnivore
Acanthodactylus scutellatus	reptile	running	ectotherm	0.0081	*80*	10.06	*80*	carnivore
Amblyrhynchus cristatus	reptile	running	ectotherm	0.0718	*80*	10.08	*80*	herbivore
Anolis carolinensis	reptile	running	ectotherm	0.006	*80*	4.32	*80*	carnivore
Anolis cristatellus	reptile	running	ectotherm	0.0081	*80*	7.76	*80*	carnivore
Anolis evermanni	reptile	running	ectotherm	0.0056	*80*	6.57	*80*	carnivore
Anolis frenatus	reptile	running	ectotherm	0.0427	*80*	9.78	*80*	carnivore
Anolis gundlachi	reptile	running	ectotherm	0.0071	*80*	7.76	*80*	carnivore
Anolis humilis	reptile	running	ectotherm	0.001	*80*	4.18	*80*	carnivore
Anolis krugi	reptile	running	ectotherm	0.0024	*80*	6.43	*80*	carnivore
Anolis lemurinus	reptile	running	ectotherm	0.0036	*80*	5.33	*80*	carnivore
Anolis limifrons	reptile	running	ectotherm	9.00E-04	*80*	4.75	*80*	carnivore
Anolis lineatopus	reptile	running	ectotherm	0.0046	*80*	7.32	*80*	carnivore
Anolis poncensis	reptile	running	ectotherm	0.0016	*80*	6.34	*80*	carnivore
Anolis pulchellus	reptile	running	ectotherm	0.0015	*80*	6.12	*80*	carnivore
Anolis sagrei	reptile	running	ectotherm	0.0029	*80*	6.52	*80*	carnivore
Anolis stratulus	reptile	running	ectotherm	0.0019	*80*	5.36	*80*	carnivore
Aspidoscelis tigris	reptile	running	ectotherm	0.01142	*27*	15.37	*27*	carnivore
Callisaurus draconoides	reptile	running	ectotherm	0.0982	*11*	25.92	*11*	carnivore
Callisaurus draconoides	reptile	running	ectotherm	0.01193	*27*	17.32	*27*	carnivore

Carlia fusca	reptile	running	ectotherm	0.00335	*27*	6.23	*27*	carnivore
Christinus marmoratus	reptile	running	ectotherm	0.0037	*80*	3.49	*80*	carnivore
Cnemidophorus inornatus arizonae	reptile	running	ectotherm	0.0042	*80*	8.15	*80*	carnivore
Cnemidophorus inornatus heptagrammus	reptile	running	ectotherm	0.004	*80*	6.75	*80*	carnivore
Cnemidophorus sexlineatus	reptile	running	ectotherm	0.2	*101*	29	*101*	carnivore
Cnemidophorus tigris marmoratus	reptile	running	ectotherm	0.0179	*80*	8.64	*80*	carnivore
Cnemidophorus tigris punctilinealis	reptile	running	ectotherm	0.0112	*80*	9.53	*80*	carnivore
Coleonyx brevis	reptile	running	ectotherm	0.0018	*80*	5.36	*80*	carnivore
Coleonyx variegatus	reptile	running	ectotherm	0.0044	*80*	5.51	*80*	carnivore
Cophosaurus texanus	reptile	running	ectotherm	0.00994	*27*	13.72	*27*	carnivore
Crotaphytus collaris	reptile	running	ectotherm	0.04015	*27*	12.10	*27*	carnivore
Ctenophorus nuchalis	reptile	running	ectotherm	0.0138	*80*	9.23	*80*	omnivore
Ctenotus regius	reptile	running	ectotherm	0.0055	*80*	3.56	*80*	carnivore
Ctenotus taeniolatus	reptile	running	ectotherm	0.0045	*80*	4.25	*80*	carnivore
Ctenotus uber	reptile	running	ectotherm	0.0054	*80*	5.94	*80*	carnivore
Dendroaspis polylepis	reptile	running	ectotherm	1.4	*101*	23	*73*	carnivore
Dendroaspis polylepis	reptile	running	ectotherm	1.4	*101*	32.2	*101*	carnivore
Dipsosaurus dorsalis	reptile	running	ectotherm	0.398	*11*	26.28	*11*	herbivore
Egernia cunninghami	reptile	running	ectotherm	0.268	*80*	9.69	*80*	herbivore
Egernia whitii	reptile	running	ectotherm	0.0251	*80*	3.92	*80*	omnivore
Elgaria kingii	reptile	running	ectotherm	0.00973	*27*	4.21	*27*	carnivore
Eremias lineoocellata	reptile	running	ectotherm	0.0042	*80*	9.47	*80*	carnivore
Eremias lugubris	reptile	running	ectotherm	0.004	*80*	5.69	*80*	carnivore
Eremias namaquensis	reptile	running	ectotherm	0.0025	*80*	9.65	*80*	carnivore
Eremiascincus fasciolatus	reptile	running	ectotherm	0.0125	*80*	2.99	*80*	carnivore
Eublepharis macularius	reptile	running	ectotherm	0.0495	*80*	2.38	*80*	carnivore
Eulamprus kosciuskoi	reptile	running	ectotherm	0.0083	*80*	3.74	*80*	carnivore
Eulamprus quoyi	reptile	running	ectotherm	0.0211	*80*	5.47	*80*	carnivore
Eulamprus tympanum	reptile	running	ectotherm	0.0144	*80*	5.36	*80*	carnivore
Gallotia atlantica	reptile	running	ectotherm	0.0054	*80*	6.55	*80*	omnivore
Gallotia caesaris	reptile	running	ectotherm	0.0098	*80*	7.74	*80*	omnivore
Gallotia simonyi	reptile	running	ectotherm	0.23	*80*	8.28	*80*	omnivore
Gallotia stehlini	reptile	running	ectotherm	0.208	*80*	11.34	*80*	omnivore

Gambelia wislizenii	reptile	running	ectotherm	0.01981	*27*	11.81	*27*	omnivore
Gekko gecko	reptile	running	ectotherm	0.0381	*80*	5.44	*80*	carnivore
Gonatodes concinnatus	reptile	running	ectotherm	0.0023	*80*	3.74	*80*	carnivore
Hemidactylus frenatus	reptile	running	ectotherm	0.0033	*80*	7.96	*80*	carnivore
Hemidactylus turcicus	reptile	running	ectotherm	0.0028	*80*	5.90	*80*	carnivore
Hemiergis decresiensis	reptile	running	ectotherm	8.00E-04	*80*	2.30	*80*	carnivore
Hemiergis peronii	reptile	running	ectotherm	0.0015	*80*	1.76	*80*	carnivore
Holbrookia elegans	reptile	running	ectotherm	0.00405	*27*	10.62	*27*	carnivore
Lacerta agilis	reptile	running	ectotherm	0.0091	*80*	6.04	*80*	carnivore
Lacerta bedriagae	reptile	running	ectotherm	0.0096	*80*	6.43	*80*	carnivore
Lacerta monticola	reptile	running	ectotherm	0.0077	*80*	5.64	*80*	carnivore
Lacerta schreiberi	reptile	running	ectotherm	0.0212	*80*	6.43	*80*	carnivore
Lacerta viridis	reptile	running	ectotherm	0.0284	*80*	9.64	*80*	carnivore
Lacerta vivipara	reptile	running	ectotherm	0.0028	*80*	3.24	*80*	carnivore
Laudakia stellio	reptile	running	ectotherm	0.04854	*27*	10.91	*27*	carnivore
Laudakia stellio	reptile	running	ectotherm	0.0401	*80*	9.72	*80*	carnivore
Laudakia stellio	reptile	running	ectotherm	0.0411	*80*	9	*80*	carnivore
Laudakia stellio	reptile	running	ectotherm	0.0419	*80*	8.28	*80*	carnivore
Laudakia stellio	reptile	running	ectotherm	0.0551	*80*	8.64	*80*	carnivore
Leiolepis belliana	reptile	running	ectotherm	0.04	*80*	7.92	*80*	omnivore
Lepidodactylus lugubris	reptile	running	ectotherm	0.0011	*80*	5.54	*80*	carnivore
Nucras tessellata	reptile	running	ectotherm	0.0047	*80*	7.38	*80*	carnivore
Petrosaurus mearnsi	reptile	running	ectotherm	0.0113	*80*	8.46	*80*	omnivore
Phrynosoma cornutum	reptile	running	ectotherm	0.03362	*27*	6.34	*27*	carnivore
Phrynosoma mcallii	reptile	running	ectotherm	0.01146	*27*	5.54	*27*	carnivore
Phrynosoma modestum	reptile	running	ectotherm	0.00595	*27*	4.5	*27*	carnivore
Phrynosoma platyrhinos	reptile	running	ectotherm	0.01626	*27*	5.58	*27*	carnivore
Plestiodon fasciatus	reptile	running	ectotherm	0.00735	*27*	6.48	*27*	carnivore
Plestiodon skiltonianus	reptile	running	ectotherm	0.0052	*80*	2.74	*80*	carnivore
Podarcis bocagei	reptile	running	ectotherm	0.0033	*80*	5.12	*80*	carnivore
Podarcis hispanica	reptile	running	ectotherm	0.0025	*80*	7.30	*80*	carnivore
Podarcis hispanica atrata	reptile	running	ectotherm	0.0076	*80*	5.50	*80*	carnivore
Podarcis lilfordi	reptile	running	ectotherm	0.0078	*80*	8.41	*80*	carnivore

Podarcis muralis	reptile	running	ectotherm	0.0031	*80*	7.69	*80*	carnivore
Podarcis pityusensis	reptile	running	ectotherm	0.0098	*80*	9.14	*80*	carnivore
Podarcis sicula	reptile	running	ectotherm	0.00539	*27*	8.64	*27*	carnivore
Podarcis sicula	reptile	running	ectotherm	0.0071	*80*	6.01	*80*	carnivore
Podarcis tiliguerta	reptile	running	ectotherm	0.0048	*80*	8.68	*80*	carnivore
Psammodromus algirus	reptile	running	ectotherm	0.011	*80*	9.09	*80*	carnivore
Psammodromus hispanicus	reptile	running	ectotherm	0.0014	*80*	5.40	*80*	carnivore
Pseudemoia entrecasteauxii	reptile	running	ectotherm	0.0033	*80*	3.20	*80*	carnivore
Pseudemoia entrecasteauxii	reptile	running	ectotherm	0.0047	*80*	4.25	*80*	carnivore
Sceloporus clarkii	reptile	running	ectotherm	0.012	*80*	6.80	*80*	carnivore
Sceloporus cowlesi	reptile	running	ectotherm	0.00451	*27*	7.92	*27*	carnivore
Sceloporus graciosus	reptile	running	ectotherm	0.00703	*27*	8.35	*27*	carnivore
Sceloporus jarrovi	reptile	running	ectotherm	0.0153	*80*	6.23	*80*	carnivore
Sceloporus magister	reptile	running	ectotherm	0.03101	*27*	11.20	*27*	carnivore
Sceloporus merriami	reptile	running	ectotherm	0.0042	*80*	7.01	*80*	carnivore
Sceloporus merriami	reptile	running	ectotherm	0.0048	*80*	7.64	*80*	carnivore
Sceloporus occidentalis	reptile	running	ectotherm	0.0074	*80*	6.95	*80*	carnivore
Sceloporus undulatus	reptile	running	ectotherm	0.0056	*80*	6.23	*80*	carnivore
Sceloporus undulatus	reptile	running	ectotherm	0.0059	*80*	5.83	*80*	carnivore
Sceloporus undulatus hyacinthus	reptile	running	ectotherm	0.01	*80*	7.70	*80*	carnivore
Sceloporus virgatus	reptile	running	ectotherm	0.00523	*27*	6.34	*27*	carnivore
Sceloporus woodi	reptile	running	ectotherm	0.0028	*80*	8.93	*80*	carnivore
Scincella lateralis	reptile	running	ectotherm	8.00E-04	*80*	1.37	*80*	carnivore
Takydromus septentrionalis	reptile	running	ectotherm	0.0055	*80*	2.92	*80*	carnivore
Tiliqua scincoides	reptile	running	ectotherm	0.438	*80*	3.85	*80*	omnivore
Trachylepis occidentalis	reptile	running	ectotherm	0.0137	*80*	6.23	*80*	carnivore
Trachylepis spilogaster	reptile	running	ectotherm	0.0095	*80*	8.53	*80*	carnivore
Trachylepis striata	reptile	running	ectotherm	0.0158	*80*	7.56	*80*	carnivore
Trachylepis variegata	reptile	running	ectotherm	0.0013	*80*	4.90	*80*	carnivore
Trapelus savignyi	reptile	running	ectotherm	0.022	*80*	9.72	*80*	carnivore
Uma rufopunctata	reptile	running	ectotherm	0.02967	*27*	11.92	*27*	carnivore
Uma scoparia	reptile	running	ectotherm	0.0185	*80*	8.57	*80*	carnivore
Urosaurus graciosus	reptile	running	ectotherm	0.0036	*80*	6.37	*80*	carnivore

Urosaurus nigricaudus	reptile	running	ectotherm	0.0023	*80*	6.44	*80*	carnivore
Urosaurus ornatus	reptile	running	ectotherm	0.00347	*27*	8.24	*27*	carnivore
Urosaurus ornatus	reptile	running	ectotherm	0.0035	*80*	7.60	*80*	carnivore
Uta stansburiana	reptile	running	ectotherm	0.00383	*27*	7.81	*27*	carnivore
Uta stansburiana	reptile	running	ectotherm	0.003	*80*	6.66	*80*	carnivore
Varanus acanthurus	reptile	running	ectotherm	0.0589	*18*	10.98	*18*	carnivore
Varanus brevicauda	reptile	running	ectotherm	0.0206	*18*	5.72	*18*	carnivore
Varanus caudolineatus	reptile	running	ectotherm	0.0181	*18*	8.42	*18*	carnivore
Varanus eremius	reptile	running	ectotherm	0.0485	*18*	13.36	*18*	carnivore
Varanus giganteus	reptile	running	ectotherm	2.9667	*18*	31.57	*18*	carnivore
Varanus gilleni	reptile	running	ectotherm	0.0271	*18*	8.028	*18*	carnivore
Varanus glauerti	reptile	running	ectotherm	0.0357	*18*	11.12	*18*	carnivore
Varanus gouldii	reptile	running	ectotherm	0.4294	*18*	20.59	*18*	carnivore
Varanus kingorum	reptile	running	ectotherm	0.0183	*18*	9.36	*18*	carnivore
Varanus mertensi	reptile	running	ectotherm	1.0323	*18*	12.85	*18*	carnivore
Varanus mitchelli	reptile	running	ectotherm	0.1513	*18*	12.35	*18*	carnivore
Varanus panoptes	reptile	running	ectotherm	2.425	*18*	21.24	*18*	carnivore
Varanus pilbarensis	reptile	running	ectotherm	0.0303	*18*	10.19	*18*	carnivore
Varanus rosenbergi	reptile	running	ectotherm	1.025	*18*	18.97	*18*	carnivore
Varanus scalaris	reptile	running	ectotherm	0.1021	*18*	9.94	*18*	carnivore
Varanus storri	reptile	running	ectotherm	0.0269	*18*	9.18	*18*	carnivore
Varanus tristis	reptile	running	ectotherm	0.0983	*18*	14.22	*18*	carnivore
Varanus varius	reptile	running	ectotherm	7.7	*18*	14.51	*18*	carnivore
Euphausia superba	arthropod	swimming	ectotherm	0.002	*91*	1.66	*48*	herbivore
Aptenodytes forsteri	bird	swimming	endotherm	29.75	*56*	10.8	*49*	carnivore
Aptenodytes patagonicus	bird	swimming	endotherm	14	*101*	12.1	*101*	carnivore
Pygoscelis adeliae	bird	swimming	endotherm	3.36	*11*	13.68	*11*	carnivore
Pygoscelis antarcticus	bird	swimming	endotherm	4.5	*101*	32	*101*	carnivore
Pygoscelis papua	bird	swimming	endotherm	8.2	*101*	36	*101*	carnivore
Acanthocybium solandri	fish	swimming	ectotherm	13.31	*11*	77.4	*11*	carnivore
Acanthocybium solandri	fish	swimming	ectotherm	16.64	*79*	77	*101*	carnivore
Alburnus alburnus	fish	swimming	ectotherm	0.001	*5*	1.8	*5*	carnivore
Alosa finita	fish	swimming	ectotherm	0.0297	*5*	2.7	*5*	carnivore

Alosa pseudoharengus	fish	swimming	ectotherm	0.27	*11*	15.84	*11*	carnivore
Anguilla anguilla	fish	swimming	ectotherm	2.16	*8*	4.1	*8*	carnivore
Argyrosomus regius	fish	swimming	ectotherm	0.0295	*5*	4.07	*5*	carnivore
Barbatula barbatula	fish	swimming	ectotherm	0.0177	*78*	3.89	*78*	carnivore
Carassius auratus	fish	swimming	ectotherm	0.00343	*11*	2.7	*11*	carnivore
Carassius auratus	fish	swimming	ectotherm	0.020	*8*	10.8	*8*	carnivore
Carassius auratus	fish	swimming	ectotherm	0.276	*6*	7.2	*6*	carnivore
Carassius leucas	fish	swimming	ectotherm	9.53	*5*	14.59	*5*	carnivore
Carassius leucas	fish	swimming	ectotherm	40.07	*5*	18.76	*5*	carnivore
Carcharodon carcharias	fish	swimming	ectotherm	800	*101*	40	*101*	carnivore
Clupea harengus	fish	swimming	ectotherm	0.15625	*8*	6.12	*8*	carnivore
Clupea harengus	fish	swimming	ectotherm	7.57E-05	*90*	0.5004	*90*	carnivore
Clupea harengus	fish	swimming	ectotherm	1.30E-04	*90*	0.5472	*90*	carnivore
Cottus gobio	fish	swimming	ectotherm	0.0190	*78*	4.032	*78*	carnivore
Cottus gobio	fish	swimming	ectotherm	0.0688	*78*	4.92	*78*	carnivore
Cyprinus carpio	fish	swimming	ectotherm	0.0483	*78*	3.72	*78*	omnivore
Cyprinus carpio	fish	swimming	ectotherm	0.3277	*78*	4.83	*78*	omnivore
Cyprinus carpio	fish	swimming	ectotherm	0.0055	*5*	2.00	*5*	omnivore
Cyprinus carpio	fish	swimming	ectotherm	0.087	*5*	6.12	*5*	omnivore
Esox lucius	fish	swimming	ectotherm	0.145	*5*	7.56	*5*	carnivore
Esox lucius	fish	swimming	ectotherm	1.18	*5*	5.33	*5*	carnivore
Gadus morhua	fish	swimming	ectotherm	1.76	*8*	7.56	*8*	carnivore
Gadus morhua	fish	swimming	ectotherm	2.18E-05	*90*	0.288	*90*	carnivore
Galeocerdo cuvier	fish	swimming	ectotherm	550	*101*	32	*101*	carnivore
Helicolenus dactylopterus	fish	swimming	ectotherm	0.493	*5*	3.53	*5*	carnivore
Istiompax indica	fish	swimming	ectotherm	150	*10*	130	*10*	carnivore
Istiophorus albicans	fish	swimming	ectotherm	90	*101*	110	*101*	carnivore
Istiophorus albicans	fish	swimming	ectotherm	90	*101*	108	*10*	carnivore
Isurus oxyrinchus	fish	swimming	ectotherm	105	*101*	67.68	*103*	carnivore
Isurus oxyrinchus	fish	swimming	ectotherm	300	*101*	50	*101*	carnivore
Leuciscus leuciscus	fish	swimming	ectotherm	0.01	*11*	4.68	*11*	herbivore
Leuciscus leuciscus	fish	swimming	ectotherm	0.03375	*11*	6.3	*11*	herbivore
Leuciscus leuciscus	fish	swimming	ectotherm	0.08	*11*	7.92	*11*	herbivore

Leuciscus leuciscus	fish	swimming	ectotherm	0.279	*6*	8.64	*6*	herbivore
Leuciscus leuciscus	fish	swimming	ectotherm	0.184	*5*	6.12	*5*	herbivore
Makaira nigricans	fish	swimming	ectotherm	153.5	*95*	75	*10*	carnivore
Melanogrammus aeglefinus	fish	swimming	ectotherm	0.741	*8*	6.48	*8*	carnivore
Merlangius merlangus	fish	swimming	ectotherm	0.08	*8*	5.76	*8*	carnivore
Merluccius merluccius	fish	swimming	ectotherm	0.0237	*5*	2.84	*5*	carnivore
Micropterus salmoides	fish	swimming	ectotherm	0.276	*5*	3.17	*5*	carnivore
Mugil cephalus	fish	swimming	ectotherm	0.026	*5*	2.20	*5*	omnivore
Perca fluviatilis	fish	swimming	ectotherm	0.0184	*5*	2.38	*5*	carnivore
Platichthys flesus	fish	swimming	ectotherm	1.21E-05	*90*	0.234	*90*	carnivore
Pleuronectes platessa	fish	swimming	ectotherm	3.57E-04	*11*	0.2304	*11*	carnivore
Pleuronectes platessa	fish	swimming	ectotherm	5.71E-04	*11*	0.4104	*11*	carnivore
Pleuronectes platessa	fish	swimming	ectotherm	0.15625	*8*	4.64	*8*	carnivore
Pollachius virens	fish	swimming	ectotherm	0.266	*8*	7.2	*8*	carnivore
Rutilus rutilus	fish	swimming	ectotherm	0.0057	*78*	2.34	*78*	omnivore
Rutilus rutilus	fish	swimming	ectotherm	0.1275	*78*	5.02	*78*	omnivore
Salmo irideus	fish	swimming	ectotherm	0.551	*6*	9.72	*6*	carnivore
Salmo irideus	fish	swimming	ectotherm	0.235	*5*	6.12	*5*	carnivore
Salmo salar	fish	swimming	ectotherm	0.0023	*5*	0.472	*5*	carnivore
Salmo salar	fish	swimming	ectotherm	0.0048	*5*	0.601	*5*	carnivore
Salmo salar	fish	swimming	ectotherm	0.0078	*5*	0.778	*5*	carnivore
Salmo salar	fish	swimming	ectotherm	6.66	*5*	21.6	*5*	carnivore
Salmo salar	fish	swimming	ectotherm	7.85	*5*	17.532	*5*	carnivore
Salmo trutta	fish	swimming	ectotherm	0.12167	*8*	8.424	*8*	carnivore
Salmo trutta	fish	swimming	ectotherm	0.54872	*8*	11.52	*8*	carnivore
Salmo trutta	fish	swimming	ectotherm	0.0341	*5*	3.312	*5*	carnivore
Salmo trutta fario	fish	swimming	ectotherm	0.0217	*78*	4.54	*78*	carnivore
Salmo trutta fario	fish	swimming	ectotherm	0.969	*5*	12.6	*5*	carnivore
Scardinius erythrophthalmus	fish	swimming	ectotherm	0.0188	*5*	4.104	*5*	omnivore
Scardinius erythrophthalmus	fish	swimming	ectotherm	0.299	*5*	4.68	*5*	omnivore
Scomber scombrus	fish	swimming	ectotherm	0.54872	*8*	5.72	*8*	carnivore
Scomber scombrus	fish	swimming	ectotherm	0.0252	*5*	2.92	*5*	carnivore
Sphyraena argentea	fish	swimming	ectotherm	4.5	*101*	44	*101*	carnivore

Sphyraena barracuda	fish	swimming	ectotherm	26.56	*5*	43.89	*5*	carnivore
Squalinus cephalus	fish	swimming	ectotherm	0.0015	*5*	0.864	*5*	omnivore
Tetrapturus audax	fish	swimming	ectotherm	163	*101*	81	*101*	carnivore
Thunnus albacares	fish	swimming	ectotherm	9.41	*11*	74.88	*11*	carnivore
Thunnus albacares	fish	swimming	ectotherm	13.11	*82*	75	*82*	carnivore
Thunnus orientalis	fish	swimming	ectotherm	250	*101*	70	*101*	carnivore
Thunnus thynnus	fish	swimming	ectotherm	27.22	*5*	70.81	*5*	carnivore
Trachinus vipera	fish	swimming	ectotherm	0.0224	*5*	1.44	*5*	carnivore
Trigla sp	fish	swimming	ectotherm	0.21	*5*	4.72	*5*	carnivore
Trisopterus luscus	fish	swimming	ectotherm	0.0165	*5*	1.98	*5*	carnivore
Xiphias gladius	fish	swimming	ectotherm	98	*101*	97	*101*	carnivore
Balaenoptera musculus	mammal	swimming	endotherm	108400	*11*	37.08	*11*	carnivore
Delphinapterus leucas	mammal	swimming	endotherm	1380	*56*	22	*59*	carnivore
Delphinus delphis	mammal	swimming	endotherm	118	*68*	28.8	*68*	carnivore
Delphinus delphis	mammal	swimming	endotherm	95.32	*11*	37.08	*11*	carnivore
Enhydra lutris	mammal	swimming	endotherm	30	*101*	9	*101*	carnivore
Megaptera novaeangliae	mammal	swimming	endotherm	30000	*101*	27	*101*	carnivore
Megaptera novaeangliae	mammal	swimming	endotherm	30000	*56*	23.3	*58*	carnivore
Orcinus orca	mammal	swimming	endotherm	4100	*101*	48	*101*	carnivore
Orcinus orca	mammal	swimming	endotherm	4300	*56*	25	*63*	carnivore
Orcinus orca	mammal	swimming	endotherm	4300	*56*	55.44	*99*	carnivore
Physeter catodon	mammal	swimming	endotherm	10100	*56*	39	*84*	carnivore
Pseudorca crassidens	mammal	swimming	endotherm	1378.5	*68*	28.8	*68*	carnivore
Pusa hispida	mammal	swimming	endotherm	88.07	*56*	30	*100*	carnivore
Tursiops truncatus	mammal	swimming	endotherm	250	*101*	35	*101*	carnivore
Tursiops truncatus	mammal	swimming	endotherm	250	*68*	29.5	*68*	carnivore
Zalophus californianus	mammal	swimming	endotherm	158	*56*	40	*97*	carnivore
Aequipecten opercularis	mollusc	swimming	ectotherm	0.0143	*50*	0.9	*72*	omnivore
Illex illecebrosus	mollusc	swimming	ectotherm	0.6	*61*	5.04	*61*	carnivore
Loligo vulgaris	mollusc	swimming	ectotherm	0.35	*72*	7.2	*72*	carnivore
Octopus vulgaris	mollusc	swimming	ectotherm	17	*101*	40	*101*	carnivore
Sepia officinalis	mollusc	swimming	ectotherm	0.25	*72*	2.88	*72*	carnivore
Dermochelys coriacea	reptile	swimming	ectotherm	420	*56*	35.28	*99*	carnivore

When only body length was given, the following mass-lengths regressions were used to calculate body mass:

terrestrial arthropods	Jurkschat L. Allometric scaling relationships in the morphology of temperate and tropical arthropods. Master's Thesis. Univ. of Göttingen (2015)
others	Peters, R. H. *The ecological implications of body size* . **2,** (Cambridge University Press, 1986).

References

peer reviewed

1 Amaya, C. C., Klawinski, P. D. & Formanowicz, J., Daniel R. The Effects of Leg Autotomy on Running Speed and Foraging Ability in Two Species of Wolf Spider, (Lycosidae). Am. Midl. Nat. 145, 201–205 (2001).

2 Apontes, P. & Brown, C. A. Between-sex variation in running speed and a potential cost of leg autotomy in the wolf spider *Pirata sedentarius* . *Am. Midl. Nat.* **154,** 115–125 (2005).

3 Auerbach, P. S. *Wilderness Medicine: Expert Consult Premium Edition - Enhanced Online Features*. (Elsevier Health Sciences, 2011).

4 Azuma, A. & Watanabe, T. Flight performance of a dragonfly. *J. Exp. Biol.* **137,** 221–252 (1988).

5 Bainbridge, R. The speed of swimming of fish as related to size and to the frequency and amplitude of the tail beat. *J. Exp. Biol.* **35,** 109–133 (1958).

6 Bainbridge, R. Speed and stamina in three fish. *J. Exp. Biol.* **37,** 129–153 (1960).

7 Bejan, A. & Marden, J. H. Unifying constructal theory for scale effects in running, swimming and flying. *J. Exp. Biol.* **209,** 238–248 (2006).

8 Blaxter, J. H. S. & Dickson, W. Observations on the swimming speeds of fish. *J. Cons.* **24,** 472–479 (1959).

9 Bleckmann, H. & Barth, F. G. Sensory ecology of a semi-aquatic spider (*Dolomedes triton*). Behav. Ecol. Sociobiol. 14, 303–312 (1984).

10 Block, B. A., Booth, D. & Carey, F. G. Direct Measurement of Swimming Speeds and Depth of Blue Marlin. *J. Exp. Biol.* **166,** 267–284 (1992).

11 Bonner, J. T. *Size and Cycle: An Essay on the Structure of Biology* . (Princeton University Press, 2015).

12 Capainolo, P. & Butler, C. A. *How Fast Can A Falcon Dive?: Fascinating Answers to Questions about Birds of Prey* . (Rutgers University Press, 2010).

13 Casas, J., Steinmann, T. & Dangles, O. The Aerodynamic Signature of Running Spiders. *PLoS ONE* **3,** e2116 (2008).

14 Catry, P., Phillips, R. A. & Croxall, J. P. Sustained fast travel by a gray-headed albatross (*Thalassarche chrysostoma*) riding an antarctic storm. *The Auk* **121,** 1208–1213 (2004).

15 Chambers, C. L. *et al.* Roosts and home ranges of spotted bats (*Euderma maculatum*) in northern Arizona. *Can. J. Zool.* **89,** 1256–1267 (2011).

16 Christiansen, P. Locomotion in terrestrial mammals: the influence of body mass, limb length and bone proportions on speed. *Zool. J. Linn. Soc.* **136,** 685–714 (2002).

17 Clark, C. J. & Dudley, R. Flight costs of long, sexually selected tails in hummingbirds. *Proc. R. Soc. Lond. B Biol. Sci.* rspb.2009.0090 (2009). doi:10.1098/rspb.2009.0090

18 Clemente, C. J., Thompson, G. G. & Withers, P. C. Evolutionary relationships of sprint speed in Australian varanid lizards. *J. Zool.* **278,** 270–280 (2009).

19 Clements, A. N. The sources of energy for flight in mosquitoes. *J. Exp. Biol.* **32,** 547–554 (1955).

20 Collett, T. S. & Land, M. F. How hoverflies compute interception courses. *J. Comp. Physiol.* **125,** 191–204 (1978).

21 Combes, S. A. & Dudley, R. Turbulence-driven instabilities limit insect flight performance. *Proc. Natl. Acad. Sci.* **106,** 9105–9108 (2009).

22 Corbett, R. J. M., Chambers, C. L. & Herder, M. J. Roosts and activity areas of Nyctinomops macrotis in northern Arizona. *Acta Chiropterologica* **10,** 323–329 (2008).

23 Cottam, C., Williams, C. S. & Sooter, C. A. Flight and Running Speeds of Birds. *Wilson Bull.* **54,** 121–131 (1942).

24 Dangles, O., Ory, N., Steinmann, T., Christides, J.-P. & Casas, J. Spider's attack versus cricket's escape: velocity modes determine success. *Anim. Behav.* **72,** 603–610 (2006).

25 David, C. T. The relationship between body angle and flight speed in free-flying Drosophila. *Physiol. Entomol.* **3,** 191–195 (1978).

26 Davis, R. B., Herreid, C. F. & Short, H. L. Mexican Free-Tailed Bats in Texas. *Ecol. Monogr.* **32,** 311–346 (1962).

27 de Albuquerque, R. L., Bonine, K. E. & Garland Jr, T. Speed and endurance do not trade off in phrynosomatid lizards. *Physiol. Biochem. Zool.* **88,** 634–647 (2015).

45 Kamoun, S. & Hogenhout, S. A. Flightlessness and Rapid Terrestrial Locomotion in Tiger Beetles of the Cicindela L. Subgenus Rivacindela van Nidek from Saline Habitats of Australia (Coleoptera: Cicindelidae). *Coleopt. Bull.* **50,** 221–230 (1996).

46 March, A. I., Bradley, C. W. & Garcia, E. Aerodynamic Properties of Avian Flight as a Function of Wing Shape. 955–963 (2005). doi:10.1115/IMECE2005-83011

47 Kikuchi, Y. & Fukatsu, T. Live imaging of symbiosis: spatiotemporal infection dynamics of a GFP-labelled Burkholderia symbiont in the bean bug Riptortus pedestris. *Mol. Ecol.* **23,** 1445–1456 (2014).

48 Kils, U. *The swimming behavior, swimming performance and energy balance of Antarctic krill, Euphausia superba*. (SCAR and SCOR, Scott Polar Research Institute, 1981).

49 Kooyman, G. L. *et al.* Heart rates and swim speeds of emperor penguins diving under sea ice. *J. Exp. Biol.* **165,** 161–180 (1992).

50 Laming, S. R., Jenkins, S. R. & McCarthy, I. D. Repeatability of escape response performance in the queen scallop, *Aequipecten opercularis* . *J. Exp. Biol.* **216,** 3264–3272 (2013).

51 Li, X., Ma, L., Sun, L. & Zhu, C. Biotic characteristics in the deltamethrin-susceptible and resistant strains of *Culex pipiens pallens* (Diptera: Culicidae) in China. *Appl. Entomol. Zool.* **37,** 305–308 (2002).

52 Marden, J. H., Wolf, M. R. & Weber, K. E. Aerial performance of Drosophila melanogaster from populations selected for upwind flight ability. *J. Exp. Biol.* **200,** 2747–2755 (1997).

53 Marsh, A. C. Microclimatic factors influencing foraging patterns and success of the thermophilic desert ant, *Ocymyrmex barbiger. Insectes Sociaux* **32,** 286–296 (1985).

54 McGinley, R. H., Prenter, J. & Taylor, P. W. Whole-organism performance in a jumping spider, *Servaea incana* (Araneae: Salticidae): links with morphology and between performance traits. *Biol. J. Linn. Soc.* **110,** 644–657 (2013).

55 McKibben, G. H., Willers, J. L., Smith, J. W. & Wagner, T. L. Stochastic model for studying boll weevil dispersal. *Environ. Entomol.* **20,** 1327–1332 (1991).

56 Myhrvold, N. P. *et al.* An amniote life-history database to perform comparative analyses with birds, mammals, and reptiles. *Ecology* **96,** 3109–3109 (2015).

57 Nelson, M. K. & Formanowicz, D. R. Relationship between escape speed and flight distance in a wolf spider, *Hogna carolinensis* (walckenaer 1805). *J. Arachnol.* **33,** 153–158 (2005).

58 Noad, M. J. & Cato, D. H. Swimming Speeds of Singing and Non-Singing Humpback Whales During Migration. *Mar. Mammal Sci.* **23,** 481–495 (2007).

59 Nowak, R. M. *Walker's Mammals of the World* . **1,** (JHU Press, 1999).

60 O'Donnell, C. F. J. Home range and use of space by *Chalinolobus tuberculatus* , a temperate rainforest bat from New Zealand. *J. Zool.* **253,** 253–264 (2001).

61 O'DOR, R. & Webber, D. M. Invertebrate athletes: trade-offs between transport efficiency and power density in cephalopod evolution. *J. Exp. Biol.* **160,** 93–112 (1991).

62 Patterson, A. P. & Hardin, J. W. Flight speeds of five species of vespertilionid bats. *J. Mammal.* 152–153 (1969).

63 Pistorius, P. A. *et al.* Distribution, movement, and estimated population size of killer whales at Marion Island, December 2000. *South Afr. J. Wildl. Res.* **32,** p–86 (2002).

64 Pitnick, S., Markow, T. A. & Spicer, G. S. Delayed male maturity is a cost of producing large sperm in *Drosophila* . *Proc. Natl. Acad. Sci.* **92,** 10614–10618 (1995).

65 Prenter, J., Pérez-Staples, D. & Taylor, P. W. Functional relations between locomotor performance traits in spiders and implications for evolutionary hypotheses. *BMC Res. Notes* **3,** 306 (2010).

66 Pruitt, J. N. & Husak, J. F. Context-dependent running speed in funnel-web spiders from divergent populations. *Funct. Ecol.* **24,** 165–171 (2010).

67 Roberts, M. J. & others. *Spiders of Britain & Northern Europe.* (HarperCollins Publishers, 1995).

68 Rohr, J. J., Fish, F. E. & Gilpatrick, J. W. Maximum swim speeds of captive and free-ranging delphinids: Critical analysis of extraordinary performance. *Mar. Mammal Sci.* **18,** 1–19 (2002).

69 Rubin, S., Young, M. H.-Y., Wright, J. C., Whitaker, D. L. & Ahn, A. N. Exceptional running and turning performance in a mite. *J. Exp. Biol.* **219,** 676–685 (2016).

70 Rüppell, G. Kinematic analysis of symmetrical flight manoeuvres of Odonata. *J. Exp. Biol.* **144,** 13–42 (1989).

71 Sachs, G. *et al.* Flying at no mechanical energy cost: disclosing the secret of wandering albatrosses. *PloS One* **7,** e41449 (2012).

72 Saleuddin, A. S. M. & Wilbur, K. M. *The Mollusca: Physiology* . **5,** (Academic Press, 2012).

73 Schmidt, W. *Reptiles & Amphibians of Southern Africa* . (Struik, 2006).

74 Spagna, J. C., Valdivia, E. A. & Mohan, V. Gait characteristics of two fast-running spider species (*Hololena adnexa* and *Hololena curta*), including an aerial phase (Araneae: Agelenidae). *J. Arachnol.* **39,** 84–91 (2011).

75 Stevenson, R., Corbo, K., Baca, L. & Le, Q. Cage size and flight speed of the tobacco hawkmoth *Manduca sexta* . *J. Exp. Biol.* **198,** 1665–1672 (1995).

76 Ting, L. H., Blickhan, R. & Full, R. J. Dynamic and static stability in hexapedal runners. *J. Exp. Biol.* **197,** 251–269 (1994).

77 Tsunoda, T. & Moriya, S. Measurement of flight speed and estimation of flight distance of the bean bug, *Riptortus pedestris* (Fabricius)(Heteroptera: Alydidae) and the rice bug, *Leptocorisa chinensis* Dallas (Heteroptera: Alydidae) with a speed sensor and flight mills. *Appl. Entomol. Zool.* **43,** 451–456 (2008).

78 Tudorache, C., Viaene, P., Blust, R., Vereecken, H. & De Boeck, G. A comparison of swimming capacity and energy use in seven European freshwater fish species. *Ecol. Freshw. Fish* **17,** 284–291 (2008).

79 Uchiyama, J. H. & Boggs, C. H. Length-weight relationships of dolphinfish, *Coryphaena hippurus* , and wahoo, *Acanthocybium solandri* : seasonal effects of spawning and possible migration in the central North Pacific. *Mar. Fish. Rev.* **68,** 19–29 (2006).

80 Van Damme, R. & Vanhooydonck, B. Origins of interspecific variation in lizard sprint capacity. *Funct. Ecol.* **15,** 186–202 (2001).

81 Vogel, S. Flight in Drosophila I. Flight performance of tethered flies. *J. Exp. Biol.* **44,** 567–578 (1966).

82 Walters, V. & Fierstine, H. L. Measurements of swimming speeds of yellowfin tuna and wahoo. *Biol. Sci.* 2 (1964).

83 Wehner, R., Fukushi, T. & Isler, K. On being small: brain allometry in ants. *Brain. Behav. Evol.* **69,** 220–228 (2007).

84 Whitehead, H. *Sperm Whales: Social Evolution in the Ocean* . (University of Chicago Press, 2003).

85 Williams, T. M. *et al.* Running energetics of the North American river otter: do short legs necessarily reduce efficiency on land? *Comp. Biochem. Physiol. A. Mol. Integr. Physiol.* **133,** 203–212 (2002).

86 Willmott, A. P. & Ellington, C. P. The mechanics of flight in the hawkmoth *Manduca sexta* . I. Kinematics of hovering and forward flight. *J. Exp. Biol.* **200,** 2705–2722 (1997).

87 Wilson, D. S. Prudent Predation: A Field Study Involving Three Species of Tiger Beetles. *Oikos* 31, 128–136 (1978).

88 Winter, Y. Flight speed and body mass of nectar-feeding bats (Glossophaginae) during foraging. *J. Exp. Biol.* **202,** 1917–1930 (1999).

89 Wu, G. C., Wright, J. C., Whitaker, D. L. & Ahn, A. N. Kinematic evidence for superfast locomotory muscle in two species of teneriffiid mites. *J. Exp. Biol.* **213,** 2551–2556 (2010).

90 Yin, M. C. & Blaxter, J. H. S. Escape speeds of marine fish larvae during early development and starvation. *Mar. Biol.* **96,** 459–468 (1987).

non-peer reviewed

91 Gierak, R. 2013. "*Euphausia superba* " (On-line), Animal Diversity Web. http://animaldiversity.org/accounts/Euphausia_superba/

92 Glyshaw, P. and E. Wason 2013."*Anopheles quadrimaculatus* "(On-line), Animal Diversity Web. http://animaldiversity.org/accounts/Anopheles_quadrimaculatus/

93 Ivory, A. 2002. "*Aquila chrysaetos* " (On-line), Animal Diversity Web. http://animaldiversity.org/accounts/Aquila_chrysaetos/

94 Thompson, B. 2001. "*Anthonomus grandis* " (On-line), Animal Diversity Web. http://animaldiversity.org/accounts/Anthonomus_grandis/

95 Tung, L. 2003. "*Makaira nigricans* " (On-line), Animal Diversity Web. http://animaldiversity.org/accounts/Makaira_nigricans/

96 www.allaboutbirds.org/guide/Peregrine_Falcon/lifehistory

97 www.nationalgeographic.com/animals/mammals/c/california-sea-lion/

98 www.howfastcanarun.com/how-fast-can-a-pig-run.html

99 www.livescience.com/32772-what-animal-is-the-fastest-swimmer.html

100 www.oceanwide-expeditions.com/to-do/wildlife/ringed-seal-1

101 www.speedofanimals.com

102 www.theanimalfiles.com/mammals/hoofed_mammals/chital.html

103 www.wikipedia.org/wiki/Shortfin_mako_shark

104 http://www.pgc.pa.gov/Education/WildlifeNotesIndex/Documents/snowgoose.pdf

Supplementary Information for Research Chapter 2

Hirt, M. R., T. Lauermann, U. Brose, L. P. J. J. Noldus, and A. I. Dell. 2017. “The little things that run: a general scaling of invertebrate exploratory speed with body mass”. Ecology 98: 2751–2757.

Supplementary Table 2.1 | Body mass and mean exploratory speed of terrestrial invertebrates.

class	order	species	body mass [g]	mean exploratory speed [mm/s]	feeding type
Arachnida	Araneae	Agelenidae Sp.	0.0189	16.17	Carnivore
Arachnida	Araneae	Agelenidae Sp.	0.0109	12.56	Carnivore
Arachnida	Araneae	Agelenidae Sp.	0.0113	6.53	Carnivore
Arachnida	Araneae	Agelenidae Sp.	0.0014	2.95	Carnivore
Arachnida	Araneae	Agelenidae Sp.	0.1009	25.54	Carnivore
Arachnida	Araneae	Agelenidae Sp.	0.0721	19.65	Carnivore
Arachnida	Araneae	Agelenidae Sp.	0.1084	26.32	Carnivore
Arachnida	Araneae	Clubionidae Sp.	0.0218	1.22	Carnivore
Arachnida	Araneae	Clubionidae Sp.	0.0247	1.68	Carnivore
Arachnida	Araneae	Clubionidae Sp.	0.0381	17.96	Carnivore
Arachnida	Araneae	Clubionidae Sp.	0.0016	3.71	Carnivore
Arachnida	Araneae	Clubionidae Sp.	0.0068	4.15	Carnivore
Arachnida	Araneae	Clubionidae Sp.	0.0029	11.48	Carnivore
Arachnida	Araneae	Clubionidae Sp.	0.0026	8.30	Carnivore
Arachnida	Araneae	Clubionidae Sp.	0.0145	2.83	Carnivore
Arachnida	Araneae	Clubionidae Sp.	0.0120	2.07	Carnivore
Arachnida	Araneae	Cybaeidae Sp.	0.0044	5.41	Carnivore
Arachnida	Araneae	Cybaeidae Sp.	0.0129	13.88	Carnivore
Arachnida	Araneae	Cybaeidae Sp.	0.0040	3.16	Carnivore
Arachnida	Araneae	Cybaeidae Sp.	0.0031	1.65	Carnivore
Arachnida	Araneae	Dictynidae Sp.	0.0014	5.36	Carnivore
Arachnida	Araneae	Dysderidae Sp.	0.0114	7.19	Carnivore
Arachnida	Araneae	Dysderidae Sp.	0.0038	3.31	Carnivore
Arachnida	Araneae	Dysderidae Sp.	0.0105	5.81	Carnivore
Arachnida	Araneae	Gnaphosidae Sp.	0.0023	8.16	Carnivore
Arachnida	Araneae	Linyphiidae Sp.	0.0045	7.68	Carnivore
Arachnida	Araneae	Linyphiidae Sp.	0.0028	8.04	Carnivore
Arachnida	Araneae	Linyphiidae Sp.	0.0073	6.55	Carnivore
Arachnida	Araneae	Lycosidae Sp.	0.0030	3.39	Carnivore
Arachnida	Araneae	Lycosidae sp.	0.0122	15.94	Carnivore
Arachnida	Araneae	Lycosidae sp.	0.0143	18.55	Carnivore
Arachnida	Araneae	Lycosidae sp.	0.0099	16.74	Carnivore
Arachnida	Araneae	Lycosidae sp.	0.0083	6.29	Carnivore
Arachnida	Araneae	Lycosidae sp.	0.0267	18.21	Carnivore
Arachnida	Araneae	Thomisidae Sp.	0.0232	5.10	Carnivore
Arachnida	Opiliones	*Nemastoma lugubre*	0.0031	7.57	Carnivore
Arachnida	Opiliones	*Nemastoma lugubre*	0.0029	6.93	Carnivore
Arachnida	Opiliones	*Nemastoma lugubre*	0.0017	9.62	Carnivore
Arachnida	Opiliones	*Nemastoma lugubre*	0.0157	20.36	Carnivore
Arachnida	Opiliones	*Nemastoma lugubre*	0.0032	5.67	Carnivore
Arachnida	Opiliones	*Paranemastoma sp.*	0.0029	3.52	Carnivore

class	order	species	body mass [g]	mean exploratory speed [mm/s]	feeding type
Arachnida	Opiliones	*Phalangiidae sp.*	0.0106	3.06	Carnivore
Arachnida	Opiliones	*Phalangiidae sp.*	0.0099	20.69	Carnivore
Arachnida	Opiliones	*Trogulidae sp.*	0.0161	7.10	Carnivore
Arachnida	Pseudoscorpiones	*Roncus lubricus*	0.0030	2.14	Carnivore
Arachnida	Pseudoscorpiones	*Roncus lubricus*	0.0027	3.10	Carnivore
Arachnida	Pseudoscorpiones	*Roncus lubricus*	0.0027	1.70	Carnivore
Arachnida	Pseudoscorpiones	*Roncus lubricus*	0.0018	2.38	Carnivore
Arachnida	Pseudoscorpiones	*Roncus lubricus*	0.0034	2.77	Carnivore
Arachnida	Pseudoscorpiones	*Roncus lubricus*	0.0017	1.94	Carnivore
Arachnida	Pseudoscorpiones	*Roncus lubricus*	0.0009	1.83	Carnivore
Arachnida	Sarcoptiformes	*Damaeus onustus*	0.0009	0.64	Detritivore
Chilopoda	Lithobiomorpha	*Lithobius calcaratus*	0.0259	15.73	Carnivore
Chilopoda	Lithobiomorpha	*Lithobius forficatus*	0.1311	32.55	Carnivore
Chilopoda	Lithobiomorpha	*Lithobius forficatus*	0.0306	23.57	Carnivore
Chilopoda	Lithobiomorpha	*Lithobius forficatus*	0.0846	30.45	Carnivore
Chilopoda	Lithobiomorpha	*Lithobius forficatus*	0.0267	9.27	Carnivore
Chilopoda	Lithobiomorpha	*Lithobius melanops*	0.0388	3.29	Carnivore
Chilopoda	Lithobiomorpha	*Lithobius melanops*	0.0176	9.68	Carnivore
Chilopoda	Lithobiomorpha	*Lithobius melanops*	0.0030	3.68	Carnivore
Chilopoda	Lithobiomorpha	*Lithobius melanops*	0.0170	7.94	Carnivore
Chilopoda	Lithobiomorpha	*Lithobius microps*	0.0024	2.91	Carnivore
Chilopoda	Scolopendromorpha	*Cryptops hortensi*	0.0062	8.38	Carnivore
Chilopoda	Scolopendromorpha	*Cryptops hortensi*	0.0447	16.93	Carnivore
Diplopoda	Glomerida	*Glomeris marginata*	0.0482	2.58	Detritivore
Diplopoda	Glomerida	*Glomeris marginata*	0.1445	3.07	Detritivore
Diplopoda	Glomerida	*Glomeris marginata*	0.0947	1.77	Detritivore
Diplopoda	Glomerida	*Glomeris marginata*	0.0737	2.96	Detritivore
Diplopoda	Glomerida	*Glomeris marginata*	0.1326	2.15	Detritivore
Diplopoda	Glomerida	*Glomeris marginata*	0.1501	3.89	Detritivore
Diplopoda	Glomerida	*Glomeris marginata*	0.1765	3.69	Detritivore
Diplopoda	Glomerida	*Glomeris marginata*	0.1908	2.30	Detritivore
Diplopoda	Julida	*Allajulus nitidus*	0.0726	3.57	Detritivore
Diplopoda	Julida	Julidae sp.	0.0418	5.82	Detritivore
Diplopoda	Julida	Julidae Sp.	0.0280	2.91	Detritivore
Diplopoda	Julida	Julidae sp.	0.0790	2.93	Detritivore
Diplopoda	Julida	Julidae sp.	0.0052	1.96	Detritivore
Diplopoda	Julida	Julidae sp.	0.0074	1.67	Detritivore
Diplopoda	Julida	Julidae sp.	0.0219	4.68	Detritivore
Diplopoda	Julida	Julidae sp.	0.1027	6.58	Detritivore
Diplopoda	Julida	*Julus scandinavius*	0.0152	1.84	Detritivore
Diplopoda	Julida	*Kryphioiulus occultus*	0.1793	7.05	Detritivore
Diplopoda	Polydesmida	*Polydesmidae Sp.*	0.0567	9.06	Detritivore
Diplopoda	Polydesmida	*Polydesmidae Sp.*	0.0521	7.86	Detritivore
Diplopoda	Polydesmida	*Polydesmus sp.*	0.0009	1.67	Detritivore
Diplopoda	Polydesmida	*Polydesmus sp.*	0.0075	3.76	Detritivore
Diplopoda	Polydesmida	*Polydesmus sp.*	0.0279	6.75	Detritivore

class	order	species	body mass [g]	mean exploratory speed [mm/s]	feeding type
Diplopoda	Polydesmida	*Polydesmus superus*	0.0077	3.89	Detritivore
Diplopoda	Polydesmida	*Polydesmus testaceus*	0.0314	8.48	Detritivore
Diplopoda	Polydesmida	*Polydesmus testaceus*	0.0370	7.25	Detritivore
Entognatha	Entomobryomorpha	*Entomobrya corticalis*	0.0020	4.39	Detritivore
Entognatha	Entomobryomorpha	*Entomobrya corticalis*	0.0006	3.43	Detritivore
Entognatha	Entomobryomorpha	*Entomobrya handschini*	0.0019	4.07	Detritivore
Entognatha	Entomobryomorpha	*Entomobrya handschini*	0.0008	3.89	Detritivore
Entognatha	Entomobryomorpha	*Mesentotoma dollfusi*	0.0002	4.07	Detritivore
Entognatha	Entomobryomorpha	*Neophorella dubia*	0.0017	3.70	Detritivore
Entognatha	Entomobryomorpha	*Tomocerus longicornis*	0.0015	5.27	Detritivore
Entognatha	Entomobryomorpha	*Tomocerus longicornis*	0.0052	4.79	Detritivore
Insecta	Blattodea	*Ectobius sylvestris*	0.0209	8.12	Detritivore
Insecta	Coleoptera	Anobiidae sp.	0.0006	7.75	Detritivore
Insecta	Coleoptera	Buprestidae sp.	0.0042	4.37	Detritivore
Insecta	Coleoptera	Carabidae sp.	0.0451	3.66	Carnivore
Insecta	Coleoptera	Carabidae sp.	0.0519	8.50	Carnivore
Insecta	Coleoptera	Carabidae sp.	0.1270	21.70	Carnivore
Insecta	Coleoptera	Carabidae sp.	0.0744	56.63	Carnivore
Insecta	Coleoptera	Carabidae sp.	0.2779	46.82	Carnivore
Insecta	Coleoptera	Carabidae Sp.	0.0052	3.20	Carnivore
Insecta	Coleoptera	Carabidae sp.	0.0144	39.06	Carnivore
Insecta	Coleoptera	Carabidae sp.	0.2016	17.55	Carnivore
Insecta	Coleoptera	Carabidae sp.	0.0161	31.51	Carnivore
Insecta	Coleoptera	Carabidae sp.	0.0345	21.76	Carnivore
Insecta	Coleoptera	Carabidae sp.	0.0024	4.79	Carnivore
Insecta	Coleoptera	Carabidae sp.	0.0030	6.26	Carnivore
Insecta	Coleoptera	Carabidae sp.	0.2895	38.16	Carnivore
Insecta	Coleoptera	Cerambycidae sp.	0.0038	17.69	Herbivore
Insecta	Coleoptera	Endomychidae sp.	0.0048	2.93	Detritivore
Insecta	Coleoptera	*Omalisus fontisbellaquaei*	0.0169	3.34	Carnivore
Insecta	Coleoptera	Scarabaeidae sp.	0.4594	11.96	Omnivore
Insecta	Coleoptera	Staphyliidae sp.	0.1639	41.03	Carnivore
Insecta	Coleoptera	Staphyliidae sp.	0.0030	8.74	Carnivore
Insecta	Coleoptera	Staphyliidae sp.	0.0059	12.12	Carnivore
Insecta	Coleoptera	Staphyliidae sp.	0.0191	6.09	Carnivore
Insecta	Coleoptera	Staphyliidae sp.	0.0022	3.88	Carnivore
Insecta	Coleoptera	Staphyliidae sp.	0.0014	4.86	Carnivore
Insecta	Coleoptera	Staphyliidae sp.	0.0136	9.19	Carnivore
Insecta	Coleoptera	Staphyliidae sp.	0.0015	5.77	Carnivore
Insecta	Coleoptera	Staphyliidae sp.	0.0028	10.85	Carnivore
Insecta	Coleoptera	Staphylinidae Sp.	0.1468	45.88	Carnivore
Insecta	Coleoptera	Staphylinidae Sp.	0.0058	19.64	Carnivore
Insecta	Coleoptera	Staphylinidae Sp.	0.0077	16.90	Carnivore
Insecta	Dermaptera	*Chelidurella acanthopygia*	0.0126	2.28	Detritivore
Insecta	Dermaptera	*Chelidurella acanthopygia*	0.1124	4.08	Detritivore
Insecta	Dermaptera	*Chelidurella acanthopygia*	0.1114	1.61	Detritivore

class	order	species	body mass [g]	mean exploratory speed [mm/s]	feeding type
Insecta	Dermaptera	*Chelidurella acanthopygia*	0.0067	7.95	Detritivore
Insecta	Dermaptera	*Chelidurella acanthopygia*	0.0152	6.63	Detritivore
Insecta	Dermaptera	*Chelidurella acanthopygia*	0.0135	5.91	Detritivore
Insecta	Dermaptera	*Chelidurella acanthopygia*	0.0241	13.12	Detritivore
Insecta	Dermaptera	*Chelidurella acanthopygia*	0.0270	2.14	Detritivore
Insecta	Hemiptera	*Errhomenus brachypterus*	0.0214	3.00	Herbivore
Insecta	Hemiptera	Nabidae sp.	0.0020	10.36	Herbivore
Insecta	Hemiptera	Nabidae sp.	0.0026	11.41	Herbivore
Insecta	Hemiptera	Nabidae sp.	0.0019	7.36	Herbivore
Insecta	Hemiptera	*Pyrrhocoris apterus*	0.0429	11.04	Herbivore
Insecta	Hemiptera	*Pyrrhocoris apterus*	0.0424	8.51	Herbivore
Insecta	Hemiptera	*Pyrrhocoris apterus*	0.0376	7.75	Herbivore
Insecta	Hemiptera	*Pyrrhocoris apterus*	0.0551	3.15	Herbivore
Insecta	Hymenoptera	*Lasius fuliginosus*	0.0172	8.12	Omnivore
Insecta	Hymenoptera	*Tetramorium caespitum*	0.0025	9.75	Omnivore
Insecta	Hymenoptera	*Tetramorium caespitum*	0.0025	5.84	Omnivore
Insecta	Hymenoptera	*Tetramorium caespitum*	0.0024	9.46	Omnivore
Insecta	Hymenoptera	*Tetramorium caespitum*	0.0024	11.70	Omnivore
Insecta	Hymenoptera	*Tetramorium caespitum*	0.0029	6.71	Omnivore
Insecta	Hymenoptera	*Tetramorium caespitum*	0.0004	1.66	Omnivore
Malacostraca	Isopoda	*Armadillidiidae pictum*	0.1065	5.80	Detritivore
Malacostraca	Isopoda	*Oniscus asellus*	0.0348	7.14	Detritivore
Malacostraca	Isopoda	*Oniscus asellus*	0.0550	6.40	Detritivore
Malacostraca	Isopoda	*Oniscus asellus*	0.0822	7.78	Detritivore
Malacostraca	Isopoda	*Oniscus asellus*	0.0634	11.15	Detritivore
Malacostraca	Isopoda	*Oniscus asellus*	0.0032	1.26	Detritivore
Malacostraca	Isopoda	*Oniscus asellus*	0.0790	9.31	Detritivore
Malacostraca	Isopoda	*Oniscus asellus*	0.0387	5.61	Detritivore
Malacostraca	Isopoda	*Oniscus asellus*	0.0467	3.33	Detritivore
Malacostraca	Isopoda	*Oniscus asellus*	0.0184	6.65	Detritivore
Malacostraca	Isopoda	*Oniscus asellus*	0.0174	4.75	Detritivore
Malacostraca	Isopoda	*Oniscus asellus*	0.0574	6.55	Detritivore
Malacostraca	Isopoda	*Philoscia muscorum*	0.0072	3.82	Detritivore
Malacostraca	Isopoda	*Philoscia muscorum*	0.0075	3.26	Detritivore
Malacostraca	Isopoda	*Philoscia muscorum*	0.0194	5.06	Detritivore
Malacostraca	Isopoda	*Trachelipus rathkei*	0.0177	7.58	Detritivore
Malacostraca	Isopoda	*Trachelipus rathkei*	0.0385	9.27	Detritivore
Malacostraca	Isopoda	*Trachelipus rathkei*	0.0028	0.95	Detritivore
Malacostraca	Isopoda	*Trachelipus rathkei*	0.0026	2.16	Detritivore
Malacostraca	Isopoda	*Trachelipus rathkei*	0.0022	1.52	Detritivore

Supplementary Information for Research Chapter 3

Hirt, M. R., V. Grimm, Y. Li, B.C. Rall, B. Rosenbaum, and U. Brose. "Bridging scales - Linking movement ecology and biodiversity research by allometric random walks".

Beta distribution derivation based on type of speed

The beta distribution is parameterized by two positive shape parameters, α and β. Approximations are used to estimate the proportion of maximum speed that is used during different types of movement. For exemplary purpose, we assume animals to move at 5% of their maximum speed during foraging, at 10% during travel and at 90% during attack or escape. The respective beta distributions have these proportions as means μ. Thus, our means for the different behaviors are $\mu_f = 0.05$ for foraging speeds, $\mu_t = 0.1$ for travel speeds and $\mu_h = 0.9$ for attack or escape speeds. The parameters α and β are related to the mean (μ)

$$\mu = \frac{\alpha}{\alpha+\beta} \tag{1}$$

and the variance

$$\sigma^2 = \frac{\alpha\,\beta}{(\alpha+\beta)^2\,(\alpha+\beta+1)} \ . \tag{2}$$

Solved for α and β, this gives

$$\alpha = \left(\frac{1-\mu}{\sigma^2} - \frac{1}{\mu}\right)\mu^2 \tag{3}$$

and

$$\beta = \alpha\,(\frac{1}{\mu} - 1) \ . \tag{4}$$

As variance, we assume 5% ($\sigma = 0.05$). Inserting these empirical values of the mean (μ) and the variance (σ^2) in eqn (3) and (4) yields the shape parameters α and β for the different beta distributions (Figure 3.2a).

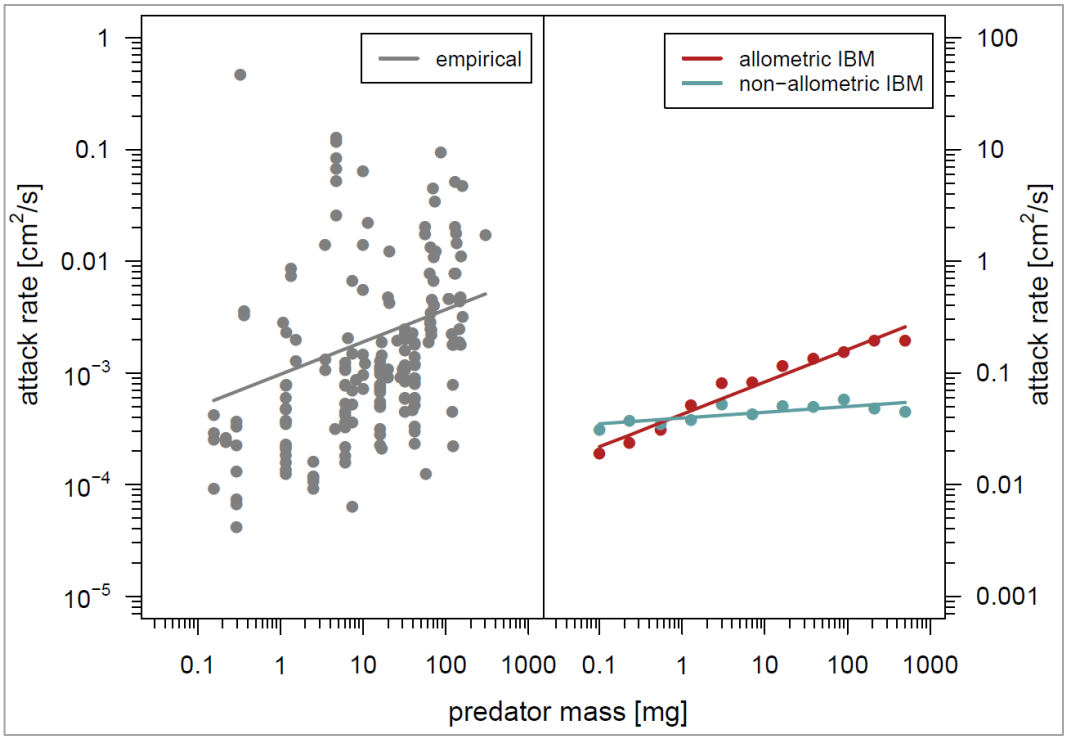

Supplementary Figure 3.1 | Body-mass scaling of predator attack rates. (**a**) Empirical data on terrestrial invertebrates by Li et al. 2017 (**b**) Predicted attack rates by standard IBM (blue) and allometric IBM (red).

Supplementary Information for Research Chapter 4

Hirt, M. R., T. Müller, B. Rosenbaum, M. Tucker, and U. Brose. "Rethinking trophic niches: speed and body mass co-limit prey space of mammalian predators".

Estimation of prey space

The prey space is defined by the 90% confidence region of a bivariate normal distribution, with the constraint that its first principal component (the axis of largest variation) crosses the origin. It is computed as follows.

The first principal component P_1 is determined by a major axis regression with fixed intercept zero (see below). Using its slope b, the principal component reads $P_1 = \binom{1}{b}$. The second principal component is orthogonal to the first one and therefore reads $P_2 = \binom{1}{-1/b}$ (such that $P_1^T P_2 = 0$). After normalization $P_1^{norm} = P_1/\|P_1\|$ and $P_2^{norm} = P_2/\|P_2\|$ ($\|\cdot\|$ denoting the Euclidean norm), the orthogonal 2x2 matrix of principal components is given by $P = [P_1^{norm}, P_2^{norm}]$.

Let $X = [x^1, \dots, x^n]$ be a 2xn matrix of n observations $x^i = \binom{x_1^i}{x_2^i}$. We perform a change of basis using the new basis P and transform the data $\tilde{X} = P^T X$. In this new space, the principal components are defined by the identity matrix $I = \begin{bmatrix} 1 & 0 \\ 0 & 1 \end{bmatrix}$, i.e. the data $\tilde{X}$ are uncorrelated. We fit an uncorrelated bivariate normal distribution to this transformed data $\tilde{X}$ by calculating its empirical mean vector $\mu_1 = \frac{1}{n}\sum_{i=1}^n \tilde{x}_1^i, \mu_2 = 0$ (to ensure that the mean vector is located on the first principal component) and empirical variances $\sigma_1^2 = \frac{1}{n-1}\sum_{i=1}^n (\tilde{x}_1^i - \mu_1)^2, \sigma_2^2 = \frac{1}{n-1}\sum_{i=1}^n (\tilde{x}_2^i - 0)^2$.

Using the mean vector $\mu = \binom{\mu_1}{\mu_2}$ and the covariance matrix $\Sigma = \begin{bmatrix} \sigma_1^2 & 0 \\ 0 & \sigma_2^2 \end{bmatrix}$, we determine the boundary $\tilde{E}$ (still in the transformed space) of the normal distribution's 90% confidence region with the R-package "ellipse". The prey space E for the original data X is calculated by performing a change of basis back to the original space $E = P\tilde{E}$.

Bayesian major axis regression

We use Bayesian methods for parameter estimation, i.e. we compute the posterior distribution of the parameters θ observing the data

$$P(\theta|data) = P(data|\theta) * P(\theta) / P(data),$$

where $P(data|\theta)$ denotes the likelihood function, $P(\theta)$ is the parameters' prior distribution and $P(data)$ is a constant. Samples from the posterior distribution were drawn using Hamiltonian Monte Carlo sampling in *Stan*, accessed via the *RStan package* (Stan Development Team 2017).

For the Bayesian major axis regression, intercept *a* and slope *b* are sought, which minimize the sum of squared orthogonal distances of the observations (x,y) to the regression line (Warton et al. 2006). For any observation, the nearest point on the line is given by $x^*=(y+x/b-a)/(b+1/b)$ and $y^*=a+bx^*$ (orthogonal projection). The residuals are the Euclidean distances $d((x,y),(x^*,y^*))$ between the observations and their projections on the regression line and are modelled normally distributed with zero mean and standard deviation σ, which defines the likelihood function.

We fitted a model with a fixed intercept $a=0$ for all three groups of data (pursuit predator, group hunter, ambusher). Each group was fitted with its own slope b_i and standard deviation σ_i ($i=1,2,3$). We used vague priors for the slopes (normal distribution with mean 0 and standard deviation 10.0). For the residuals' standard deviations, a positive half-Cauchy prior (location 0.0, scale 2.0) was chosen (Gelman and Hill 2007). This Bayesian approach allows direct inference on all parameters and their combinations. I.e., from the samples of the posterior distribution, we can directly compute statistics on differences in slopes (b_i-b_j). We tested for significant differences by calculating posterior probabilities $P(b_i>b_j)$.

Supplementary Table 4.1 | Database on body masses and maximum speeds of mammalian predator-prey pairs.

predator species	predator mass [kg]	mass ref.	predator max. speed [km/h]	speed ref.	hunting strategy	prey species	prey mass [kg]	mass ref.	prey max. speed [km/h]	speed ref.
Acinonyx jubatus	65.00	1	120.00	1	pursuit predator	*Aepyceros melampus*	54.42	1	74.99	1
Acinonyx jubatus	65.00	1	120.00	1	pursuit predator	*Antidorcas marsupialis*	39.50	1	97.00	1
Acinonyx jubatus	65.00	1	120.00	1	pursuit predator	*Eudorcas thomsonii*	25.00	1	65.00	1
Canis aureus	9.20	1	55.98	1	pursuit predator	*Mus musculus*	0.02	1	13.00	1
Canis aureus	9.20	1	55.98	1	pursuit predator	*Rattus*	0.25	1	9.43	1
Canis latrans	18.00	1	69.04	1	pursuit predator	*Lepus americanus*	1.50	1	48.55	1
Gulo gulo	12.79	3	48.00	4	pursuit predator	*Lepus timidus*	3.03	3	61.24	1
Lynx canadensis	9.68	3	64.00	5	pursuit predator	*Lepus americanus*	1.50	1	48.55	1
Urocyon cinereoargenteus	5.50	1	67.60	1	pursuit predator	*Neotoma lepida*	0.11	1	16.62	1
Urocyon cinereoargenteus	5.50	1	67.60	1	pursuit predator	*Peromyscus spp.*	0.02	1	13.90	1
Urocyon cinereoargenteus	5.50	1	67.60	1	pursuit predator	*Sylvilagus floridanus*	1.17	1	48.00	1
Vulpes vulpes	4.59	1	72.00	1	pursuit predator	*Antechinomys laniger*	0.03	1	14.51	1
Vulpes vulpes	4.59	1	72.00	1	pursuit predator	*Microtus pennsylvanicus*	0.05	1	10.68	1
Vulpes vulpes	4.59	1	72.00	1	pursuit predator	*Microtus pinetorum*	0.03	1	6.60	1
Canis lupus	40.00	1	63.97	1	group hunter	*Bison bison*	865	1	54.43	1
Canis lupus	40.00	1	63.97	1	group hunter	*Capreolus capreolus*	25	1	59.98	1
Canis lupus	40.00	1	63.97	1	group hunter	*Cervus canadensis*	270	1	72.40	1
Lycaon pictus	27.00	1	72.42	1	group hunter	*Aepyceros melampus*	50.00	1	74.99	1
Lycaon pictus	27.00	1	72.42	1	group hunter	*Eudorcas thomsonii*	25.00	1	65.00	1
Panthera leo	199.00	1	80.00	1	group hunter	*Syncerus caffer*	529.77	1	56.23	1
Panthera leo	199.00	1	80.00	1	group hunter	*Connochaetes gnou*	133.50	1	90.00	1
Panthera leo	199.00	1	80.00	1	group hunter	*Connochaetes taurinus*	180.00	1	79.98	1
Panthera leo	199.00	1	80.00	1	group hunter	*Giraffa camelopardalis*	1555.00	1	60.00	1
Panthera leo	199.00	1	80.00	1	group hunter	*Taurotragus derbianus*	680.77	1	69.98	1
Panthera leo	199.00	1	80.00	1	group hunter	*Taurotragus oryx*	559.76	1	69.98	1
Crocuta crocuta	63.00	3	62.32	1	group hunter	*Connochaetes taurinus*	180.00	1	79.98	1
Crocuta crocuta	63.00	3	62.32	1	pursuit predator	*Eudorcas thomsonii*	25.00	1	65.00	1
Gulo gulo	12.79	3	48.00	4	ambusher	*Alces alces*	351.00	3	55.26	1
Gulo gulo	12.79	3	48.00	4	ambusher	*Capreolus capreolus*	21.67	3	59.98	1
Gulo gulo	12.79	3	48.00	4	ambusher	*Rangifer tarandus*	101.25	3	75.92	1

predator species	predator mass [kg]	mass ref.	predator max. speed [km/h]	speed ref.	hunting strategy	prey species	prey mass [kg]	mass ref.	prey max. speed [km/h]	speed ref.
Panthera pardus	51.00	1	59.98	1	ambusher	*Aepyceros melampus*	50.00	1	74.99	1
Panthera pardus	51.00	1	59.98	1	ambusher	*Phacochoerus aethiopicus*	87.9	1	54.95	1
Panthera tigris	144.88	1	55.98	1	ambusher	*Axis axis*	45.5	1	65.00	1
Panthera tigris	144.88	1	55.98	1	ambusher	*Cervus canadensis*	270	1	72.40	1
Panthera tigris	144.88	1	55.98	1	ambusher	*Sus scrofa*	135.00	1	61.21	1
Puma concolor	53.70	3	80.00	2	ambusher	*Alces alces*	410.20	1	55.27	1
Puma concolor	53.70	3	80.00	2	ambusher	*Odocoileus hemionus*	54.95	1	63.97	1
Puma concolor	53.70	3	80.00	2	ambusher	*Odocoileus virginianus*	61.94	1	63.97	1
Puma concolor	53.70	3	80.00	2	ambusher	*Pecari tajacu*	21.98	1	34.99	1

References

1 Hirt, M. R., W. Jetz, B. C. Rall, and U. Brose. 2017. A general scaling law reveals why the largest animals are not the fastest. Nature ecology & evolution 1:1116–1122.

2 http://mountainlion.org/FAQfrequentlyaskedquestions.asp, retrieved 04.08.2017

3 Myhrvold, N. P., E. Baldridge, B. Chan, D. Sivam, D. L. Freeman, and S. K. Ernest. 2015. An amniote life-history database to perform comparative analyses with birds, mammals, and reptiles. Ecology 96:3109–3109.

4 http://a-z-animals.com/animals/wolverine/, retrieved 24.11.2017, 15:56

5 http://dinoanimals.com/animals/the-fastest-animals-in-the-world-top-100/, retrieved 24.11.2017

Supplementary Table 4.2 | Body-mass and maximum-speed ratios of the predator-prey pairs of Supplementary Table 4.1 given as ratios from predator to prey and prey to predator.

		predator/prey				prey/predator			
predator species	prey species	mass ratio	log10 (mass ratio)	speed ratio	log10 (speed ratio)	mass ratio	log10 (mass ratio)	speed ratio	log10 (speed ratio)
Acinonyx jubatus	*Aepyceros melampus*	1.19	0.08	1.60	0.20	0.84	-0.08	0.62	-0.20
Acinonyx jubatus	*Antidorcas marsupialis*	1.65	0.22	1.24	0.09	0.61	-0.22	0.81	-0.09
Acinonyx jubatus	*Eudorcas thomsonii*	2.60	0.41	1.85	0.27	0.38	-0.41	0.54	-0.27
Canis aureus	*Mus musculus*	460.00	2.66	4.31	0.63	0.00	-2.66	0.23	-0.63
Canis aureus	*Rattus*	36.80	1.57	5.94	0.77	0.03	-1.57	0.17	-0.77
Canis latrans	*Lepus americanus*	12.00	1.08	1.42	0.15	0.08	-1.08	0.70	-0.15
Gulo gulo	*Lepus timidus*	4.22	0.63	0.78	-0.11	0.24	-0.63	1.28	0.11
Lynx canadensis	*Lepus americanus*	6.46	0.81	1.32	0.12	0.15	-0.81	0.76	-0.12
Urocyon cinereoargenteus	*Neotoma lepida*	50.00	1.70	4.07	0.61	0.02	-1.70	0.25	-0.61
Urocyon cinereoargenteus	*Peromyscus spp.*	275.00	2.44	4.86	0.69	0.00	-2.44	0.21	-0.69
Urocyon cinereoargenteus	*Sylvilagus floridanus*	4.70	0.67	1.41	0.15	0.21	-0.67	0.71	-0.15
Vulpes vulpes	*Antechinomys laniger*	153.00	2.18	4.96	0.70	0.01	-2.18	0.20	-0.70
Vulpes vulpes	*Microtus pennsylvanicus*	91.80	1.96	6.74	0.83	0.01	-1.96	0.15	-0.83
Vulpes vulpes	*Microtus pinetorum*	153.00	2.18	10.91	1.04	0.01	-2.18	0.09	-1.04
Canis lupus	*Bison bison*	0.05	-1.33	1.18	0.07	21.63	1.33	0.85	-0.07
Canis lupus	*Capreolus capreolus*	1.60	0.20	1.07	0.03	0.63	-0.20	0.94	-0.03
Canis lupus	*Cervus canadensis*	0.15	-0.83	0.88	-0.05	6.75	0.83	1.13	0.05
Lycaon pictus	*Aepyceros melampus*	0.54	-0.27	0.97	-0.02	1.85	0.27	1.04	0.02
Lycaon pictus	*Eudorcas thomsonii*	1.08	0.03	1.11	0.05	0.93	-0.03	0.90	-0.05
Panthera leo	*Syncerus caffer*	0.38	-0.43	1.42	0.15	2.66	0.43	0.70	-0.15
Panthera leo	*Connochaetes gnou*	1.49	0.17	0.89	-0.05	0.67	-0.17	1.13	0.05
Panthera leo	*Connochaetes taurinus*	1.11	0.04	1.00	0.00	0.90	-0.04	1.00	0.00
Panthera leo	*Giraffa camelopardalis*	0.13	-0.89	1.33	0.12	7.81	0.89	0.75	-0.12
Panthera leo	*Taurotragus derbianus*	0.29	-0.53	1.14	0.06	3.42	0.53	0.87	-0.06
Panthera leo	*Taurotragus oryx*	0.36	-0.45	1.14	0.06	2.81	0.45	0.87	-0.06
Crocuta crocuta	*Connochaetes taurinus*	0.35	-0.46	0.78	-0.11	2.86	0.46	1.28	0.11
Crocuta crocuta	*Eudorcas thomsonii*	2.52	0.40	0.96	-0.02	0.40	-0.40	1.04	0.02
Gulo gulo	*Alces alces*	0.04	-1.44	0.87	-0.06	27.44	1.44	1.15	0.06
Gulo gulo	*Capreolus capreolus*	0.59	-0.23	0.80	-0.10	1.69	0.23	1.25	0.10
Gulo gulo	*Rangifer tarandus*	0.13	-0.90	0.63	-0.20	7.92	0.90	1.58	0.20
Panthera pardus	*Aepyceros melampus*	1.02	0.01	0.80	-0.10	0.98	-0.01	1.25	0.10
Panthera pardus	*Phacochoerus aethiopicus*	0.58	-0.24	1.09	0.04	1.72	0.24	0.92	-0.04
Panthera tigris	*Axis axis*	3.18	0.50	0.86	-0.06	0.31	-0.50	1.16	0.06
Panthera tigris	*Cervus canadensis*	0.54	-0.27	0.77	-0.11	1.86	0.27	1.29	0.11
Panthera tigris	*Sus scrofa*	1.07	0.03	0.91	-0.04	0.93	-0.03	1.09	0.04
Puma concolor	*Alces alces*	0.13	-0.88	1.45	0.16	7.64	0.88	0.69	-0.16
Puma concolor	*Odocoileus hemionus*	0.98	-0.01	1.25	0.10	1.02	0.01	0.80	-0.10
Puma concolor	*Odocoileus virginianus*	0.87	-0.06	1.25	0.10	1.15	0.06	0.80	-0.10
Puma concolor	*Pecari tajacu*	2.44	0.39	2.29	0.36	0.41	-0.39	0.44	-0.36

Ehrenwörtliche Erklärung

Ich versichere, dass ich die vorliegende Arbeit selbständig und ohne unerlaubte Hilfe Dritter verfasst und keine anderen als die angegebenen Quellen und Hilfsmittel verwendet habe. Alle Stellen, die inhaltlich oder wörtlich aus Veröffentlichungen stammen, sind kenntlich gemacht. Diese Arbeit lag in der gleichen oder ähnlichen Weise noch keiner Prüfungsbehörde vor und wurde bisher noch nicht veröffentlicht.

Myriam Brose-Hirt

Leipzig, den 29.06.2018